Letters in Applied NanoBioScience
Open-Access Journal (ISSN: 2284-6808)

Article
Volume 12, Issue 4, 2023, 118
https://doi.org/10.33263/LIANBS124.118

Effect of Mutations in the SARS-CoV-2 Spike RBD Region of Delta and Delta-Plus Variants on its Interaction with ACE2 Receptor Protein

Chainee Das [1], Dorothy Das [1], Venkata Satish Kumar Mattaparthi [1,*]

[1] Molecular Modeling and Simulation Laboratory, Department of Molecular Biology and Biotechnology, Tezpur University, Tezpur, Assam, 784028, India; chaineedas97@gmail.com (C.D.); dorthyds.1010@gmail.com (D.D.); mvenkatasatishkumar@gmail.com (V.S.K.M.), venkata@tezu.ernet.in (V.S.K.M.)
* Correspondence: mvenkatasatishkumar@gmail.com (V.S.K.M.); venkata@tezu.ernet.in (V.S.K.M.);
Scopus Author ID 54962670000
Received: 26.03.2022; Accepted: 29.04.2022; Published: 18.09.2022

Abstract: The outbreak of severe acute respiratory syndrome coronavirus 2 (SARS CoV-2) has undergone multiple significant mutations since its detection in 2019 in Wuhan, China. The emergence of new SARS-CoV-2 variants that can spread rapidly and undermine vaccine-induced immunity threatens the end of the COVID-19 pandemic. The delta variant (B.1.617.2) that emerged in India challenges efforts to control the COVID-19 pandemic. In addition to Delta, so-called Delta Plus sub-variants (B.1.617.2.1 and B.1.617.2.2) have become a new cause of global concern. Here we compare the interaction profile of RBD of the spike protein of the Delta and Delta-Plus variant of SARS-CoV-2 with the ACE2 receptor. From the molecular dynamics simulation, we observed the spike protein of Delta and Delta-Plus variant of SARS-CoV-2 utilizes unique strategies to have stable binding with ACE2. Using MM-GBSA/MM-PBSA algorithms, we found the binding affinity of spike protein of the Delta- variant-ACE2 complex is indeed high (GB_{TOT} = -39.36 kcal mol^{-1}, PB_{TOT}= -17.52 kcal mol^{-1}) in comparison with spike protein of Delta-Plus variant-ACE2 Complex (GB_{TOT} = -36.83 kcal mol^{-1}, PB_{TOT} = -16.03 kcal mol^{-1}). Stable binding of spike protein to ACE2 is essential for virus entry, and the interactions between them should be understood well for the treatment modalities.

Keywords: SARS-CoV-2; coronavirus; ACE2 receptor; Delta-Plus, B.1.617; molecular dynamics; spike protein; COVID-19.

1. Introduction

Coronavirus disease 2019 (COVID-19), a disease caused by the severe acute respiratory syndrome coronavirus 2 (SARS-CoV-2), has killed over 5.4 million people globally, making it the deadliest global health catastrophe since the 1918 influenza pandemic. The virus has continued to strike destruction since the World Health Organization (WHO) proclaimed it a global pandemic on March 11, 2020, with many countries seeing numerous waves of breakouts. Adaptive mutations can alter the pathogenic capacity of a virus in its genome. Even a single amino acid substitution can significantly impact a virus's ability to elude the immune system, making vaccine development difficult. SARS-CoV-2, like other RNA viruses, is prone to genetic evolution as it adapts to new human hosts, creating various variants with distinct characteristics from the ancestral strains. Periodic genomic sequencing of viral samples aids in the detection of new SARS-CoV-2 genetic variations circulating in populations, particularly in

the event of a worldwide pandemic. During the early stages of the pandemic, SARS-genetic CoV-2's evolution was limited, except for the appearance of a worldwide dominant variant known as D614G, which was linked to higher transmissibility but not increased disease severity compared to its ancestral strain. Another human variant linked to infection of farmed mink in Denmark was discovered, although it was not linked to greater transmissibility. Multiple SARS-CoV-2 variants have been identified since then, with a number of them being classified as variants of concern (VOCs) due to their public health implications. VOCs have been linked to increased transmissibility or virulence, decreased neutralization by antibodies obtained from natural infection or vaccination, the potential to elude detection, and a reduction in therapeutic or vaccine efficiency. Five SARS-CoV-2 VOCs (Alpha (B.1.1.7), Beta (B.1.351), Gamma (P.1), Delta (B.1.617.2), and Omicron (B.1.1.529)) have been detected since the start of the pandemic, according to a recent WHO epidemiological update, as of December 11, 2021. The fourth variant of concern, B.1.617.2 (also known as the Delta variant), was first discovered in India in December 2020 and was responsible for the deadly second wave of COVID-19 infections in India in April 2021. This variant was first found in the United States in March 2021 and has turned into the most prevalent SARS-CoV-2 strain in the country. With cases reported in over 96 countries, the spread of the delta variant, which originated in India [1], has generated concern worldwide. Many countries, including the United States, Africa, Brazil, Australia, and Europe, are threatened by these variants.

India is still fighting a resurgence of the delta variant, which appeared in early 2021. The Delta variant has been observed to avoid neutralizing antibodies and is 60 percent more transmissible than the Alpha variant (B.1.1.7), which is already highly infectious[1-4]. The recent studies on the variant have ignited fresh attention to how SARS-CoV-2 can adapt and mutate with the existing environment [5]. Another variant very similar to the Delta variant is the Delta Plus variant (AY.1), which was first detected in Europe and declared a “variant of concern” by the U.K. governmental agency Health England. The delta Plus variant is a sub-lineage of the delta variant, with a notable difference of possessing K417N mutation in the spike protein. The majority of the changes in these variants have occurred in the RBD domain of the spike protein [6,7], and these alterations correspond to improved virus transmissibility [8,9], evasion [10,11], and flexibility in the spike protein’s interaction with the host receptors [12]. Due to decreased vaccination efficacy due to mutations and the lack of viable antiviral medication candidates against SARS-CoV-2, the globe is still fighting to defeat the pandemic. With a decrease in vaccine efficacy due to mutations [13] and the absence of strong anti-viral drug candidates against SARS-CoV-2, the world is still battling to overcome the Pandemic. In this situation, one can look into nature for a cure and a solution. [14-33]. The mutations present in the RBD region of the spike protein of Delta and Delta Plus variants may affect its binding affinity to human cell-surface protein angiotensin I-converting enzyme 2 (ACE2). Modifications in the spike protein’s RBD region may lead to changes in the virus’s ACE2 binding specificity and alter its antigenicity, that is, recognition by immune antibodies. Here, we seek to investigate the binding interactions between RBD region of the spike protein of Delta and Delta Plus variants of SARS-CoV-2 with the ACE2 by employing Molecular dynamics and other computational approaches.

2. Materials and Methods

The initial 3-D structure of the SARS-CoV-2 spike receptor-binding domain bound with ACE2 (S protein-ACE2) (PDB ID: 6lzg with a resolution of 2.50 Å) (Figure 1A) was

retrieved from the Research Collaboratory for Structural Bioinformatics Protein Data bank (www.rcsb.org) [34]. The 3-D structure of the SARS-CoV-2 receptor-binding domain of Delta (L452R and T478K) (Figure 1A) and Delta-Plus (L452R, K417N, and T478K) (Figure 1B) variants bound with ACE2 were obtained by inducing punctual mutation of PDB: 6lzg crystal structure using UCSF Chimera package alpha v.1.12 [35]. The complex structures were then energy minimized by employing the steepest descents and conjugate gradient minimization.

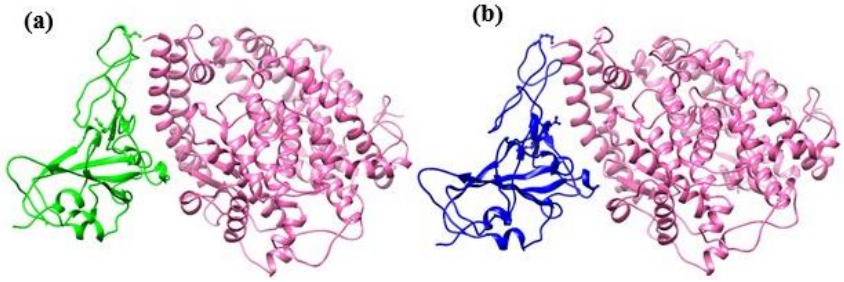

Figure 1. Three-dimensional structure of (a) SARS-CoV-2 spike receptor-binding domain Delta variant bound with ACE2 (S protein(Delta)-ACE2); (b) SARS-CoV-2 spike receptor-binding domain Delta Plus variant bound with ACE2 (S protein(Delta Plus)-ACE2).

2.1. Molecular dynamics simulations.

The Delta, as well as the Delta-Plus variants of the complex of SARS-CoV-2 spike receptor-binding domain bound with ACE2, were subjected to MD simulations. The MD simulation was performed using AMBER ff14SB force field [36] with AMBER software package [36]. To ensure the overall neutrality of the two complex systems, appropriate numbers of counter ions were added. The two complex systems were subjected to MD simulations in explicit solvent and were solvated with TIP3P [37] water model with a solvent buffer of 10 Å in all directions. In the first minimization step, spike receptor-binding domain and ACE2 were fixed with a 500 kcal/mol/Å^2 and minimized the energy of all water molecules and counterions for 10000 steps of steepest descents (SD) followed by 10000 steps of the conjugate gradient (CG). Subsequently, in the second step of minimization, to remove conflicting contacts, the entire complex system was repeated for 12000 steps of SD minimization and 8000 steps of CG minimization. Next, both the complex systems were gradually heated from 0-300 K in constant volume (NVT) conditions, thereby applying harmonic restraints with a force constant of 10 kcal/mol/Å^2 on the solute atoms, and equilibration was performed three times with 3000 ps using a force constant of 5.0 kcal/mol/Å. Finally, 100 ns MD simulations were performed using the NPT ensemble without restraints. We used the Particle mesh Ewald [38,39] technique with a non-bonded cutoff of 12.0 Å to limit the direct space sum to treat the long-range electrostatic interactions. The SHAKE algorithm was used to constrain all of the system's bonds [40]. The pressure and temperature (0.5 ps of heat bath and 0.2 ps of pressure relaxation) were kept constant by the Berendsen weak coupling algorithm [41] throughout the simulation process. The time step of MD simulation was set to 2 fs, and sampling was performed every 10 ps into the MD file.

After completion of the 100 ns of production dynamics of the complexes, the lowest energy conformer of the individual complex (S protein(Delta)-ACE2 and S protein(Delta-Plus)-ACE2) was extracted using the RMSD clustering algorithm from the highly populated clusters and submitted to PDBsum server (http://www.ebi.ac.uk/thornton-srv/databases/pdbsum/Generate.html) to analyze for their residue-specific interactions which are considered to be important to know about the nature of interactions. PDBsum [42] is a

database that, among other things, shows schematic diagrams of the non-bonded contacts between amino acid residues at the interface of molecules in a multimer complex.

2.2. Binding free energy calculations.

The binding free energy and free energy decomposition of the two complex systems (S protein(Delta)-ACE2 and S protein(Delta-Plus)-ACE2) were calculated using the Molecular Mechanics Poisson-Boltzmann Surface Area (MM-PBSA) and Molecular Mechanics Generalized Born Surface Area (MM-GBSA) methods implemented in the AMBER 16 [43,44] package. For each complex system, 200 snapshots were selected from the last 10 ns of MD trajectories to calculate the relevant energies.

The equations (1-6) show the formulas for computing the BFE and their decomposed energetic components. The free energy difference between the bound state complex (Gcomplex) and the free state individuals of the receptor ($G_{receptor}$) and ligand (G_{ligand}). is represented by the total BFE (ΔG_{bind}). ΔG_{bind} can be decomposed into enthalpy (ΔH) and entropy ($T\Delta S$) according to the second law of thermodynamics. Here the enthalpies were calculated by Poisson–Boltzmann or Generalized-Born surface area continuum solvation (MM-PBSA/MM-GBSA) methods with a modest computational effort [45,46], and the entropy was estimated with normal mode (nmode) analysis [47]. After taking all the trajectories for MM-PBSA/MM-GBSA calculation, analysis was done for three components of the individual two complexes (i) ligand (S protein) (ii) receptor (ACE2) (iii) complex (S protein-ACE2). The approaches and protocols that we have considered in this study to estimate the binding free energy have been used in many recent *in-silico* studies [48-58].

BFE for the two complex systems was calculated using Eqn. (1):

$$\Delta G_{binding} = \Delta G_{complex} - [\Delta G_{receptor} + \Delta G_{ligand}] \quad (1)$$

where, $\Delta G_{binding}$ is the total binding free energy.

Thermodynamically,

$$\Delta G = \Delta H - T\Delta S \quad (2)$$

$$\Delta G = \Delta E_{MM} + \Delta G_{sol} - T\Delta S \quad (3)$$

$$\Delta E_{MM} = \Delta E_{int} + \Delta E_{ele} + \Delta E_{vdw} \quad (4)$$

$$\text{and } \Delta G_{sol} = \Delta G_{PB/GB} + \Delta G_{SURF} \quad 5)$$

$$\Delta G_{SURF} = E_{NP} + E_{dis} \quad (6)$$

Enthalpy calculations with MM-GBSA/PBSA: As shown in the Eqn. (1), for the two complex systems (S protein(Delta)-ACE2 and S protein(Delta-Plus)-ACE2), $\Delta G_{complex,}$ $\Delta G_{receptor,}$ and ΔG_{ligand} represent free energy contributions from S protein-ACE2 (complex), ACE2 (receptor), and S protein (ligand) respectively.

The enthalpy part is calculated by summation of change in molecular mechanics components in the gas phase (ΔE_{MM}) and the stabilization energy due to solvation (ΔG_{sol}) as shown in Eqn. (3). ΔE_{MM} represents the summation of internal energy (Δ_{Eint}) (bond, angle, and dihedral energies), electrostatic interaction (ΔE_{ele}), and Van der Waals interaction (ΔE_{vdw}). The solvation free energy (ΔG_{sol}) is divided into electrostatic solvation free energy ($\Delta G_{PB/GB}$) and the non-polar solvation free energy (ΔG_{SURF}) contribution eqn. (5). $\Delta G_{PB/GB}$ is calculated by Poisson-Boltzmann/Generalized-Boltzmann models and ΔG_{SURF}, the summation of non-polar contribution calculated by PB (E_{NP}) and dispersion energy (E_{dis}) using Solvent accessibility surface area (SASA).

Energy decompositions were performed to identify the important residues within the two complex systems. Here, only per-residue decomposition was included, which was used to

separate the energy contribution of each residue from the combination of Protein (ACE2) with the ligand (S protein) into three terms: van der Waals contribution (ΔE_{vdW}), electrostatic contribution (ΔE_{ele}), and solvation contribution ($\Delta G_{GB} + \Delta G_{SA}$).

3. Results and Discussion

In May 2021, India faced the world's most devastating coronavirus infection wave since the COVID-19 pandemic. The situation remained grim as the country records a staggering number of daily new infections at around four lakh. Despite the pain and suffering, scientists are working round the clock to identify the case's reason for such a 'tsunami'. And one of the main suspects remains the emergence of the more virulent mutant variants of the coronavirus. The new Delta-Plus variant from India carries the genetic code from two other mutations, T478K and L452R, which were already circulating globally. While both the mutations, traced across separate variants, are characteristic of their high infectivity and transmission rates, this is the first time they have merged, making them many times more infectious and deadly. Therefore, the mutations in this variant are expected to develop resistant resistance to antibodies generated by vaccination or natural infection. However, the impact of this newly reported variant has not yet been investigated. Here, we performed a computational study to investigate the effect of these mutations on the binding affinity of spike protein for ACE2 and its impact on transmission.

3.1. MD simulation of the Delta type and Delta-Plus structure of SARS-CoV-2 spike receptor-binding domain bound with ACE2.

The RBD domain of the wild-type strain of COVID-19 has been explored, and the structure of this SARS-CoV-2 spike receptor-binding domain bound with ACE2 protein has been reported. From the wild-type structure of the SARS-CoV-2 spike receptor-binding domain bound with ACE2, the 3-D structure of the Delta (L452R and T478K) and Delta-Plus (L452R, K417N, and T478K) of SARS-CoV-2 spike receptor-binding domain bound with ACE2 were obtained by punctual mutation. Then the energy minimization was carried out on both the complex structures using the steepest descents and conjugate gradient minimization. Both the complexes were then submitted to MD simulations with the AMBER program.

3.1.1. RMSD analysis.

To test the stability of the (S protein (Delta)-ACE2) and (S protein (Delta-Plus)-ACE2) complexes, 100 ns of MD simulation studies were carried out. The conformational snapshots of the (S protein (Delta)-ACE2) and (S protein (Delta-Plus)-ACE2) complexes during the course of 100 ns MD simulation time were depicted in Figure S1 and Figure S2. The average deviations in the atomic positions and the stability through the trajectory of 100 ns of the MD simulations, and the RMSD (root mean square deviation) values of the backbone atoms of the complexes along with the S protein (Apo form) were calculated (Figure 2). The RMSD of Delta type and the Delta-Plus complex appeared stable after 10 ns, revealing that good convergence was achieved for each system. Interestingly, we noticed the RMSD values of the Delta and Delta-Plus complexes to depict lower values and observed them be stable. The average of RMSD is 1.84 Å (± 0.12) for the Delta type complex structure and 1.42 Å (± 0.14) for the Delta-Plus complex structure, which could indicate greater stability of the mutated complex structure. We have also compared the average deviations in the atomic positions of the residues

exclusively at the mutation sites 452 and 478 (Figure 3). At residue indexes 452 and 478, we observed RMSD fluctuations to be relatively lower in the case of Delta and Delta-Plus complexes than in the Wild type complex. RMSD plot of the residue at position 417 in S protein (WILD)-ACE2 complex (black) and S protein (Delta-Plus)-ACE2 complex (green) was also analyzed (Figure 4) and found the RMSD fluctuations to be lower in Delta-Plus complex. We also noticed that the binding of ACE2 reduced the perturbation of S protein to a significant extent in both Delta and Delta-Plus complex systems.

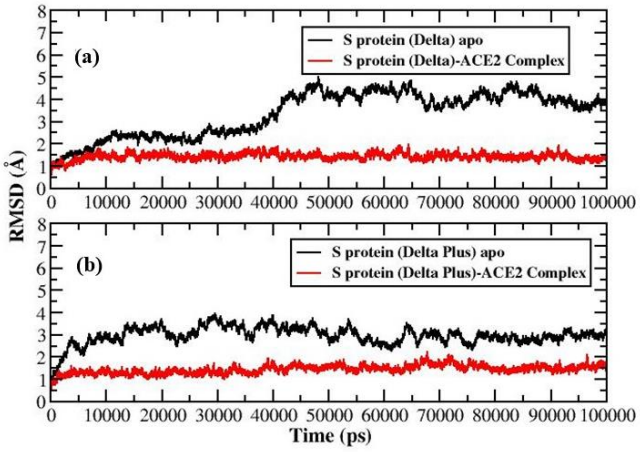

Figure 2. Backbone RMSD's for (a) S protein (Delta) Apo (black), S protein (Delta)-ACE2 complex (red); (b) S protein (Delta-Plus) Apo (black), S protein (Delta-Plus)-ACE2 complex (red).

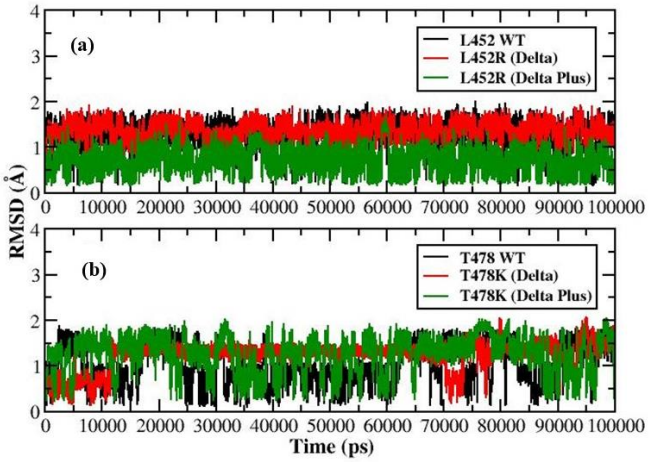

Figure 3. RMSD plot of the residue at position (a) 452 (b) 478 in S protein (WILD)-ACE2 complex (black), S protein (Delta)-ACE2 complex (red) and S protein (Delta-Plus)-ACE2 complex (green).

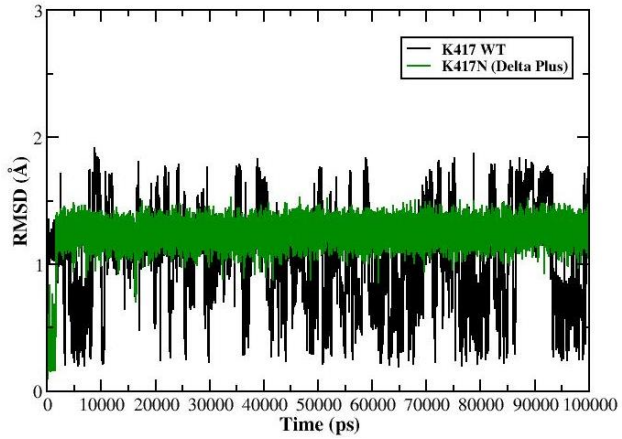

Figure 4. RMSD plot of the residue at position 417 in S protein (WILD)-ACE2 complex (black) and S protein (Delta-Plus)-ACE2 complex (green).

3.1.2. RMSF analysis.

We further explored the S protein flexibility by RMSF values of the Cα from the MD simulations of the (S protein (Delta)-ACE2) and (S protein (Delta-Plus)-ACE2) complexes (Figure 5). We observed significant differences in the flexibility of S protein in Delta and Delta-Plus complexes, particularly in the region in and around the mutation position (452, 478, and 417). The RMSF values of the Cα atoms of S protein in Delta and Delta-Plus complexes show relatively lower values than in Wild-type complexes. From Figure 5, it is more apparent that there is a significant reduction in structural fluctuations and increased stability in the case of Delta and Delta-Plus complexes.

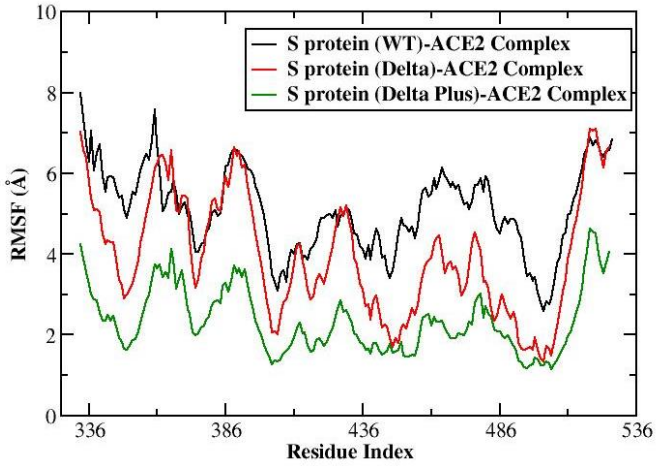

Figure 5. Backbone RMSF's for S protein in A) S protein (WILD)-ACE2 complex (black) B) S protein (Delta)-ACE2 complex (red) and C) S protein (Delta-Plus)-ACE2 complex (green).

3.1.3. Hydrogen bond analysis.

Additionally, we also calculated and plotted the number of intermolecular hydrogen bonds present in the (S protein (Delta)-ACE2) and (S protein(Delta-Plus)-ACE2) complexes (Figure 6), as these hydrogen bonds play a crucial role in conferring the stability to the protein complexes. The number of intermolecular hydrogen bonds was found to be higher in S protein (Delta-Plus)-ACE2 and S protein (Delta)-ACE2 complex. The list of intermolecular hydrogen bonds between the S protein (acceptor/donor) and ACE2 (donor/acceptor) during the last 20 ns of MD simulation of the Delta and Delta-Plus complexes was summarized in Table S1-S4.

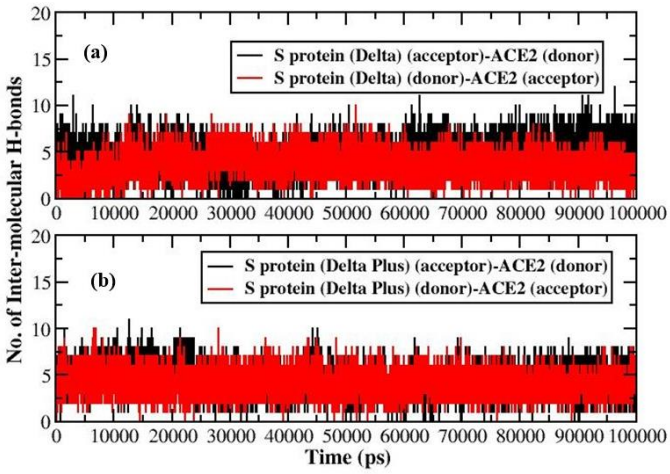

Figure 6. The number of intermolecular hydrogen bonds between S protein and ACE2 in (a) S protein (Delta)-ACE2 complex; (b) S protein (Delta-Plus)-ACE2 complex.

3.1.4. Determination of the interface interactions of the S protein (Delta)-ACE2) and (S protein(Delta-Plus)-ACE2 complexes.

An interface area is usually defined as a region where two sets of proteins come in contact with each other. Surface residues with large surface regions accessible to the solvent available usually characterize them. The interface statistics for the S protein(Delta)-ACE2 and S protein(Delta-Plus)-ACE2 complexes were obtained upon submitting the corresponding lowest energy complex structure extracted from the 100 ns MD simulation trajectory using RMSD clustering algorithm to the PDBsum server. The interface statistics for both complexes have been shown in Table 1.

Table 1. Interface statistics for the S protein(Delta)-ACE2 and S protein(Delta-Plus)-ACE2 complexes.

Complex system	Chain	No. of interface residues	Interface area (Å^2)	No. of salt bridges	No. of disulfide bonds	No. of hydrogen bonds	No. of non-bonded contacts
S protein (Delta)-ACE2	ACE2	19	916	2	-	15	149
	S protein (Delta)	20	921				
S protein (Delta Plus)-ACE2	ACE2	20	956	1	-	13	179
	S protein (Delta PLUS)	20	969				

The summarized intermolecular interactions between S protein and ACE2 of the Delta type and mutant complexes at the residue levels are shown in Figure 7. The detailed contributions of each interface residue stabilizing the Delta type and Delta-Plus complexes were summarized in Table S5 and S6. The total number of interface residues in the S protein(Delta)-ACE2 and S protein(Delta-Plus)-ACE2 complexes were found to be thirty-nine and forty, respectively. In the S protein(Delta)-ACE2 complex, the interface area for the S protein chain and the ACE2 chain involved in the interaction was observed to be 916 Å^2 and 921 Å^{2,} respectively, while in the S protein(Delta-Plus)-ACE2 complex, the S protein chain and the ACE2 chain involved in the interaction was observed to be 956 Å^2 and 969 Å^2 respectively. Both the Delta and Delta-Plus complexes were stabilized by molecular interactions like salt bridges, hydrogen bonding, and non-bonded contacts. From Table S5A, S5B, S5C, and S6A, S6B, and S6C, we can see the presence of one hundred and forty-nine non-bonded contacts, two salt bridges, and fifteen hydrogen bonds at the interface of S protein and ACE2 in the S protein(Delta)-ACE2 complex. However, at the interface of S protein and ACE2 in the S protein(Delta-Plus)-ACE2 complex, we observed one hundred and seventy-nine non-bonded contacts, one salt bridge, and thirteen hydrogen bonds. Overall, we see the number of intermolecular interactions and the interface area shared by S protein and ACE2 in forming complex is larger in the Delta-Plus complex than in the Delta-type complex. Therefore, the Delta-Plus complex's stability was higher than the Delta-type complex.

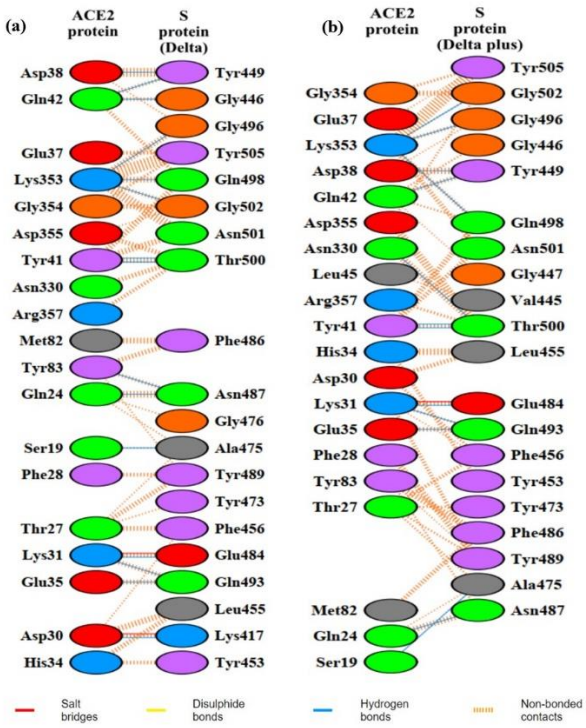

Figure 7. Intermolecular interactions at residue level between ACE2 and S protein in (a) S protein(Delta)-ACE2; (b) S protein(Delta-Plus)-ACE2 complexes.

3.1.5. Binding free energy and per residue energy decomposition (PRED) analysis.

Binding free energies of the S protein(Delta)-ACE2 and S protein(Delta-Plus)-ACE2 complexes were calculated from the last 10 ns of the MD simulation using the MM-PBSA/GBSA approach. The values represent only the relative binding free energy rather than absolute or total binding energy, as MM-PBSA/GBSA approach uses a continuum solvent approach to determine the binding free energies of a system. The binding free energies determined for the Delta and Delta-Plus complexes and the energy terms were summarized in Tables 2 and 3. From the Table 2 and 3, it can be seen that the S protein(Delta)-ACE2 complex (GB_{TOT} = -39.36 kcal mol^{-1}, ΔG_{bind} (GBSA)= -36.08 kcal mol^{-1}, PB_{TOT}= -17.52 kcal mol^{-1}, ΔG_{bind} (PBSA)= -14.24kcal mol^{-1}) was energetically more favourable than S protein(Delta-Plus)-ACE2 complex (GB_{TOT} = -36.83 kcal mol^{-1}, ΔG_{bind} (GBSA)= -33.19 kcal mol^{-1}, PB_{TOT}= --16.03 kcal mol^{-1}, ΔG_{bind} (PBSA)= -12.39 kcal mol^{-1}). Analyzing Tables 2 and 3, we observed that all the derived components for the BFE analysis contributed to the binding of S protein and ACE2 to form the S protein (Delta/Delta-Plus)-ACE2 complex.

Table 2. Binding free energies (kcal/mol) and its components of S protein(Delta)-ACE2 and S protein(Delta-Plus)-ACE2 complexes obtained using the MM-GBSA approach.

	$\Delta G_{(S\ protein(Delta)-ACE2)} - [\Delta G_{S\ protein(Delta)} + \Delta G_{ACE2}]$		$\Delta G_{(S\ protein(Delta-Plus)-ACE2)} - [\Delta G_{S\ protein(Delta-Plus)} + \Delta G_{ACE2}]$	
	Average	**std. dev. (±)**	**Average**	**std. dev. (±)**
VDW	-88.44	4.00	-91.08	4.36
ELE	-1082.33	15.46	-838.42	21.20
GB	1144.23	13.49	906.46	22.31
GBSUR	-12.82	0.34	-13.78	0.40
GAS	-1170.78	15.37	-929.50	22.50
GBSOL	1131.41	13.46	892.67	22.13
GBTOT	-39.36	4.97	-36.83	4.43
TΔS	-3.28	0.22	-3.64	1.44
ΔG_{bind}	**-36.08**		**-33.19**	

Table 3. Binding free energies (kcal/mol) and its components of S protein(Delta)-ACE2 and S protein(Delta-Plus)-ACE2 complexes obtained using MM-PBSA approach.

	$\Delta G_{(S\ protein(Delta)\text{-}ACE2)} - [\Delta G_{S\ protein(Delta)} + \Delta G_{ACE2}]$		$\Delta G_{(S\ protein(Delta\text{-}Plus)\text{-}ACE2)} - [\Delta G_{S\ protein(Delta\text{-}Plus)} + \Delta G_{ACE2}]$	
	Average	std. dev. (±)	Average	std. dev. (±)
VDW	-88.44	4.00	-91.08	4.36
ELE	-1082.33	15.46	-838.4252	21.2098
PB	1069.90	13.47	847.8183	21.6188
ENPOLAR	-64.76	2.20	-68.5126	1.9070
EDISPER	133.11	2.8868	134.1634	2.2987
GAS	-1170.78	15.3736	-929.5060	22.5022
PBSOL	1168.25	13.6110	913.4691	22.0820
PBTOT	-17.52	7.3209	-16.0368	6.5460
TΔS	-3.28	0.22	-3.64	1.44
ΔG_{bind}	**-14.24**		**-12.39**	

To gain insights into the contribution of the individual amino acid residues to the overall PPI of the S protein (Delta/Delta-Plus)-ACE2 complexes, PRED values were calculated. In this analysis, the total binding energy was decomposed into residues to identify key residues for ACE2 binding to S protein (Delta/Delta-Plus). Essential residues with the binding energy value below -1.00 kcal/mol were shown in Figures 8 and 9. The highest energy contributions for S protein (Delta) come from the residues GLN498, GLN493, LYS417, PHE486, TYR505, TYR449, TYR489, PHE456, LEU492, LEU455, and ASN487, while in S protein (Delta-Plus) come from the residues GLY496, ASN487, GLN498, GLN493, TYR505, PHE486, TYR449, TYR489, PHE456, ALA475, LEU492, and LEU455.

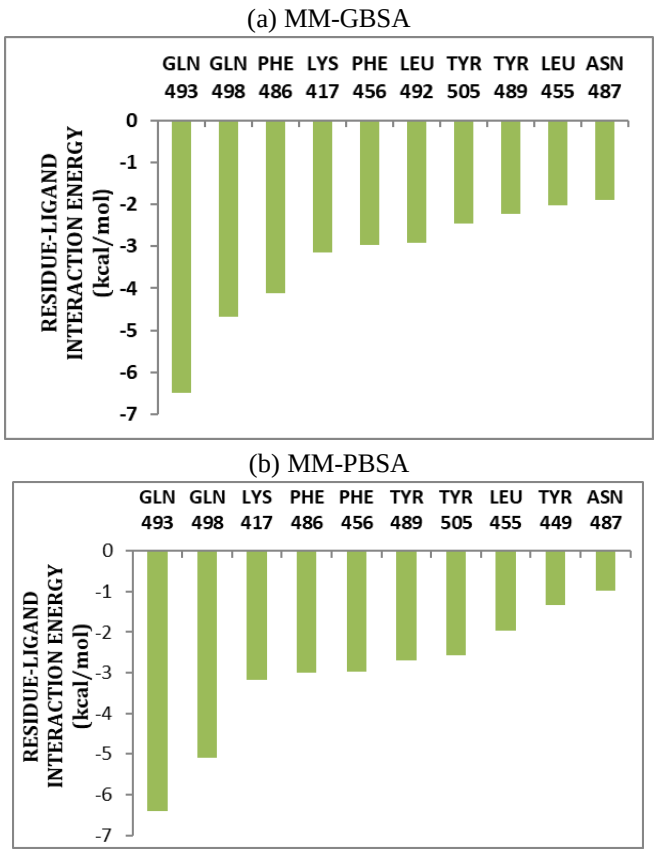

Figure 8. Decomposition of binding free energy (kcal/mol) on per residue basis for ACE2 binding to S protein (Delta) obtained using (a) MM-GBSA approach; (b) MM-PBSA approach.

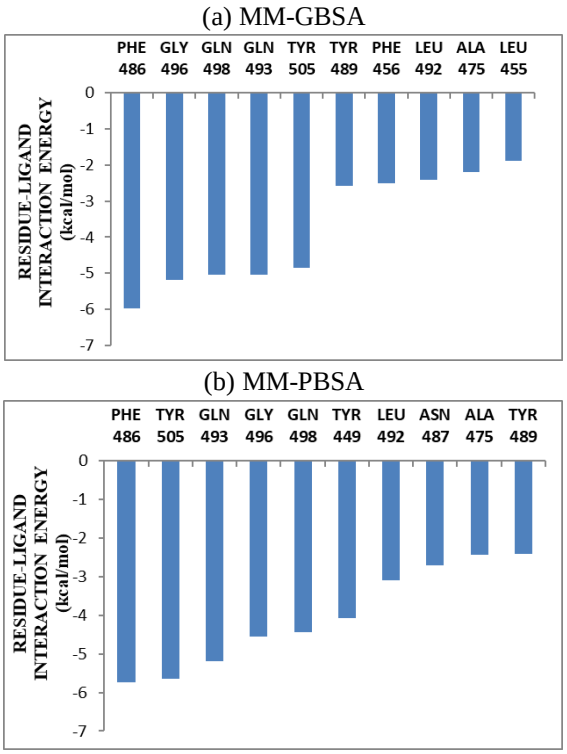

Figure 9. Decomposition of binding free energy (kcal/mol) on per residue basis for ACE2 binding to S protein (Delta-Plus) obtained using (a) MM-GBSA approach; (b) MM-PBSA approach.

4. Conclusions

The present study demonstrates the effect of Delta (L452R and T478K) and Delta-Plus (K417N, L452R, and T478K) on the binding of RBD of S protein of SARS-CoV-2 with the ACE2 by employing Molecular dynamics and other computational approaches. From the MD simulation of S protein(Delta)-ACE2 and S protein(Delta-Plus)-ACE2 complexes, we found significant structural changes in the spike protein near the point of mutations (K417N, L452R, and T478K). From the RMSD, RMSF, and PPI analysis, we found S protein(Delta-Plus)-ACE2 complex to have enhanced stability than the S protein(Delta)-ACE2 complex. The binding free energy was found to be subtly higher in the case of the S protein(Delta)-ACE2 than S protein(Delta-Plus)-ACE2 complex. The salient interactions we have reported in this study pertaining to the S protein and ACE2 in the Delta and the Delta-Plus complexes could be used to design novel inhibitors against the newly emerging coronavirus strains.

Funding

This research received no external funding.

Acknowledgments

The authors extend their deepest gratitude to Tezpur University and University Grants Commission, India, for the start-up grant.

Conflicts of Interest

The authors declare no conflict of interest.

References

1. Callaway, E. Delta coronavirus variant: scientists brace for impact. *Nature* **2021**, *595*, 17–18, https://doi.org/10.1038/d41586-021-01696-3.
2. Planas, D.; Veyer, D.; Baidaliuk, A. Reduced sensitivity of SARS-CoV-2 variant Delta to antibody neutralization. *Nature* **2021**, *596*, 276–280, https://doi.org/10.1038/s41586-021-03777-9.
3. Chowdhury, S.; Bappy, M.H. On the Delta Plus Variant of SARS-CoV-2. *European Journal of Medical and Health Sciences **2021***, 3, 52-55, https://doi.org/10.24018/ejmed.2021.3.6.1134
4. Bernal, J.L.; Andrews, N.; Gower, C.; Gallagher, E.; Simmons, R.; Thelwall, S.; Stowe, J.; Tessier, E.; Groves, N.; Dabrera, G.; Myers, R.; Campbell, C.; Amirthalingam, G.; Edmunds, M.; Zambon, M.; Brown, K. E.; Hopkins, S.; Chand, M.; Ramsay, M. Effectiveness of Covid-19 Vaccines against the B.1.617.2 (Delta) Variant. *The New England journal of medicine **2021***, 385, 585-594, http://doi.org/10.1056/NEJMoa2108891.
5. Salvatore, M.; Bhattacharyya, R.; Purkayastha, S.; Zimmermann, L.; Ray, D.; Hazra, A.; Kleinsasser, M.; Mellan, T.; Whittaker, Charlie.; Flaxman, Seth.; Bhatt, Samir.; Mishra, Swapnil.; Mukherjee, B. Resurgence of SARS-CoV-2 in India: Potential Role of theB.1.617.2 (Delta) Variant and Delayed Interventions. *medRvix* **2021**, https://doi.org/10.1101/2021.06.23.21259405.
6. Shu, Y.; McCauley, J. Gisaid: global initiative on sharing all influenza data—from vision to reality. *Euro Surveill* **2017**, *22*, https://doi.org/10.2807/1560-7917.ES.2017.22.13.30494.
7. Khateeb, J.; Li, Y.; Zhang, H. Emerging SARS-CoV-2 variants of concern and potential intervention approaches. *Crit. Care*, **2021**, *25*, https://doi.org/10.1186/s13054-021-03662-x.
8. Weisblum, Y. Escape from neutralizing antibodies by sars-cov-2 spike protein variants. *BioRxiv* **2020**, *12*, 556-561, https://doi.org/10.1101/2020.07.21.214759.
9. Verma, J.; Subbarao, N. Insilico study on the effect of SARS-CoV-2 RBD hotspot mutants' interaction with ACE2 to understand the binding affinity and stability. *Virology* **2021**, *561*, 107–116, https://doi.org/10.1016/j.virol.2021.06.009.
10. Teruel, N.; Mailhot, O.; Najmanovich, R.J. Modelling conformational state dynamics and its role on infection for SARS-CoV-2 Spike protein variants. *PLoS Comput. Biol.* **2021**, *17*, https://doi.org/10.1371/journal.pcbi.1009286.
11. Zhang, L.; Jackson, C.B.; Mou, H. SARS-CoV-2 spike-protein D614G mutation increases virion spike density and infectivity. *Nat. Commun*. **2020**, *11*, https://doi.org/10.1038/s41467-020-19808-4.
12. Volz, E.; Hill, V.; John, T. Evaluating the effects of SARS-CoV-2 spike mutation D614G on transmissibility and pathogenicity. *Cell* **2021**, *184*, 64–75, https://doi.org/10.1016/j.cell.2020.11.020.
13. Noh, J.Y.; Jeong, H.W.; Shin, E.C. SARS-CoV-2 mutations, vaccines, and immunity: implication of variants of concern. *Sig. Transduct. Target. Ther*. **2021**, *6*, https://doi.org/10.1038/s41392-021-00623-2.
14. Abdellatiif, M. H.; Ali, A.; Ali, A.; Hussien, M. Computational studies by molecular docking of some antiviral drugs with COVID-19 receptors are an approach to medication for COVID-19. *Open Chem.* **2021**, *19*, 245-264, https://doi.org/10.1515/chem-2021-0024.
15. Muralidharan, N.; Sakthivel, R.; Velmurugan, D.; Gromiha, M.M. Computational studies of drug repurposing and synergism of lopinavir, oseltamivir and ritonavir binding with SARS-CoV-2 protease against COVID-19. *J. Biomol. Struct. Dyn.* **2021,** *39*, 2673-2678, http://doi.org/10.1080/07391102.2020.1752802.
16. Mongia, A.; Saha, S.K.; Chouzenoux, E.; Majumdar, A. A computational approach to aid clinicians in selecting anti-viral drugs for COVID-19 trials. *Sci. Rep.* **2021**, *11*, https://doi.org/10.1038/s41598-021-88153-3.
17. Behera, S.K.; Vhora, N.; Contractor,D.; Shard, A.; Kumar, D.; Kalia, K.; Jain, A. Computational drug repurposing study elucidating simultaneous inhibition of entry and replication of novel corona virus by Grazoprevir. *Sci. Rep.* **2021**, *11*, https://doi.org/10.1038/s41598-021-86712-2.
18. Egieyeh, S.; Egieyeh, E.; Malan, S.; Christofells, A.; Fielding, B. Computational drug repurposing strategy predicted peptide-based drugs that can potentially inhibit the interaction of SARS-CoV-2 spike protein with its target (humanACE2). *PLoS ONE* **2021**, *16*, https://doi.org/10.1371/journal.pone.0245258.
19. Coban, M.A.; Morrison, J.; Maharjan, S.; Hernandez, M.D.H.; Li, W.; Zhang, Y.S.; Freeman, W.D.; Radisky, E.S.; Le, R.K.G.; Weisend, C.M.; Ebihara, H.; Caulfield, T.R. Attacking COVID-19 progression using multi-drug therapy for synergetic target engagement. *Biomolecules* **2021**, *11*, http://doi.org/10.3390/biom11060787.
20. Basak, S.C.; Kier, L.B. COVID-19 pandemic: how can computer-assisted methods help to rein in this global menace? *Curr. Comput.-Aided Drug Des.* **2021**, *17*, http://dx.doi.org/10.2174/1573409917012101121032l5.
21. Ibrahim, M.A.A.; Abdelrahman, A.H.M.; Allemailem, K.S.; Almatroudi, A.; Moustafa, M.F.; Hegazy, M.E.F. In silico evaluation of prospective anti-COVID-19 drug candidates as potential SARS-CoV-2 main protease inhibitors. *Protein J.* **2021**, *40*, 1–14, https://doi.org/10.1007/s10930-020-09945-6.
22. Singh, S.K.; Upadhyay, A.K.; Reddy, M.S. Screening of potent drug inhibitors against SARS-CoV-2 RNA polymerase: an in silico approach. *3 Biotech* **2021**, *11*, 1–13, http://doi.org/10.1007/s13205-020-02610-w.
23. Enmozhi, S.K.; Raja, K.; Sebastine, I.; Joseph, J. Andrographolide as a potential inhibitor of SARS-CoV-2 main protease: an in silico approach. *J. Biomol. Struct. Dyn.* **2021**, *39*, 3092–3098, http://doi.org/10.1080/07391102.2020.1760136.
24. Mahanta, S.; Chowdhury, P.; Gogoi, N.; Borah, D.; Kumar, R.; Chetia, D.; Borah, P.; Buragohain,A.K.; Gogoi, B. Potential anti-viral activity of approved repurposed drug against main protease of SARS-CoV-2:

an in silico based approach. *J. Biomol. Struct. Dyn.* **2021**, *39*, 3802–3811, http://doi.org/10.1080/07391102.2020.1768902.
25. Beura, S.; Chetti, P. In-silico strategies for probing chloroquine based inhibitors against SARS-CoV-2. *J. Biomol. Struct. Dyn*. **2021**, *39*, 3747–3759, http://doi.org/10.1080/07391102.2020.1772111.
26. Mittal, L.; Kumari, A.; Srivastava, M.; Singh, M.; Asthana, S. Identification of potential molecules against COVID-19 main protease through structure-guided virtual screening approach. *J. Biomol. Struct. Dyn*. **2021**, *39*, 3662–3680, http://doi.org/10.1080/07391102.2020.1768151.
27. Wahedi, H.M.; Ahmad, S.; Abbasi, S.W. Stilbene-based natural compounds as promising drug candidates against COVID-19. *J. Biomol. Struct. Dyn*. **2021**, *39*, 3225–3234, http://doi.org/10.1080/07391102.2020.1762743.
28. Selvaraj, C.; Dinesh, D.C.; Panwar, U.; Abhirami, R.; Boura, E.; Singh, S.K. Structure-based virtual screening and molecular dynamics simulation of SARS-CoV-2 guanine-N7 methyltransferase (nsp 14) for identifying antiviral inhibitors against COVID-19. *J. Biomol. Struct. Dyn.* **2021**, *39*, 4582-4593, http://doi.org/10.1080/07391102.2020.1778535.
29. Hassab, M.A.E.; Ibrahim, T.M.; Al-Rashood, S.T.; Alharbi, A.; Eskandrani, R.O.; Eldehna, W.M. In silico identification of novel SARS-COV-2 2-O-methyltransferase (nsp16) inhibitors: structure-based virtual screening, molecular dynamics simulation and MM-PBSA approaches. *J. Enzyme Inhib. Med. Chem.* **2021**, *36*, 727–736, http://doi.org/10.1080/14756366.2021.1885396.
30. Elmaaty, A.A.; Darwish, K.M.; Khattab, M.; Elhady, S.S.; Salah, M.; Hamed, M.I.A.; Al-Karmalawy, A.A.; Saleh, M.M. In a search for potential drug candidates for combating COVID-19: computational study revealed salvianolic acid B as a potential therapeutic targeting 3CLpro and spike proteins. *J. Biomol. Struct. Dyn*. **2021**, 1-28, https://doi.org/10.1080/07391102.2021.1918256.
31. Al-Karmalawy, A.; Alnajjar, R.; Dahab, M.; Metwaly, A.; Eissa, I.H. Molecular docking and dynamics simulations reveal the potential of anti-HCV drugs to inhibit COVID-19 main protease. *Pharm. Sci.* **2021**, *27*, S109-S121, https://doi.org/10.34172/PS.2021.3.
32. Sharanya, C.S.; Sabu, A.; Haridas, M. Potent phytochemicals against COVID-19 infection from phyto-materials used as antivirals in complementary medicines: a review. *Futur. J. Pharm. Sci.* **2021**, *7*, https://doi.org/10.1186/s43094-021-00259-7.
33. Nabi, F.; Ahmad, O.; Khan, Y.A.; Nabi, A.; Amiruddin, H.M.; Qais, F.A.; Masroor, A.; Hisamuddin, M.; Uversky, V.N.; Khan, R.H. Computational studies on phylogeny and drug designing using molecular simulations for COVID-19. *J. Biomol. Struct. Dyn.* **2021**, 1-10, http://doi.org/10.1080/07391102.2021.1947895.
34. Berman, H.M.; Westbrook, J.; Feng, Z.; Gilliland, G.; Bhat, T.N.; Weissig, H.; Shindyalov, I.N.; Bourne, P.E. The protein data bank. *Nucl. Acids Res.* **2000**, *28*, 235-242, https://doi.org/10.1107/97809553602060000722.
35. Pettersen, E.F.; Goddard, T.D.; Huang, C.C.; Couch, G.S.; Greenblatt, D.M.; Meng, E.C.; Ferrin, T.E. UCSF Chimera? A visualization system for exploratory research and analysis. *J. of Comp. Chem*. **2004**, *25*, 1605−1612, https://doi.org/10.1002/jcc.20084.
36. Salomon-Ferrer, R.; Gotz, A.W.; Poole, D.; Le Grand, S.; Walker, R.C. Routine microsecond molecular dynamics simulations with AMBER on GPUs. 2. Explicit solvent particle mesh Ewald. *J. Chem. Theory Comput*. **2013**, *9*, 3878-3888, https://doi.org/10.1021/ct400314y.
37. Jorgensen, W.L.; Chandrasekhar, J.; Madura, J.D.; Impey, R.W.; Klein, M.L. Comparison of simple potential functions for simulating liquid water. *J. Chem. Phys*. **1983**, *79*, 926−935, http://dx.doi.org/10.1063/1.445869.
38. Darden, T.; York, D.; Pedersen, L. Particle mesh Ewald: An N· log (N) method for Ewald sums in large systems. *J. Chem. Phys.* **1993**, *98*, 10089-10092.
39. Salomon-Ferrer, R.; Gotz, A.W.; Poole, D.; Le Grand, S.; Walker, R.C. Routine microsecond molecular dynamics simulations with AMBER on GPUs. 2. Explicit solvent particle mesh Ewald. *J. Chem. Theory Comput*. **2013**, *9*, 3878-3888, https://doi.org/10.1021/ct400314y.
40. Ryckaert, J.P.; Ciccotti, G.; Berendsen, H.J.C. Numerical integration of the cartesian equations of motion of a system with constraints: molecular dynamics of n-alkanes. *J. Comp. Phys.* **1977**, *23*, 327−341, https://doi.org/10.1016/0021-9991(77)90098-5.
41. Berendsen, H.J.; Postma, J.V.; Van, G.W.F.; Dinola, A.R.H.J.; Haak, J.R. Molecular dynamics with coupling to an external bath. *J. Chem. Phys.* **1984**, *81*, 3684-3690, https://doi.org/10.1063/1.448118.
42. Laskowski, R.A.; Hutchinson, E.G.; Michie, A.D.; Wallace, A.C.; Jones, M.L.; Thornton, J.M. PDBsum: a Web-based database of summaries and analyses of all PDB structures. *Trends Biochem. Sci*. **1997**, *22*, 488–490, https://doi.org/10.1016/s0968-0004(97)01140-7.
43. Chen, F.; Liu, H.; Sun, H.; Pan, P.; Li, Y.; Li, D.; Hou, T. Assessing the performance of the MM/PBSA and MM/GBSA methods. 6. Capability to predict protein–protein binding free energies and re-rank binding poses generated by protein–protein docking. *Phys. Chem. Chem. Phys.* **2016**, *18*, 22129-22139, http://doi.org/10.1261/rna.065896.118.
44. Genheden, S.; Ryde, U. The MM/PBSA and MM/GBSA methods to estimate ligand-binding affinities. *Expert Opin. Drug Discov.* **2015**, *10*, 449-461, http://doi.org/10.1517/17460441.2015.1032936.

45. Sun, H.; Duan, L.; Chen, F.; Liu, H.; Wang, Z.; Pan, P.; Zhu, F.; Zhang, J.Z.H.; Hou, T. Assessing the performance of MM/PBSA and MM/GBSA methods. 7. Entropy effects on the performance of end-point binding free energy calculation approaches. *Phys. Chem. Chem. Phys* **2018**, *20*, 14450-14460, https://doi.org/10.1039/c7cp07623a.
46. Wang, E.; Sun, H.; Wang, J.; Wang, Z.; Liu, H.; Zhang, J.Z.H.; Hou, T. End-Point Binding Free Energy Calculation with MM/PBSA and MM/GBSA: Strategies and Applications in Drug Design. *Chem. Rev.* **2019**, *119*, 9478-9508, https://doi.org/10.1021/acs.chemrev.9b00055.
47. Case, D.A. Normal mode analysis of protein dynamics. *Curr. Opin. Struct. Biol.* **1994**, *4*, 285-290, https://doi.org/10.1016/S0959-440X(94)90321-2.
48. Chen, J.; Yin, B.; Pang, L.; Wang, W.; Zhang, J.Z.; Zhu, T. Binding modes and conformational changes of FK506-binding protein 51 induced by inhibitor bindings: insight into molecular mechanisms based on multiple simulation technologies. *J. Bio. Struc. Dyn*. **2019**, *38*, 1-15, http://doi.org/10.1021/acs.jcim.0c01470.
49. Du, Q.; Qian, Y.; Yao, X.; Xue, W. Elucidating the tight-binding mechanism of two oral anticoagulants to factor Xa by using induced-fit docking and molecular dynamics simulation. *J. Bio. Struct. Dyn.* **2019**, 1-9, https://doi.org/10.1080/07391102.2019.1583605.
50. Eduardo, S.C.E.; Betancourt-Conde, I.; Hernandez-Campos, A.; Tellez-Valencia, A.; Castillo, R. In silico hit optimization toward AKT inhibition: fragment-based approach, molecular docking and molecular dynamics study. *J. Bio. Struc. Dyn.* **2019**, *37*, 4301-4311, http://doi.org/10.1080/07391102.2018.1546618.
51. Gao, J.; Wang, Y.; Chen, Q.; Yao, R. Integrating molecular dynamics simulation and molecular mechanics/generalized Born surface area calculation into pharmacophore modeling: a case study on the proviral integration site for Moloney murine leukemia virus (Pim)-1 kinase inhibitors. *J. Bio. Struc. Dyn*. **2019**, *38*, 1-8, http://doi.org/10.1080/07391102.2019.1571946.
52. Joshi, T.; Joshi, T.; Sharma, P.; Chandra, S.; Pande, V. Molecular docking and molecular dynamics simulation approach to screen natural compounds for inhibition of Xanthomonas oryzae pv. Oryzae by targeting Peptide Deformylase. *J. Bio. Struc. Dyn.* **2020**, *39*, 1-40, https://doi.org/10.1080/07391102.2020.1719200.
53. Sk, M.F.; Roy, R.; Kar, P. Exploring the potency of currently used drugs against HIV-1 protease of subtype D variant by using multiscale simulations. *J. Bio. Struct. Dyn.* **2020**, *130*, https://doi.org/10.1080/07391102.2020.1724196.
54. Sun, H.; Duan, L.; Chen, F.; Liu, H.; Wang, Z.; Pan, P.; Zhu, F.; Zhang, J.Z.H.; Hou, T. Assessing the performance of MM/PBSA and MM/GBSA methods. 7. Entropy effects on the performance of end-point binding free energy calculation approaches. *Phys. Chem. Chem. Phys.* **2018**, *20*, 14450-14460, https://doi.org/10.1039/C9CP01674K.
55. Tian, S.; Ji, C.; Zhang, J.Z. Molecular basis of SMAC–XIAP binding and the effect of electrostatic polarization. *J. Bio. Struc. Dyn*. **2020**, *39*, 1-26, https://doi.org/10.1080/07391102.2020.1713892.
56. Wan, Y.; Guan, S.; Qian, M.; Huang, H.; Han, F.; Wang, S.; Zhang, H. Structural basis of fullerene derivatives as novel potent inhibitors of protein acetylcholinesterase without catalytic active site interaction: insight into the inhibitory mechanism through molecular modeling studies. *J. Bio. Struc. Dyn*. **2019**, *38*, 410-425, http://doi.org/10.1080/07391102.2019.1576543.
57. Wang, E.; Sun, H.; Wang, J.; Wang, Z.; Liu, H.; Zhang, J.Z.H.; Hou, T. End-Point Binding Free Energy Calculation with MM/PBSA and MM/GBSA: Strategies and Applications in Drug Design. *Chem. Rev*. **2019**, *119*, 9478- 9508, https://doi.org/10.1021/acs.chemrev.9b00055.
58. Zhang, W.; Yang, F.; Ou, D.; Lin, G.; Huang, A.; Liu, N.; Li, P. Prediction, docking study and molecular simulation of 3D DNA aptamers to their targets of endocrine disrupting chemicals. *J. Bio. Struc. Dyn*. **2019**, *37*, 4274-4282, https://doi.org/10.1080/07391102.2018.1547222.

Supplementary Data

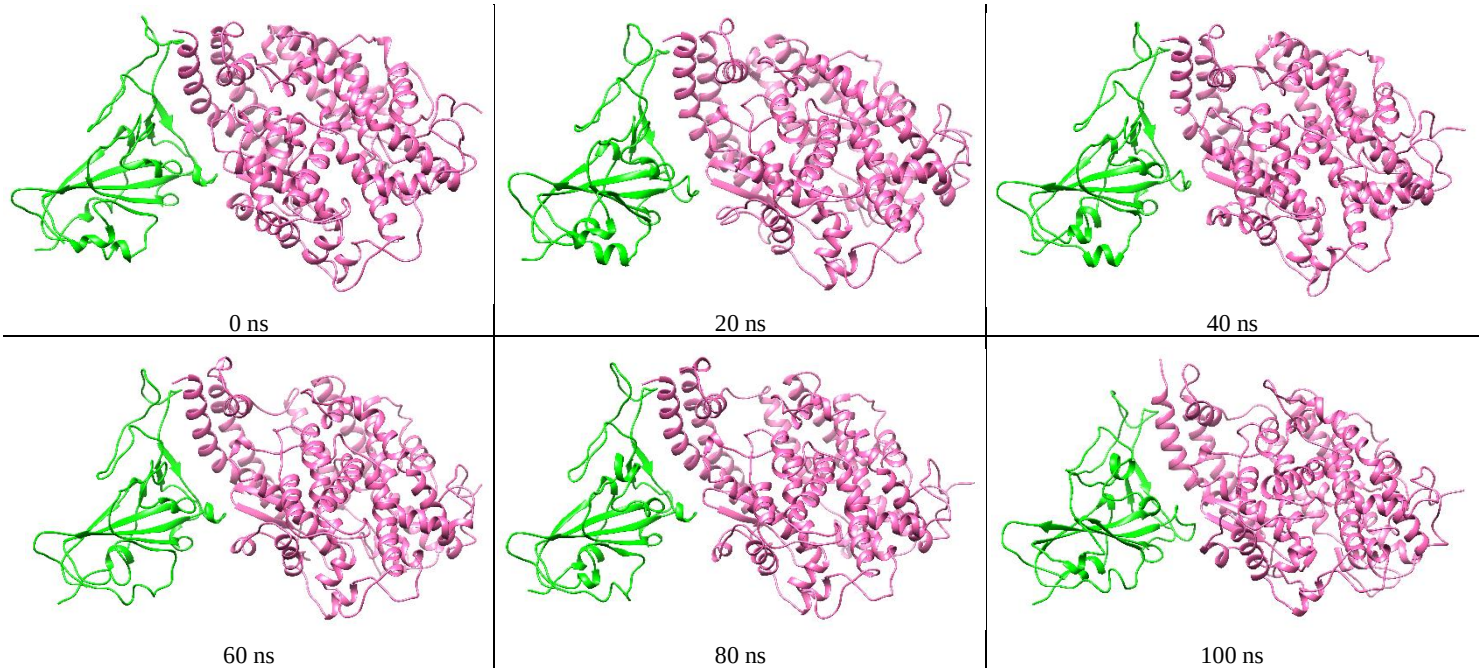

Figure S1. Snapshots of SARS-CoV-2 ACE2-Spike Protein (Delta variant) structures at discrete separation distance (in Å) between their center of mass.

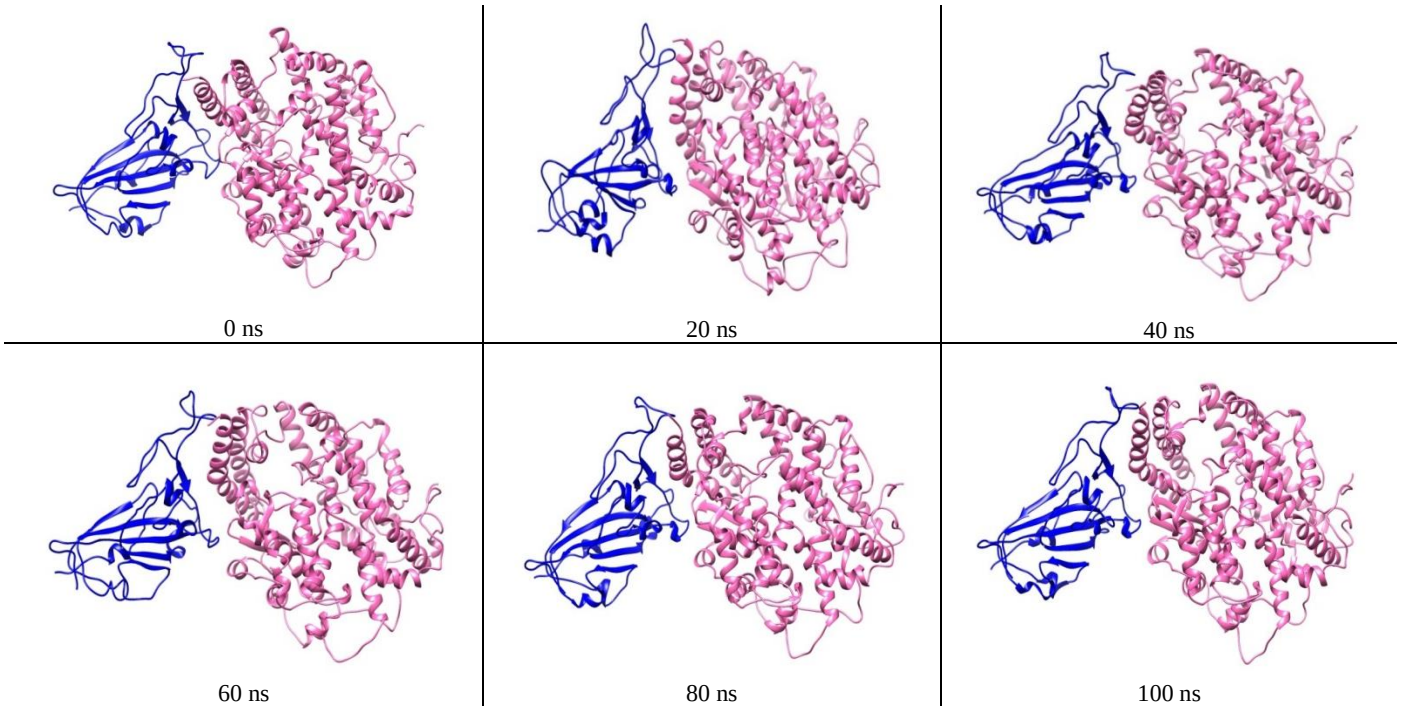

Figure S2. Snapshots of SARS-CoV-2 ACE2-Spike Protein (Delta-plus variant) structures at discrete separation distance (in Å) between their center of mass.

Table S1. Hydrogen bond analysis of S protein (DELTA)-ACE2 complex during the last 20 ns of MD simulation with S protein as acceptor and ACE2 as a donor.

#Acceptor	DonorH	Donor	Frac	AvgDist	AvgAng
GLN_498@OE1	GLN_42@HE21	GLN_42@NE2	0.5507	2.8653	162.2189
GLN_498@OE1	LYS_353@HZ2	LYS_353@NZ	0.3066	2.8136	159.1395
GLN_498@OE1	LYS_353@HZ1	LYS_353@NZ	0.2856	2.8066	156.3792
GLN_493@OE1	LYS_31@HZ1	LYS_31@NZ	0.1892	2.7974	158.1674
GLN_493@OE1	LYS_31@HZ2	LYS_31@NZ	0.1814	2.8015	158.5917
GLN_498@OE1	LYS_353@HZ3	LYS_353@NZ	0.1814	2.8075	156.0259
ALA_475@O	GLN_24@HE22	GLN_24@NE2	0.1598	2.8663	156.5649

#Acceptor	DonorH	Donor	Frac	AvgDist	AvgAng
GLN_493@OE1	LYS_31@HZ3	LYS_31@NZ	0.1472	2.8018	158.6927
ASN_501@OD1	LYS_353@HZ3	LYS_353@NZ	0.1373	2.8063	149.3355
ALA_475@O	SER_19@H2	SER_19@N	0.0741	2.8471	153.6287
TYR_489@OH	TYR_83@HH	TYR_83@OH	0.0725	2.8337	155.5629
ALA_475@O	SER_19@H3	SER_19@N	0.0704	2.8454	153.7257
ASN_501@OD1	LYS_353@HZ2	LYS_353@NZ	0.0684	2.8117	150.3018
LEU_492@O	LYS_31@HZ3	LYS_31@NZ	0.0641	2.8284	151.3374
GLY_502@HA3	GLY_354@HA3	GLY_354@CA	0.0593	2.9211	141.7867
GLU_484@OE1	LYS_31@HZ1	LYS_31@NZ	0.0575	2.7989	153.0558
LEU_492@O	LYS_31@HZ2	LYS_31@NZ	0.0559	2.8233	150.5004
LEU_492@O	LYS_31@HZ1	LYS_31@NZ	0.0556	2.8285	151.0206
ALA_475@O	SER_19@H1	SER_19@N	0.0553	2.8421	153.8468
ALA_475@O	SER_19@HG	SER_19@OG	0.0476	2.713	161.3645
GLY_496@O	LYS_353@HZ3	LYS_353@NZ	0.0454	2.8587	153.6011
PHE_490@O	LYS_31@HZ2	LYS_31@NZ	0.0439	2.855	152.2969
GLU_484@OE1	LYS_31@HZ2	LYS_31@NZ	0.0407	2.7942	151.9281
GLU_484@OE1	LYS_31@HZ3	LYS_31@NZ	0.0394	2.8022	152.7312
PHE_490@O	LYS_31@HZ3	LYS_31@NZ	0.0333	2.8631	153.6305
TYR_489@HE1	PHE_28@HB2	PHE_28@CB	0.0276	2.9389	139.9999
GLU_484@OE2	LYS_31@HZ1	LYS_31@NZ	0.0271	2.8381	151.5963
GLY_496@O	LYS_353@HZ2	LYS_353@NZ	0.0248	2.8564	154.3297
GLU_484@OE2	LYS_31@HZ2	LYS_31@NZ	0.0241	2.8329	152.6549
GLN_493@HE21	GLU_35@HB2	GLU_35@CB	0.023	2.871	146.8194
GLU_484@OE2	LYS_31@HZ3	LYS_31@NZ	0.0182	2.8353	152.8463
TYR_489@HH	PHE_28@HB2	PHE_28@CB	0.0182	2.8842	151.9685
THR_500@O	ASN_330@HD21	ASN_330@ND2	0.0153	2.8748	146.8897
PHE_490@O	LYS_31@HZ1	LYS_31@NZ	0.0152	2.8769	151.5013
THR_500@HG1	ARG_357@HH21	ARG_357@NH2	0.0132	2.8624	139.8828
PHE_490@HB3	LYS_31@HE3	LYS_31@CE	0.0132	2.8944	144.6722
GLY_496@O	LYS_353@HZ1	LYS_353@NZ	0.0126	2.873	154.5785
PHE_490@H	LYS_31@HE3	LYS_31@CE	0.0112	2.902	152.8467
ASN_501@OD1	LYS_353@HZ1	LYS_353@NZ	0.0088	2.8302	150.9196
PHE_490@HB3	LYS_31@HE2	LYS_31@CE	0.0082	2.9014	145.6414
TYR_489@HH	LEU_79@HD21	LEU_79@CD2	0.0078	2.8133	148.1638
TYR_449@HH	GLN_42@HE22	GLN_42@NE2	0.007	2.8976	142.1551
TYR_489@HH	LEU_79@HD22	LEU_79@CD2	0.007	2.8214	148.9876
TYR_449@OH	GLN_42@HE22	GLN_42@NE2	0.0069	2.9052	150.3965
THR_500@HG1	TYR_41@HH	TYR_41@OH	0.0064	2.8204	141.0035
LEU_455@HD13	HIE_34@HE2	HIE_34@NE2	0.0049	2.8313	143.7435
ASN_501@OD1	LYS_353@HE3	LYS_353@CE	0.0049	2.9609	141.7058
PHE_486@HE2	TYR_83@HA	TYR_83@CA	0.0046	2.9407	141.6148
ALA_475@HB2	GLN_24@HG2	GLN_24@CG	0.0044	2.9449	140.898
ALA_475@HB3	GLN_24@HG2	GLN_24@CG	0.0042	2.9494	141.0908
PHE_456@HZ	LYS_31@HB2	LYS_31@CB	0.0041	2.9549	144.864
LEU_455@HD11	HIE_34@HE2	HIE_34@NE2	0.004	2.8474	142.8438
ALA_475@HB1	GLN_24@HG2	GLN_24@CG	0.0038	2.947	140.6587
PHE_456@HE2	LYS_31@HB2	LYS_31@CB	0.0036	2.9536	143.1534
TYR_489@HH	LEU_79@HD23	LEU_79@CD2	0.0034	2.8138	147.8788
LEU_455@HD12	HIE_34@HE2	HIE_34@NE2	0.0032	2.8212	143.5735
PHE_456@HE2	LYS_31@HD3	LYS_31@CD	0.0032	2.9566	142.8444
THR_500@HG21	ARG_357@HH22	ARG_357@NH2	0.0032	2.8795	143.057
LEU_455@HD23	LYS_31@HA	LYS_31@CA	0.0032	2.9363	140.4649
ALA_475@HB1	SER_19@HB2	SER_19@CB	0.0029	2.9283	142.2612
THR_500@HG23	ARG_357@HH22	ARG_357@NH2	0.0029	2.8925	142.8801
ASN_501@HD21	LYS_353@HD2	LYS_353@CD	0.0029	2.9057	150.3464
THR_500@HG22	ARG_357@HH22	ARG_357@NH2	0.0028	2.8813	143.328
THR_500@HB	ASN_330@HD21	ASN_330@ND2	0.0027	2.7502	145.6902
TYR_489@HH	LEU_79@HD11	LEU_79@CD1	0.0026	2.8787	147.7328
PHE_456@CZ	THR_27@HG1	THR_27@OG1	0.0024	2.921	151.1962
ALA_475@HB3	SER_19@HB2	SER_19@CB	0.0024	2.9377	143.188
PHE_490@HD2	LYS_31@HZ1	LYS_31@NZ	0.0024	2.8493	143.5614
GLN_493@HE21	GLU_35@HG2	GLU_35@CG	0.0024	2.7856	144.3027
PHE_456@HE2	LYS_31@HD2	LYS_31@CD	0.0024	2.9492	143.5004
PHE_486@HA	LEU_79@HD13	LEU_79@CD1	0.0024	2.9492	142.0671
PHE_490@H	LYS_31@HE2	LYS_31@CE	0.0022	2.9273	154.5146
GLN_493@HE22	HIE_34@HB3	HIE_34@CB	0.0022	2.9317	141.8993

#Acceptor	DonorH	Donor	Frac	AvgDist	AvgAng
LEU_455@HD21	LYS_31@HA	LYS_31@CA	0.0019	2.9429	140.1966
PHE_490@HD2	LYS_31@HZ3	LYS_31@NZ	0.0019	2.9008	144.4712
ASN_501@HD21	LYS_353@HZ2	LYS_353@NZ	0.0019	2.9295	146.8572
GLY_502@H	GLY_354@HA3	GLY_354@CA	0.0019	2.8417	141.65
LEU_455@HD21	HIE_34@HD2	HIE_34@CD2	0.0019	2.9356	142.5781
ALA_475@HB2	SER_19@HB2	SER_19@CB	0.0018	2.9193	140.7925
ALA_475@HB1	GLN_24@HA	GLN_24@CA	0.0018	2.9583	143.8502
GLU_484@OE1	LYS_31@HE2	LYS_31@CE	0.0018	2.9425	140.0895
PHE_486@HA	LEU_79@HD11	LEU_79@CD1	0.0018	2.9515	143.2077
ALA_475@HB2	GLN_24@HA	GLN_24@CA	0.0017	2.9515	139.9443
PHE_486@HA	LEU_79@HD12	LEU_79@CD1	0.0017	2.9528	143.1182
PHE_490@HD2	LYS_31@HZ2	LYS_31@NZ	0.0017	2.8856	142.4585
GLY_446@O	GLN_42@HE21	GLN_42@NE2	0.0016	2.873	145.4339
LEU_455@HD22	LYS_31@HE2	LYS_31@CE	0.0016	2.9325	147.505
PHE_486@HE1	TYR_83@HA	TYR_83@CA	0.0016	2.9378	140.7391
TYR_489@HH	LEU_79@HD12	LEU_79@CD1	0.0016	2.8596	146.9403
GLN_493@HE21	GLU_35@HA	GLU_35@CA	0.0016	2.9008	141.0137
GLN_498@HE21	TYR_41@HE2	TYR_41@CE2	0.0016	2.8841	144.9482
LEU_455@HD23	HIE_34@HD2	HIE_34@CD2	0.0016	2.9395	143.4051
TYR_473@HE2	THR_27@HG23	THR_27@CG2	0.0016	2.9528	139.8288
PHE_486@HB2	MET_82@HG2	MET_82@CG	0.0016	2.955	145.9443
ALA_475@HB2	GLN_24@HE22	GLN_24@NE2	0.0015	2.7936	143.5724
GLU_484@OE1	LYS_31@HE3	LYS_31@CE	0.0015	2.9561	138.782
GLN_498@HB3	LYS_353@HZ3	LYS_353@NZ	0.0015	2.8963	139.1842
GLY_496@HA3	LYS_353@HE2	LYS_353@CE	0.0015	2.8712	150.8568
PHE_456@HZ	ASP_30@HB3	ASP_30@CB	0.0014	2.9525	144.5573
ALA_475@HB3	GLN_24@HA	GLN_24@CA	0.0014	2.9519	140.9137
LEU_455@HD21	LYS_31@HD3	LYS_31@CD	0.0014	2.9597	138.9274
LEU_455@HD22	LYS_31@HA	LYS_31@CA	0.0014	2.9292	140.7335
LEU_455@HD22	LYS_31@HD3	LYS_31@CD	0.0014	2.9579	140.9739
ALA_475@HB3	GLN_24@HE22	GLN_24@NE2	0.0014	2.8356	148.1018
LEU_455@HD22	HIE_34@HD2	HIE_34@CD2	0.0013	2.9519	141.7248
PHE_456@HE2	LYS_31@HE2	LYS_31@CE	0.0012	2.8783	143.5895
GLY_476@HA2	SER_19@HB3	SER_19@CB	0.0012	2.9284	142.1802
ASN_487@OD1	GLN_24@HE22	GLN_24@NE2	0.0012	2.8957	157.0248
THR_500@HG21	ASN_330@HD21	ASN_330@ND2	0.0012	2.8529	143.7543
TYR_473@HE2	THR_27@HG21	THR_27@CG2	0.0011	2.9516	140.743
ASN_487@HD21	GLN_24@HG2	GLN_24@CG	0.0011	2.9117	139.4355
GLN_493@HE21	GLU_35@HG3	GLU_35@CG	0.0011	2.8342	147.0016
GLN_498@HE21	GLN_42@HE21	GLN_42@NE2	0.0011	2.8599	140.3977
TYR_473@HE2	THR_27@HG22	THR_27@CG2	0.0011	2.9382	139.9857
ASN_487@HD21	GLN_24@HE22	GLN_24@NE2	0.0011	2.9392	145.43
LEU_455@HD21	LYS_31@HE2	LYS_31@CE	0.001	2.9177	149.7512
LEU_455@HD23	LYS_31@HD3	LYS_31@CD	0.001	2.9521	140.6354
PHE_490@HB3	LYS_31@HZ3	LYS_31@NZ	0.001	2.8897	142.9276
LEU_455@HD23	LYS_31@HE2	LYS_31@CE	0.001	2.9309	148.3557
ASN_501@HD21	LYS_353@HZ3	LYS_353@NZ	0.001	2.9192	151.641
PHE_490@O	LYS_31@HE3	LYS_31@CE	0.0009	2.9727	142.5201
TYR_489@HH	LEU_79@HD13	LEU_79@CD1	0.0008	2.8866	152.276
THR_500@HG23	ASN_330@HD21	ASN_330@ND2	0.0008	2.8638	145.4477
ASN_501@HD21	LYS_353@HZ1	LYS_353@NZ	0.0008	2.933	149.9917
TYR_489@HE1	PHE_28@HD1	PHE_28@CD1	0.0008	2.9457	139.0899
GLY_485@O	TYR_83@HH	TYR_83@OH	0.0008	2.8809	146.6101
TYR_489@HB3	LYS_31@HG2	LYS_31@CG	0.0008	2.9474	139.2828
TYR_489@HE1	PHE_28@HA	PHE_28@CA	0.0008	2.9509	138.0567
LEU_455@HD12	HIE_34@HD2	HIE_34@CD2	0.0007	2.9469	140.138
LEU_455@HD13	HIE_34@HD2	HIE_34@CD2	0.0007	2.9434	139.6838
PHE_456@HE1	THR_27@HG22	THR_27@CG2	0.0007	2.962	139.8631
ASN_487@HB2	GLN_24@HE22	GLN_24@NE2	0.0007	2.786	149.7811
GLN_498@HB3	LYS_353@HZ2	LYS_353@NZ	0.0007	2.9155	138.583
GLN_498@HE22	LYS_353@HE3	LYS_353@CE	0.0007	2.9365	147.7473
ALA_475@HB1	GLN_24@HE22	GLN_24@NE2	0.0006	2.9014	145.7651
THR_500@O	TYR_41@HH	TYR_41@OH	0.0006	2.8113	140.1306
LEU_455@HD22	LYS_31@HG2	LYS_31@CG	0.0006	2.9428	140.4576
TYR_489@HB3	LYS_31@HE3	LYS_31@CE	0.0006	2.9394	145.2765
GLN_493@HE21	LYS_31@HZ2	LYS_31@NZ	0.0006	2.8898	153.1135

#Acceptor	DonorH	Donor	Frac	AvgDist	AvgAng
GLN_493@HE22	HIE_34@HB2	HIE_34@CB	0.0006	2.8065	141.3884
GLN_493@HE22	LYS_31@HE2	LYS_31@CE	0.0006	2.9239	151.8607
ASN_501@HD21	LYS_353@HD3	LYS_353@CD	0.0006	2.8772	147.4528
PHE_456@CE1	THR_27@HG1	THR_27@OG1	0.0006	2.9375	160.6948
TYR_489@HE1	LEU_79@HD22	LEU_79@CD2	0.0006	2.9752	142.4893
PHE_490@HB3	LYS_31@HZ1	LYS_31@NZ	0.0006	2.8031	141.1282
GLN_493@OE1	LYS_31@HE2	LYS_31@CE	0.0006	2.9534	138.2307
GLN_493@HE21	LYS_31@HE2	LYS_31@CE	0.0006	2.9199	146.5394
THR_500@HG22	ASN_330@HD21	ASN_330@ND2	0.0006	2.8776	142.7676
PHE_486@HZ	ILE_21@HG23	ILE_21@CG2	0.0005	2.9424	138.4986
TYR_489@HE1	LEU_79@HD21	LEU_79@CD2	0.0005	2.9518	140.8133
GLN_493@HG2	HIE_34@HB3	HIE_34@CB	0.0005	2.9392	140.5177
TYR_505@HE2	GLU_37@HG2	GLU_37@CG	0.0005	2.9595	140.371
PHE_456@HE1	ASP_30@HB3	ASP_30@CB	0.0004	2.9576	141.3306
PHE_456@HE1	THR_27@HG23	THR_27@CG2	0.0004	2.969	141.7486
PHE_456@CE2	THR_27@HG1	THR_27@OG1	0.0004	2.9547	148.157
ALA_475@HB3	GLN_24@HG3	GLN_24@CG	0.0004	2.956	147.9242
PHE_486@HA	LEU_79@HD21	LEU_79@CD2	0.0004	2.9512	147.8361
PHE_486@HZ	ILE_21@HG22	ILE_21@CG2	0.0004	2.965	138.8099
PHE_486@HD2	MET_82@HB3	MET_82@CB	0.0004	2.942	139.2249
ASN_487@ND2	GLN_24@HE22	GLN_24@NE2	0.0004	2.9169	147.7641
TYR_489@HD2	THR_27@HG22	THR_27@CG2	0.0004	2.9406	140.0117
GLN_493@HE21	LYS_31@HZ1	LYS_31@NZ	0.0004	2.9202	144.0494
GLY_496@HA3	LYS_353@HZ3	LYS_353@NZ	0.0004	2.8386	143.0141
TYR_449@HH	LYS_353@HZ1	LYS_353@NZ	0.0004	2.9432	142.7487
LEU_455@HD11	HIE_34@HD2	HIE_34@CD2	0.0004	2.9607	141.7211
PHE_456@HE1	THR_27@HG21	THR_27@CG2	0.0004	2.9643	142.209
GLY_485@HA2	LEU_79@HD22	LEU_79@CD2	0.0004	2.9454	142.5768
PHE_486@HB2	MET_82@HB3	MET_82@CB	0.0004	2.9277	141.3228
TYR_489@HE1	LEU_79@HD23	LEU_79@CD2	0.0004	2.9504	142.1387
THR_500@HA	ASN_330@HD21	ASN_330@ND2	0.0004	2.9485	146.0151
TYR_449@HH	LYS_353@HZ2	LYS_353@NZ	0.0003	2.8888	140.3075
ALA_475@HB1	GLN_24@HG3	GLN_24@CG	0.0003	2.9475	143.1565
GLY_476@HA2	SER_19@H2	SER_19@N	0.0003	2.8753	142.7028
GLY_476@HA2	SER_19@H1	SER_19@N	0.0003	2.9444	137.9828
PHE_486@HB2	LEU_79@HD13	LEU_79@CD1	0.0003	2.9156	137.6539
PHE_486@HZ	ILE_21@HG21	ILE_21@CG2	0.0003	2.9188	141.3263
TYR_489@HD1	LYS_31@HG2	LYS_31@CG	0.0003	2.9687	145.2105
GLY_496@HA3	LYS_353@HE3	LYS_353@CE	0.0003	2.9168	143.9337
GLN_498@HB3	LYS_353@HZ1	LYS_353@NZ	0.0003	2.9014	142.2068
PHE_456@HZ	ASP_30@HB2	ASP_30@CB	0.0003	2.9614	138.0887
PHE_456@HZ	THR_27@HG1	THR_27@OG1	0.0003	2.9082	155.4678
ALA_475@HB2	SER_19@HB3	SER_19@CB	0.0003	2.9096	140.3182
ALA_475@HB2	SER_19@HG	SER_19@OG	0.0003	2.8345	144.2649
ALA_475@HB3	SER_19@HG	SER_19@OG	0.0003	2.8822	142.3035
GLY_485@HA2	LEU_79@HD23	LEU_79@CD2	0.0003	2.9203	140.5166
PHE_486@HB2	LEU_79@HD12	LEU_79@CD1	0.0003	2.9372	140.7241
PHE_486@HB2	MET_82@HG3	MET_82@CG	0.0003	2.9541	143.3194
PHE_486@HD1	MET_82@HB3	MET_82@CB	0.0003	2.9371	140.6265
PHE_486@HE2	ILE_21@HD11	ILE_21@CD1	0.0003	2.9451	139.351
ASN_487@HD22	GLN_24@HE22	GLN_24@NE2	0.0003	2.8788	146.664
TYR_489@HB3	LYS_31@HG3	LYS_31@CG	0.0003	2.9562	144.4624
TYR_489@HD2	THR_27@HG23	THR_27@CG2	0.0003	2.9593	138.975
PHE_490@HB3	LYS_31@HZ2	LYS_31@NZ	0.0003	2.8763	139.6384
PHE_490@O	LYS_31@HE2	LYS_31@CE	0.0003	2.9469	139.3232
GLN_493@HE22	LYS_31@HG3	LYS_31@CG	0.0003	2.8641	154.0917
GLN_498@HE21	LEU_45@HD22	LEU_45@CD2	0.0003	2.9514	138.2983
LEU_455@HD22	ASP_30@HB3	ASP_30@CB	0.0003	2.9566	143.1572
LEU_455@HD23	HIE_34@HE2	HIE_34@NE2	0.0003	2.8636	143.5369
ALA_475@HB3	SER_19@HB3	SER_19@CB	0.0003	2.9273	140.0013
GLY_476@HA3	SER_19@HB3	SER_19@CB	0.0003	2.9539	139.7851
GLY_485@HA2	LEU_79@HD21	LEU_79@CD2	0.0003	2.9411	141.2975
PHE_486@HD1	MET_82@HB2	MET_82@CB	0.0003	2.9721	139.5955
PHE_486@HD2	MET_82@HB2	MET_82@CB	0.0003	2.9702	135.6257
TYR_489@HD1	LYS_31@HE3	LYS_31@CE	0.0003	2.9059	150.8524
LEU_492@O	LYS_31@HE2	LYS_31@CE	0.0003	2.9624	139.1642

#Acceptor	DonorH	Donor	Frac	AvgDist	AvgAng
THR_500@HG1	TYR_41@HE2	TYR_41@CE2	0.0003	2.9496	142.8663
TYR_505@HD1	GLY_354@HA3	GLY_354@CA	0.0003	2.9597	139.6307
LYS_417@HZ3	HIE_34@HE2	HIE_34@NE2	0.0002	2.8775	146.6135
TYR_453@HH	HIE_34@HB3	HIE_34@CB	0.0002	2.9444	141.7322
PHE_456@HE1	THR_27@HG1	THR_27@OG1	0.0002	2.8538	148.0666
GLY_485@HA2	LEU_79@HD12	LEU_79@CD1	0.0002	2.9232	149.8135
GLY_485@HA2	LEU_79@HD11	LEU_79@CD1	0.0002	2.9516	147.1025
PHE_486@HB2	MET_82@HE1	MET_82@CE	0.0002	2.9489	138.3771
PHE_486@HE2	ILE_21@HD12	ILE_21@CD1	0.0002	2.9708	142.8261
PHE_486@HD2	MET_82@HG3	MET_82@CG	0.0002	2.9551	143.2457
TYR_489@HH	GLN_24@HB3	GLN_24@CB	0.0002	2.9131	138.655
TYR_489@HH	PHE_28@HD1	PHE_28@CD1	0.0002	2.8927	146.3763
TYR_489@HH	THR_27@HB	THR_27@CB	0.0002	2.9332	158.2099
GLN_493@HE22	GLU_35@HG3	GLU_35@CG	0.0002	2.9004	141.1356
GLN_498@HE21	LEU_45@HD23	LEU_45@CD2	0.0002	2.8956	146.6705
GLN_498@HE22	LYS_353@HD2	LYS_353@CD	0.0002	2.9057	152.7506
THR_500@HB	ARG_357@HH21	ARG_357@NH2	0.0002	2.8675	138.1067
TYR_505@HH	ALA_387@HA	ALA_387@CA	0.0002	2.9803	144.4676
LYS_417@HE2	HIE_34@HE2	HIE_34@NE2	0.0001	2.8379	149.2014
LYS_417@HZ2	HIE_34@HE2	HIE_34@NE2	0.0001	2.887	143.3963
GLY_446@HA2	GLN_42@HE21	GLN_42@NE2	0.0001	2.8528	146.3474
LEU_455@HD21	ASP_30@HB3	ASP_30@CB	0.0001	2.9812	141.7711
LEU_455@HD21	LYS_31@HB2	LYS_31@CB	0.0001	2.9707	141.9962
LEU_455@HD22	LYS_31@HD2	LYS_31@CD	0.0001	2.9822	137.826
LEU_455@HD22	HIE_34@HE2	HIE_34@NE2	0.0001	2.834	142.8453
LEU_455@HD22	LYS_31@HB2	LYS_31@CB	0.0001	2.9694	138.3985
LEU_455@HD23	HIE_34@HB2	HIE_34@CB	0.0001	2.9837	137.0322
PHE_456@HZ	THR_27@HA	THR_27@CA	0.0001	2.8723	143.1241
PHE_456@HZ	THR_27@HG22	THR_27@CG2	0.0001	2.933	138.7571
PHE_456@HE2	LYS_31@HG2	LYS_31@CG	0.0001	2.9704	141.9825
ALA_475@HB1	SER_19@HG	SER_19@OG	0.0001	2.7242	147.8804
ALA_475@C	SER_19@HG	SER_19@OG	0.0001	2.9234	136.9574
GLY_476@HA2	SER_19@HB2	SER_19@CB	0.0001	2.9811	143.7024
GLY_476@HA2	SER_19@H3	SER_19@N	0.0001	2.9288	139.6111
GLY_476@HA2	SER_19@HG	SER_19@OG	0.0001	2.8386	140.4924
GLU_484@OE2	LYS_31@HE2	LYS_31@CE	0.0001	2.9388	138.5356
PHE_486@H	LEU_79@HD13	LEU_79@CD1	0.0001	2.9315	146.8896
PHE_486@HB2	LEU_79@HD11	LEU_79@CD1	0.0001	2.9789	143.1085
PHE_486@HD1	LEU_79@HD11	LEU_79@CD1	0.0001	2.9475	135.6258
PHE_486@HZ	ILE_21@HD12	ILE_21@CD1	0.0001	2.9789	145.8237
PHE_486@HE2	ILE_21@HD13	ILE_21@CD1	0.0001	2.9669	141.9768
TYR_489@HB3	LYS_31@HD3	LYS_31@CD	0.0001	2.9542	138.6204
TYR_489@HD2	THR_27@HG21	THR_27@CG2	0.0001	2.9192	142.2464
GLN_498@HB2	LYS_353@HZ1	LYS_353@NZ	0.0001	2.9861	139.4811
GLN_498@HB2	LYS_353@HZ2	LYS_353@NZ	0.0001	2.8464	140.8583
GLN_498@HB2	LYS_353@HZ3	LYS_353@NZ	0.0001	2.9155	143.4959
GLN_498@HG2	LYS_353@HE3	LYS_353@CE	0.0001	2.9247	136.0988
GLN_498@HE21	GLN_42@HE22	GLN_42@NE2	0.0001	2.9031	138.1461
VAL_503@HG22	THR_324@HG21	THR_324@CG2	0.0001	2.9409	142.4196
ARG_403@HH22	HIE_34@HE1	HIE_34@CE1	0.0001	2.9795	156.282
LYS_417@HZ1	HIE_34@HE2	HIE_34@NE2	0.0001	2.8646	145.6445
TYR_449@HH	LYS_353@HZ3	LYS_353@NZ	0.0001	2.9357	145.2177
LEU_455@HD13	ASP_30@HB3	ASP_30@CB	0.0001	2.9406	137.9862
LEU_455@HD21	LYS_31@HG3	LYS_31@CG	0.0001	2.9666	147.4968
LEU_455@HD22	LYS_31@HG3	LYS_31@CG	0.0001	2.943	138.0994
LEU_455@HD23	LYS_31@HG2	LYS_31@CG	0.0001	2.917	135.5201
LEU_455@HD23	LYS_31@HG3	LYS_31@CG	0.0001	2.9209	138.7176
LEU_455@HD23	ASP_30@HB3	ASP_30@CB	0.0001	2.9875	143.1941
PHE_456@HZ	THR_27@HG23	THR_27@CG2	0.0001	2.94	138.5336
TYR_473@HE2	THR_27@HG1	THR_27@OG1	0.0001	2.792	152.4781
TYR_473@HD2	THR_27@HG21	THR_27@CG2	0.0001	2.9627	139.4041
ALA_475@HB1	GLU_23@HG2	GLU_23@CG	0.0001	2.9546	148.7126
ALA_475@HB1	SER_19@HB3	SER_19@CB	0.0001	2.9645	141.4604
ALA_475@HB1	THR_27@HG1	THR_27@OG1	0.0001	2.9906	141.8613
ALA_475@HB1	THR_27@HG23	THR_27@CG2	0.0001	2.9352	135.7921
ALA_475@HB2	THR_27@HG21	THR_27@CG2	0.0001	2.9941	152.8545

#Acceptor	DonorH	Donor	Frac	AvgDist	AvgAng
ALA_475@HB2	GLU_23@HG2	GLU_23@CG	0.0001	2.9564	153.9971
ALA_475@HB3	THR_27@HG21	THR_27@CG2	0.0001	2.9227	139.2209
ALA_475@HB3	THR_27@HG1	THR_27@OG1	0.0001	2.9401	143.3999
ALA_475@HB3	GLU_23@HG2	GLU_23@CG	0.0001	2.9551	146.0805
GLY_485@HA2	LEU_79@HD13	LEU_79@CD1	0.0001	2.9448	148.1721
GLY_485@HA2	LEU_79@HG	LEU_79@CG	0.0001	2.9615	139.4342
PHE_486@H	LEU_79@HD11	LEU_79@CD1	0.0001	2.9469	146.9189
PHE_486@HB2	MET_82@HE2	MET_82@CE	0.0001	2.9705	137.0986
PHE_486@HB3	MET_82@HE1	MET_82@CE	0.0001	2.9827	138.8214
PHE_486@HD1	MET_82@HG2	MET_82@CG	0.0001	2.9148	143.0929
PHE_486@HD1	LEU_79@HD12	LEU_79@CD1	0.0001	2.9328	135.6221
PHE_486@HZ	ILE_21@HD11	ILE_21@CD1	0.0001	2.8227	137.3724
PHE_486@HE2	PRO_84@HD3	PRO_84@CD	0.0001	2.9053	138.2015
ASN_487@CG	GLN_24@HE22	GLN_24@NE2	0.0001	2.945	141.6362
TYR_489@HB3	LYS_31@HE2	LYS_31@CE	0.0001	2.8415	139.3784
TYR_489@HD1	LYS_31@HE2	LYS_31@CE	0.0001	2.8229	151.3787
TYR_489@OH	THR_27@HG1	THR_27@OG1	0.0001	2.8475	144.6474
GLN_493@HA	LYS_31@HZ2	LYS_31@NZ	0.0001	2.885	141.8104
GLN_493@HG2	HIE_34@HD2	HIE_34@CD2	0.0001	2.9878	139.6669
GLN_493@HE22	LYS_31@HA	LYS_31@CA	0.0001	2.8751	147.764
GLN_493@HE22	GLU_35@HB2	GLU_35@CB	0.0001	2.9343	162.4266
GLN_493@HE22	LYS_31@HG2	LYS_31@CG	0.0001	2.9493	144.2993
GLN_498@HG2	LYS_353@HE2	LYS_353@CE	0.0001	2.8441	143.1554
GLN_498@HG2	LYS_353@HZ2	LYS_353@NZ	0.0001	2.9634	138.2696
GLN_498@NE2	GLN_42@HE21	GLN_42@NE2	0.0001	2.9199	149.9419
GLN_498@HE21	LYS_353@HZ3	LYS_353@NZ	0.0001	2.9429	153.168
GLN_498@HE22	GLN_42@HE21	GLN_42@NE2	0.0001	2.8722	141.4323
THR_500@OG1	TYR_41@HH	TYR_41@OH	0.0001	2.8956	143.056
ASN_501@HD21	LYS_353@HE3	LYS_353@CE	0.0001	2.9499	143.0945
VAL_503@HG11	THR_324@HG22	THR_324@CG2	0.0001	2.9605	140.2352
LYS_417@HE3	HIE_34@HE2	HIE_34@NE2	0.0001	2.9616	136.8526
TYR_449@HE1	ASP_38@HB3	ASP_38@CB	0.0001	2.9918	135.9595
TYR_449@OH	GLN_42@HE21	GLN_42@NE2	0.0001	2.724	142.0443
LEU_455@HD12	ASP_30@HB3	ASP_30@CB	0.0001	2.9936	143.579
LEU_455@HD21	HIE_34@HE2	HIE_34@NE2	0.0001	2.8317	137.3926
LEU_455@HD21	HIE_34@HB2	HIE_34@CB	0.0001	2.9709	136.8276
LEU_455@HD21	LYS_31@HD2	LYS_31@CD	0.0001	2.9287	137.4034
LEU_455@HD22	LYS_31@HZ2	LYS_31@NZ	0.0001	2.7647	146.9059
LEU_455@HD23	LYS_31@HD2	LYS_31@CD	0.0001	2.9789	135.3623
PHE_456@HZ	THR_27@HG21	THR_27@CG2	0.0001	2.8392	135.7551
TYR_473@HD2	THR_27@HG1	THR_27@OG1	0.0001	2.5784	136.8598
ALA_475@HB1	THR_27@HG21	THR_27@CG2	0.0001	2.9997	138.2685
ALA_475@HB1	SER_19@H3	SER_19@N	0.0001	2.9441	160.4377
ALA_475@HB1	SER_19@H2	SER_19@N	0.0001	2.9946	149.0503
ALA_475@HB2	GLN_24@HG3	GLN_24@CG	0.0001	2.9836	153.9385
ALA_475@HB2	THR_27@HG22	THR_27@CG2	0.0001	2.9768	147.8507
ALA_475@HB2	THR_27@HG23	THR_27@CG2	0.0001	2.963	141.0238
ALA_475@HB3	GLU_23@HG3	GLU_23@CG	0.0001	2.9969	136.173
ALA_475@HB3	SER_19@HA	SER_19@CA	0.0001	2.9739	154.336
ALA_475@O	SER_19@HA	SER_19@CA	0.0001	2.9397	139.7736
GLY_476@H	GLN_24@HE22	GLN_24@NE2	0.0001	2.9651	146.715
GLY_476@HA2	SER_19@HA	SER_19@CA	0.0001	2.9746	141.307
GLY_476@HA3	GLN_24@HE22	GLN_24@NE2	0.0001	2.9897	137.4413
GLY_476@HA3	SER_19@HG	SER_19@OG	0.0001	2.6962	135.3109
GLY_476@HA3	SER_19@H1	SER_19@N	0.0001	2.9353	135.6172
GLU_484@CD	LYS_31@HZ3	LYS_31@NZ	0.0001	2.9771	154.5452
PHE_486@H	LEU_79@HD12	LEU_79@CD1	0.0001	2.9137	139.7185
PHE_486@HA	LEU_79@HD23	LEU_79@CD2	0.0001	2.9956	142.2349
PHE_486@HB2	MET_82@HE3	MET_82@CE	0.0001	2.9188	144.9748
PHE_486@HD1	MET_82@HE3	MET_82@CE	0.0001	2.9319	136.5446
PHE_486@HD1	LEU_79@HD13	LEU_79@CD1	0.0001	2.8652	137.6995
PHE_486@HE1	MET_82@HB3	MET_82@CB	0.0001	2.8994	144.739
PHE_486@HE1	GLN_24@HE21	GLN_24@NE2	0.0001	2.8966	140.9717
PHE_486@HE2	TYR_83@HE2	TYR_83@CE2	0.0001	2.9902	141.2797
PHE_486@HD2	MET_82@HG2	MET_82@CG	0.0001	2.9842	140.4538
PHE_486@HD2	LEU_79@HD12	LEU_79@CD1	0.0001	2.9384	139.5584

#Acceptor	DonorH	Donor	Frac	AvgDist	AvgAng
ASN_487@HB2	GLN_24@HG2	GLN_24@CG	0.0001	2.9999	138.2558
TYR_489@HD1	LYS_31@HG3	LYS_31@CG	0.0001	2.9466	159.1393
TYR_489@HD1	LYS_31@HZ1	LYS_31@NZ	0.0001	2.8825	137.7142
TYR_489@HD1	PHE_28@HA	PHE_28@CA	0.0001	2.9499	135.784
TYR_489@HE1	LEU_79@HD12	LEU_79@CD1	0.0001	2.9735	139.4293
TYR_489@HE1	LEU_79@HD11	LEU_79@CD1	0.0001	2.977	135.8639
TYR_489@HH	TYR_83@HH	TYR_83@OH	0.0001	2.9152	137.7338
TYR_489@HE2	THR_27@HG1	THR_27@OG1	0.0001	2.9678	138.2421
PHE_490@HB2	LYS_31@HE3	LYS_31@CE	0.0001	2.9885	152.8254
PHE_490@HD2	LYS_31@HE2	LYS_31@CE	0.0001	2.8228	140.9269
GLN_493@HA	LYS_31@HZ3	LYS_31@NZ	0.0001	2.955	136.3707
GLN_493@HB2	LYS_31@HE2	LYS_31@CE	0.0001	2.9131	156.1404
GLN_493@HG2	LYS_31@HZ1	LYS_31@NZ	0.0001	2.9941	149.5806
GLN_493@HG3	HIE_34@HB3	HIE_34@CB	0.0001	2.955	142.0177
GLN_493@HG3	HIE_34@HD2	HIE_34@CD2	0.0001	2.9905	148.3648
GLN_493@NE2	LYS_31@HZ2	LYS_31@NZ	0.0001	2.9771	142.2165
GLN_493@HE21	LYS_31@HZ3	LYS_31@NZ	0.0001	2.7883	147.3653
GLN_493@HE21	LYS_31@HD3	LYS_31@CD	0.0001	2.9604	158.2392
GLN_493@HE22	LYS_31@HZ1	LYS_31@NZ	0.0001	2.9695	168.4856
GLN_493@HE22	GLU_35@HA	GLU_35@CA	0.0001	2.7939	136.5813
GLY_496@H	LYS_353@HE2	LYS_353@CE	0.0001	2.9326	140.0924
GLY_496@HA2	LYS_353@HZ2	LYS_353@NZ	0.0001	2.9663	138.8439
GLY_496@HA3	LYS_353@HZ1	LYS_353@NZ	0.0001	2.5974	135.4773
GLN_498@HG2	LYS_353@HZ3	LYS_353@NZ	0.0001	2.9888	137.2004
GLN_498@HG2	TYR_41@HE2	TYR_41@CE2	0.0001	2.9919	147.3983
GLN_498@CD	LYS_353@HZ1	LYS_353@NZ	0.0001	2.835	139.9964
GLN_498@HE21	LYS_353@HE3	LYS_353@CE	0.0001	2.9157	156.3923
GLN_498@HE21	LYS_353@HD2	LYS_353@CD	0.0001	2.7514	135.3218
GLN_498@HE21	LEU_45@HD12	LEU_45@CD1	0.0001	2.8697	137.7011
GLN_498@HE21	LYS_353@HZ1	LYS_353@NZ	0.0001	2.9547	139.5248
GLN_498@HE21	LEU_45@HD21	LEU_45@CD2	0.0001	2.8857	140.6384
THR_500@HB	ARG_357@HH22	ARG_357@NH2	0.0001	2.933	135.2763
THR_500@HG1	ARG_357@HH22	ARG_357@NH2	0.0001	2.9623	153.4424
THR_500@HG1	LEU_45@HD11	LEU_45@CD1	0.0001	2.8364	135.2552
THR_500@HG1	LEU_45@HD22	LEU_45@CD2	0.0001	2.864	141.7225
ASN_501@HA	ASP_355@HB2	ASP_355@CB	0.0001	2.9837	142.7705
ASN_501@OD1	LYS_353@HE2	LYS_353@CE	0.0001	2.9879	172.4992
VAL_503@HB	GLN_325@HE22	GLN_325@NE2	0.0001	2.9625	145.2546
VAL_503@HG11	THR_324@HG21	THR_324@CG2	0.0001	2.9605	137.3257
VAL_503@HG12	THR_324@HB	THR_324@CB	0.0001	2.9767	142.5732
VAL_503@HG13	THR_324@HG22	THR_324@CG2	0.0001	2.9812	135.1951
VAL_503@HG13	THR_324@HG21	THR_324@CG2	0.0001	2.9476	138.6162
VAL_503@HG21	THR_324@HG23	THR_324@CG2	0.0001	2.9732	139.2007
VAL_503@HG21	GLN_325@HB2	GLN_325@CB	0.0001	2.8898	135.1781
VAL_503@HG21	GLN_325@HE21	GLN_325@NE2	0.0001	2.7157	144.2387
VAL_503@HG21	THR_324@HG21	THR_324@CG2	0.0001	2.9868	139.1054
VAL_503@HG22	THR_324@HG22	THR_324@CG2	0.0001	2.9715	136.1337
VAL_503@HG23	THR_324@HG22	THR_324@CG2	0.0001	2.8831	136.9782
VAL_503@HG23	THR_324@HG23	THR_324@CG2	0.0001	2.8972	137.5005
VAL_503@HG23	THR_324@HG21	THR_324@CG2	0.0001	2.9483	137.7205
TYR_505@HD2	LYS_353@HD2	LYS_353@CD	0.0001	2.8943	135.1409

Table S2. Hydrogen bond analysis of S protein (DELTA)-ACE2 complex during the last 20 ns of MD simulation with S protein as donor and ACE2 as acceptor.

#Acceptor	DonorH	Donor	Frac	AvgDist	AvgAng
ASP_38@OD1	TYR_449@HH	TYR_449@OH	0.6236	2.693	161.9246
LYS_353@O	GLY_502@H	GLY_502@N	0.5714	2.8778	159.9073
TYR_41@OH	THR_500@HG1	THR_500@OG1	0.4712	2.8014	158.9853
GLN_42@OE1	GLN_498@HE21	GLN_498@NE2	0.4653	2.8757	162.1953
GLU_35@OE1	GLN_493@HE21	GLN_493@NE2	0.3831	2.8265	159.8379
GLU_35@OE2	GLN_493@HE21	GLN_493@NE2	0.2372	2.829	159.9659
ASP_355@OD2	THR_500@HG1	THR_500@OG1	0.224	2.7243	162.1695
ASP_38@OD2	TYR_449@HH	TYR_449@OH	0.21	2.7279	160.7297
GLN_24@O	TYR_489@HH	TYR_489@OH	0.1513	2.812	145.4541
TYR_83@OH	ASN_487@H	ASN_487@N	0.1092	2.9232	161.806
TYR_83@OH	TYR_489@HH	TYR_489@OH	0.1014	2.8629	150.6138

#Acceptor	DonorH	Donor	Frac	AvgDist	AvgAng
ASP_30@OD1	LYS_417@HZ3	LYS_417@NZ	0.0943	2.7749	157.7357
TYR_41@HH	THR_500@HG1	THR_500@OG1	0.0693	2.871	146.7438
ASP_30@OD1	LYS_417@HZ2	LYS_417@NZ	0.0643	2.787	157.1344
GLY_354@HA3	GLY_502@HA3	GLY_502@CA	0.0557	2.9291	145.3736
HIE_34@O	GLN_493@HE22	GLN_493@NE2	0.0471	2.8642	154.2906
ASP_30@OD2	LYS_417@HZ2	LYS_417@NZ	0.0469	2.7815	156.2563
ASP_30@OD2	LYS_417@HZ3	LYS_417@NZ	0.0469	2.7831	157.8188
ASP_30@OD2	LYS_417@HZ1	LYS_417@NZ	0.0462	2.7878	157.5149
ASP_30@OD1	LYS_417@HZ1	LYS_417@NZ	0.0374	2.7788	156.1463
PHE_28@HB2	TYR_489@HH	TYR_489@OH	0.0348	2.8493	147.7873
TYR_83@HH	ASN_487@H	ASN_487@N	0.0259	2.9216	157.6922
PHE_28@HB2	TYR_489@HE1	TYR_489@CE1	0.0248	2.9497	145.6507
GLU_35@HB2	GLN_493@HE21	GLN_493@NE2	0.0205	2.8175	146.1815
LYS_31@HE3	PHE_490@HB3	PHE_490@CB	0.0174	2.9047	145.5947
LEU_79@HD21	TYR_489@HH	TYR_489@OH	0.0143	2.7658	153.9927
LEU_79@HD22	TYR_489@HH	TYR_489@OH	0.0127	2.7855	155.1003
GLU_35@HG2	GLN_493@HE21	GLN_493@NE2	0.0107	2.8125	147.6822
ALA_386@O	TYR_505@HH	TYR_505@OH	0.0107	2.7603	159.2593
TYR_41@HE2	THR_500@HG1	THR_500@OG1	0.0097	2.8635	144.891
LYS_31@HE2	PHE_490@HB3	PHE_490@CB	0.0097	2.9153	148.846
TYR_41@HE2	GLN_498@HE21	GLN_498@NE2	0.0083	2.8734	149.6651
LEU_79@HD23	TYR_489@HH	TYR_489@OH	0.0073	2.7824	152.5098
GLU_35@OE1	SER_494@HG	SER_494@OG	0.0066	2.7107	164.1631
LYS_31@HE3	PHE_490@H	PHE_490@N	0.0066	2.8645	141.7725
ASN_330@HD21	THR_500@HB	THR_500@CB	0.0057	2.8388	145.4362
ARG_357@HH21	THR_500@HG1	THR_500@OG1	0.0056	2.8404	140.5976
GLN_24@HG2	ALA_475@HB3	ALA_475@CB	0.0053	2.95	141.54
HIE_34@HE2	LEU_455@HD13	LEU_455@CD1	0.0053	2.8941	144.1877
LYS_31@HB2	PHE_456@HZ	PHE_456@CZ	0.0049	2.9423	140.0973
PHE_28@HA	TYR_489@HE1	TYR_489@CE1	0.004	2.9462	140.2618
GLN_24@HG2	ALA_475@HB2	ALA_475@CB	0.004	2.951	141.2291
TYR_83@HA	PHE_486@HE2	PHE_486@CE2	0.0037	2.9478	147.4662
HIE_34@HE2	LEU_455@HD11	LEU_455@CD1	0.0037	2.9002	143.9433
LYS_31@O	GLN_493@HE21	GLN_493@NE2	0.0036	2.8908	149.8534
GLN_24@HG2	ALA_475@HB1	ALA_475@CB	0.0035	2.9508	141.1643
TYR_41@CE2	GLN_498@HE21	GLN_498@NE2	0.0035	2.9454	146.7151
HIE_34@HE2	LEU_455@HD12	LEU_455@CD1	0.0034	2.9084	144.4722
GLU_35@HG3	GLN_493@HE21	GLN_493@NE2	0.0034	2.7956	147.6776
SER_19@HB2	ALA_475@HB1	ALA_475@CB	0.0033	2.953	145.2701
SER_19@HB2	ALA_475@HB3	ALA_475@CB	0.0032	2.9387	143.6168
LYS_31@HB2	PHE_456@HE2	PHE_456@CE2	0.0032	2.9422	139.9297
LYS_31@HD3	PHE_456@HE2	PHE_456@CE2	0.0031	2.9447	141.4446
LEU_79@HD11	TYR_489@HH	TYR_489@OH	0.0031	2.795	151.6513
TYR_83@HH	TYR_489@HH	TYR_489@OH	0.003	2.9367	146.9054
LYS_353@HZ3	GLN_498@HB3	GLN_498@CB	0.0029	2.937	144.209
LEU_79@HD12	TYR_489@HH	TYR_489@OH	0.0027	2.8342	153.6734
GLN_24@OE1	ASN_487@HD22	ASN_487@ND2	0.0027	2.8395	152.0275
THR_27@HG21	TYR_473@HE2	TYR_473@CE2	0.0027	2.9464	141.9026
LYS_31@HD2	PHE_456@HE2	PHE_456@CE2	0.0026	2.9489	142.8004
ARG_357@HH22	THR_500@HG23	THR_500@CG2	0.0024	2.9107	142.051
ARG_357@HH21	THR_500@HB	THR_500@CB	0.0023	2.9371	140.9513
THR_27@HG23	TYR_473@HE2	TYR_473@CE2	0.0022	2.9589	142.4736
LYS_31@HE2	PHE_456@HE2	PHE_456@CE2	0.0022	2.9237	147.7263
ARG_357@HH22	THR_500@HG22	THR_500@CG2	0.0022	2.8862	141.4981
LYS_31@HE2	PHE_490@H	PHE_490@N	0.0022	2.9023	139.3652
SER_19@HB2	ALA_475@HB2	ALA_475@CB	0.0021	2.9448	144.152
ASP_30@HB3	PHE_456@HZ	PHE_456@CZ	0.0021	2.9542	143.5537
LYS_31@HZ3	PHE_490@HD2	PHE_490@CD2	0.002	2.9279	153.2475
LEU_79@HD13	PHE_486@HA	PHE_486@CA	0.0019	2.9307	139.5874
THR_27@HG22	TYR_473@HE2	TYR_473@CE2	0.0019	2.953	143.4783
LYS_31@HZ1	PHE_490@HD2	PHE_490@CD2	0.0019	2.9	153.4331
GLN_325@OE1	GLN_506@HE21	GLN_506@NE2	0.0018	2.868	161.8485
LYS_353@HZ2	ASN_501@HD21	ASN_501@ND2	0.0018	2.9371	142.1742
GLU_35@HA	GLN_493@HE21	GLN_493@NE2	0.0018	2.8774	146.0882
MET_82@HG2	PHE_486@HB2	PHE_486@CB	0.0018	2.9442	142.5033
TYR_83@HA	PHE_486@HE1	PHE_486@CE1	0.0017	2.9551	146.3942

#Acceptor	DonorH	Donor	Frac	AvgDist	AvgAng
LYS_353@HD2	ASN_501@HD21	ASN_501@ND2	0.0017	2.8361	139.9704
GLN_24@HE22	ASN_487@HD21	ASN_487@ND2	0.0016	2.9345	141.6718
TYR_41@OH	GLN_498@HE21	GLN_498@NE2	0.0015	2.882	143.0881
LEU_79@HD13	TYR_489@HH	TYR_489@OH	0.0015	2.8002	147.7399
LYS_353@HE2	GLY_496@HA3	GLY_496@CA	0.0015	2.8456	142.9151
ARG_357@HH22	THR_500@HG21	THR_500@CG2	0.0013	2.9146	139.9048
LYS_31@HE2	LEU_455@HD22	LEU_455@CD2	0.0012	2.9237	143.9363
LYS_31@HZ3	PHE_490@HB3	PHE_490@CB	0.0012	2.9391	154.1935
LYS_31@HD3	LEU_455@HD21	LEU_455@CD2	0.0011	2.9476	138.8768
GLY_354@HA3	GLY_502@H	GLY_502@N	0.0011	2.8348	142.6716
SER_19@HB3	GLY_476@HA2	GLY_476@CA	0.0011	2.9232	140.8918
HIE_34@HD2	LEU_455@HD21	LEU_455@CD2	0.0011	2.9145	140.6061
LYS_31@HZ2	PHE_490@HD2	PHE_490@CD2	0.001	2.9317	161.0728
LEU_79@HD12	PHE_486@HA	PHE_486@CA	0.001	2.9227	139.0183
LYS_31@HA	LEU_455@HD23	LEU_455@CD2	0.0009	2.9532	141.0845
LEU_79@HD11	PHE_486@HA	PHE_486@CA	0.0009	2.9289	139.6701
ILE_21@HG22	PHE_486@HZ	PHE_486@CZ	0.0009	2.961	143.2995
GLN_24@HG3	ALA_475@HB3	ALA_475@CB	0.0009	2.9544	145.0829
LYS_31@HG2	TYR_489@HB3	TYR_489@CB	0.0009	2.9632	141.6229
LYS_31@HD3	LEU_455@HD22	LEU_455@CD2	0.0009	2.9497	138.7097
ASN_330@HD21	THR_500@HG23	THR_500@CG2	0.0009	2.8817	143.9549
LYS_353@HD3	ASN_501@HD21	ASN_501@ND2	0.0009	2.8877	139.6163
LYS_353@HZ3	ASN_501@HD21	ASN_501@ND2	0.0009	2.9145	140.3458
ILE_21@HG21	PHE_486@HZ	PHE_486@CZ	0.0008	2.9516	141.2366
GLN_24@HA	ALA_475@HB1	ALA_475@CB	0.0008	2.9347	140.3456
GLN_24@HE22	ALA_475@HB2	ALA_475@CB	0.0008	2.8449	149.0153
ILE_21@HG23	PHE_486@HZ	PHE_486@CZ	0.0008	2.936	141.0214
LYS_31@HZ1	PHE_490@HB3	PHE_490@CB	0.0008	2.929	159.6611
HIE_34@HD2	LEU_455@HD11	LEU_455@CD1	0.0008	2.9549	140.1684
TYR_41@HH	THR_500@HB	THR_500@CB	0.0008	2.9418	140.0653
LEU_79@HD22	GLY_485@HA2	GLY_485@CA	0.0008	2.9414	142.3284
ASN_330@HD21	THR_500@HG21	THR_500@CG2	0.0008	2.9178	145.6221
LYS_353@HZ2	GLN_498@HB3	GLN_498@CB	0.0008	2.9218	143.8703
HIE_34@HB2	GLN_493@HE22	GLN_493@NE2	0.0008	2.7595	151.637
HIE_34@HD2	LEU_455@HD22	LEU_455@CD2	0.0008	2.9538	139.907
LEU_79@HD22	TYR_489@HE1	TYR_489@CE1	0.0008	2.9441	140.0526
MET_82@HB3	PHE_486@HD2	PHE_486@CD2	0.0008	2.9459	139.2268
LYS_353@HZ1	ASN_501@HD21	ASN_501@ND2	0.0008	2.8925	143.0532
SER_19@HG	ALA_475@HB2	ALA_475@CB	0.0007	2.9211	143.9282
LYS_31@HD3	LEU_455@HD23	LEU_455@CD2	0.0007	2.9657	139.0814
LYS_31@HE2	LEU_455@HD23	LEU_455@CD2	0.0007	2.9184	146.4771
HIE_34@HB3	GLN_493@HG2	GLN_493@CG	0.0007	2.9649	139.3978
HIE_34@HD2	LEU_455@HD12	LEU_455@CD1	0.0007	2.9373	138.988
LEU_79@HD21	GLY_485@HA2	GLY_485@CA	0.0007	2.9453	142.4481
GLN_24@HA	ALA_475@HB2	ALA_475@CB	0.0006	2.9585	139.4196
GLN_24@HA	ALA_475@HB3	ALA_475@CB	0.0006	2.9332	137.3971
GLN_24@HE22	ASN_487@HB2	ASN_487@CB	0.0006	2.8401	143.6113
THR_27@HG22	TYR_489@HD2	TYR_489@CD2	0.0006	2.9407	139.1091
GLU_35@CD	GLN_493@HE21	GLN_493@NE2	0.0006	2.9693	147.8715
GLU_37@OE1	TYR_505@HH	TYR_505@OH	0.0006	2.7124	153.4794
ASP_38@CG	TYR_449@HH	TYR_449@OH	0.0006	2.9791	156.8196
GLN_42@HE21	GLN_498@HE21	GLN_498@NE2	0.0006	2.8908	145.6087
LEU_79@HD21	TYR_489@HE1	TYR_489@CE1	0.0006	2.9489	142.6538
GLN_42@HE22	TYR_449@HH	TYR_449@OH	0.0006	2.8787	138.0402
LEU_79@HD23	GLY_485@HA2	GLY_485@CA	0.0006	2.963	144.4289
MET_82@HB2	PHE_486@HD2	PHE_486@CD2	0.0006	2.9451	139.84
LYS_353@HE3	GLY_496@HA3	GLY_496@CA	0.0006	2.8978	143.8999
GLN_24@NE2	ASN_487@HD21	ASN_487@ND2	0.0006	2.9107	141.28
ASP_30@HB2	PHE_456@HZ	PHE_456@CZ	0.0006	2.9505	141.8772
LYS_31@HA	LEU_455@HD21	LEU_455@CD2	0.0006	2.9388	138.7982
LYS_31@HZ2	PHE_490@HB3	PHE_490@CB	0.0006	2.9321	151.4282
HIE_34@HD2	LEU_455@HD13	LEU_455@CD1	0.0006	2.9302	139.8252
ASN_330@HD21	THR_500@HG22	THR_500@CG2	0.0006	2.9258	143.2114
SER_19@H2	GLY_476@HA2	GLY_476@CA	0.0005	2.9337	140.4365
PHE_28@HD1	TYR_489@HE1	TYR_489@CE1	0.0005	2.9632	139.472
LYS_31@HE3	TYR_489@HB3	TYR_489@CB	0.0005	2.9313	143.8643

#Acceptor	DonorH	Donor	Frac	AvgDist	AvgAng
SER_19@HG	ALA_475@HB1	ALA_475@CB	0.0004	2.9079	146.7506
LYS_31@HG2	TYR_489@HD1	TYR_489@CD1	0.0004	2.9539	141.3179
LYS_31@HE2	LEU_455@HD21	LEU_455@CD2	0.0004	2.908	143.931
HIE_34@HD2	LEU_455@HD23	LEU_455@CD2	0.0004	2.9163	141.8469
LEU_79@HD12	PHE_486@HB2	PHE_486@CB	0.0004	2.9326	140.755
LEU_79@HD12	GLY_485@HA2	GLY_485@CA	0.0004	2.9309	142.9006
LEU_79@HD21	PHE_486@HA	PHE_486@CA	0.0004	2.9373	145.214
LYS_353@HZ3	GLN_498@HG2	GLN_498@CG	0.0004	2.9225	145.3557
LYS_31@HG3	GLN_493@HE22	GLN_493@NE2	0.0004	2.855	142.4092
HIE_34@HB3	GLN_493@HE22	GLN_493@NE2	0.0004	2.941	139.8289
MET_82@HG3	PHE_486@HB2	PHE_486@CB	0.0004	2.9571	143.3945
SER_19@HG	ALA_475@HB3	ALA_475@CB	0.0003	2.9381	139.9456
THR_27@HG21	PHE_456@HE1	PHE_456@CE1	0.0003	2.9121	141.0447
LYS_31@HA	LEU_455@HD22	LEU_455@CD2	0.0003	2.9162	141.5974
LEU_79@HD13	PHE_486@HB2	PHE_486@CB	0.0003	2.9442	139.0467
LYS_353@HZ3	GLY_496@HA3	GLY_496@CA	0.0003	2.9122	142.3697
GLU_23@HG2	ALA_475@HB1	ALA_475@CB	0.0003	2.9451	141.8607
GLN_24@HG3	ALA_475@HB1	ALA_475@CB	0.0003	2.9455	141.1737
LYS_31@HG3	TYR_489@HB3	TYR_489@CB	0.0003	2.9418	140.8438
TYR_41@CE2	THR_500@HG1	THR_500@OG1	0.0003	2.9375	149.4632
LEU_45@HD21	GLN_498@HE21	GLN_498@NE2	0.0003	2.895	151.0792
LEU_79@HD23	TYR_489@HE1	TYR_489@CE1	0.0003	2.9293	142.0844
LYS_353@HZ1	GLN_498@HB2	GLN_498@CB	0.0003	2.9121	140.7044
SER_19@H1	GLY_476@HA2	GLY_476@CA	0.0003	2.9293	137.6065
SER_19@HB2	GLY_476@HA2	GLY_476@CA	0.0003	2.9648	143.3466
SER_19@HB3	ALA_475@HB3	ALA_475@CB	0.0003	2.9482	143.2324
SER_19@HG	GLY_476@HA3	GLY_476@CA	0.0003	2.9145	150.9716
GLN_24@HE22	ALA_475@HB3	ALA_475@CB	0.0003	2.9363	149.2328
THR_27@HG21	TYR_473@HD2	TYR_473@CD2	0.0003	2.9458	139.0863
THR_27@HG21	PHE_456@HZ	PHE_456@CZ	0.0003	2.9392	144.808
THR_27@HG23	PHE_456@HZ	PHE_456@CZ	0.0003	2.9625	140.9154
LYS_31@HE2	GLN_493@HB2	GLN_493@CB	0.0003	2.9596	141.2256
LYS_31@HZ2	GLN_493@HE21	GLN_493@NE2	0.0003	2.933	137.9288
HIE_34@HE2	LYS_417@HE2	LYS_417@CE	0.0003	2.8046	152.0903
GLN_42@HE21	GLY_446@HA2	GLY_446@CA	0.0003	2.943	148.7195
GLN_42@HE21	GLN_498@HE22	GLN_498@NE2	0.0003	2.8986	139.3477
LEU_79@HD11	PHE_486@HB2	PHE_486@CB	0.0003	2.9514	140.2118
MET_82@HB2	PHE_486@HD1	PHE_486@CD1	0.0003	2.9387	138.8545
LYS_353@HZ2	GLY_496@HA3	GLY_496@CA	0.0003	2.829	141.9086
GLY_354@HA3	TYR_505@HD1	TYR_505@CD1	0.0003	2.9447	139.1565
ARG_357@HH22	THR_500@HG1	THR_500@OG1	0.0003	2.8684	147.9521
SER_19@HB3	ALA_475@HB2	ALA_475@CB	0.0002	2.9206	146.8678
SER_19@OG	SER_477@H	SER_477@N	0.0002	2.9411	157.9891
GLN_24@HE22	GLY_476@HA3	GLY_476@CA	0.0002	2.8733	142.7887
THR_27@HG21	TYR_489@HD2	TYR_489@CD2	0.0002	2.9658	144.908
THR_27@HG22	PHE_456@HE1	PHE_456@CE1	0.0002	2.9518	140.7109
PHE_28@HD1	TYR_489@HH	TYR_489@OH	0.0002	2.743	139.7899
ASP_30@HB3	PHE_456@HE1	PHE_456@CE1	0.0002	2.9032	139.5612
ASP_30@HB3	LEU_455@HD22	LEU_455@CD2	0.0002	2.9343	140.493
LYS_31@HD2	LEU_455@HD22	LEU_455@CD2	0.0002	2.9623	138.5054
LYS_31@HE3	PHE_490@HD2	PHE_490@CD2	0.0002	2.9199	151.7931
GLU_37@HG2	TYR_505@HE2	TYR_505@CE2	0.0002	2.9742	136.5463
LEU_45@HD23	GLN_498@HE21	GLN_498@NE2	0.0002	2.8698	142.3447
LEU_79@HD11	GLY_485@HA2	GLY_485@CA	0.0002	2.9644	139.1651
LEU_79@HD12	PHE_486@HD1	PHE_486@CD1	0.0002	2.9672	137.5273
LEU_79@HD23	PHE_486@HD1	PHE_486@CD1	0.0002	2.9554	142.2565
MET_82@HB3	PHE_486@HD1	PHE_486@CD1	0.0002	2.9552	140.1156
MET_82@HE1	PHE_486@HB2	PHE_486@CB	0.0002	2.9528	136.7663
TYR_83@HH	PHE_486@HA	PHE_486@CA	0.0002	2.9405	157.6066
LYS_353@HZ1	TYR_449@HH	TYR_449@OH	0.0002	2.9388	140.8282
LYS_353@HZ1	GLN_498@HB3	GLN_498@CB	0.0002	2.9437	144.3436
LYS_353@HZ1	GLY_496@HA3	GLY_496@CA	0.0002	2.8373	150.2564
ASP_355@HB2	ASN_501@HA	ASN_501@CA	0.0002	2.9629	139.7148
ARG_357@HH22	THR_500@HB	THR_500@CB	0.0002	2.8453	139.1016
SER_19@H3	GLY_476@HA2	GLY_476@CA	0.0001	2.9072	142.1616
SER_19@HG	GLY_476@HA2	GLY_476@CA	0.0001	2.9273	143.8405

#Acceptor	DonorH	Donor	Frac	AvgDist	AvgAng
ILE_21@HD12	PHE_486@HE2	PHE_486@CE2	0.0001	2.9192	143.7769
GLN_24@HG3	ALA_475@HB2	ALA_475@CB	0.0001	2.9623	141.3982
GLN_24@HE22	ALA_475@HB1	ALA_475@CB	0.0001	2.9823	151.541
THR_27@HA	PHE_456@HZ	PHE_456@CZ	0.0001	2.9531	143.1392
THR_27@HG21	ALA_475@HB2	ALA_475@CB	0.0001	2.963	144.2626
THR_27@HG23	PHE_456@HE1	PHE_456@CE1	0.0001	2.9228	138.9552
ASP_30@HB3	LEU_455@HD21	LEU_455@CD2	0.0001	2.9643	143.7053
ASP_30@HB3	LEU_455@HD13	LEU_455@CD1	0.0001	2.9672	143.5138
ASP_30@HB3	LEU_455@HD23	LEU_455@CD2	0.0001	2.9518	143.0856
ASP_30@CG	LYS_417@HZ3	LYS_417@NZ	0.0001	2.9872	155.1901
LYS_31@HA	GLN_493@HE22	GLN_493@NE2	0.0001	2.9126	140.239
LYS_31@HE2	PHE_490@HD2	PHE_490@CD2	0.0001	2.9373	148.1166
LYS_31@HZ1	GLN_493@HE21	GLN_493@NE2	0.0001	2.9646	141.2063
HIE_34@HE2	LEU_455@HD22	LEU_455@CD2	0.0001	2.8302	142.7767
TYR_41@CZ	GLN_498@HE21	GLN_498@NE2	0.0001	2.9492	139.9657
TYR_41@HE2	GLN_498@HG2	GLN_498@CG	0.0001	2.9451	140.7665
MET_82@HB2	PHE_486@HE1	PHE_486@CE1	0.0001	2.9852	137.1972
MET_82@HE2	PHE_486@HB2	PHE_486@CB	0.0001	2.9745	139.798
LYS_353@HE3	GLN_498@HG2	GLN_498@CG	0.0001	2.9141	137.6133
LYS_353@HE3	GLN_498@HB3	GLN_498@CB	0.0001	2.9645	141.4842
LYS_353@HZ2	GLN_498@HG2	GLN_498@CG	0.0001	2.9557	147.2895
LYS_353@HZ2	GLN_498@HB2	GLN_498@CB	0.0001	2.9285	155.6547
GLY_354@O	GLY_502@H	GLY_502@N	0.0001	2.8402	153.5696
SER_19@HB3	ALA_475@HB1	ALA_475@CB	0.0001	2.9932	146.0168
ILE_21@HD11	PHE_486@HE2	PHE_486@CE2	0.0001	2.9259	138.7457
ILE_21@HD12	PHE_486@HZ	PHE_486@CZ	0.0001	2.8991	140.797
GLU_23@HG2	ALA_475@HB2	ALA_475@CB	0.0001	2.926	137.8428
GLN_24@HE21	ASN_487@HD21	ASN_487@ND2	0.0001	2.9068	136.6303
THR_27@HG23	ALA_475@HB2	ALA_475@CB	0.0001	2.9529	140.3787
PHE_28@HB3	TYR_489@HE1	TYR_489@CE1	0.0001	2.96	140.4155
LYS_31@HG2	LEU_455@HD22	LEU_455@CD2	0.0001	2.9767	136.9975
LYS_31@HG2	PHE_456@HE2	PHE_456@CE2	0.0001	2.9738	138.3129
LYS_31@HG2	LEU_455@HD21	LEU_455@CD2	0.0001	2.956	140.1814
LYS_31@HG3	PHE_456@HE2	PHE_456@CE2	0.0001	2.9776	136.4053
LYS_31@HG3	TYR_489@HD1	TYR_489@CD1	0.0001	2.9537	136.0418
LYS_31@HD2	LEU_455@HD23	LEU_455@CD2	0.0001	2.9139	139.0594
LYS_31@HD2	GLN_493@HE21	GLN_493@NE2	0.0001	2.844	140.7861
LYS_31@HD2	LEU_455@HD21	LEU_455@CD2	0.0001	2.9903	142.199
LYS_31@HD3	PHE_490@H	PHE_490@N	0.0001	2.9329	137.0707
LYS_31@HE3	TYR_489@HD1	TYR_489@CD1	0.0001	2.9057	144.55
LYS_31@HZ2	GLN_493@HA	GLN_493@CA	0.0001	2.8837	151.0345
HIE_34@HB2	LEU_455@HD23	LEU_455@CD2	0.0001	2.9845	140.5611
HIE_34@HB3	GLN_493@HG3	GLN_493@CG	0.0001	2.9412	137.1974
HIE_34@HE1	ARG_403@HH12	ARG_403@NH1	0.0001	2.9209	141.6122
HIE_34@HE2	LYS_417@HZ3	LYS_417@NZ	0.0001	2.9349	137.477
HIE_34@HE2	LYS_417@HZ2	LYS_417@NZ	0.0001	2.9648	144.8985
HIE_34@HE2	LEU_455@HD23	LEU_455@CD2	0.0001	2.8333	136.5901
HIE_34@HE2	LEU_455@HD21	LEU_455@CD2	0.0001	2.9258	139.2984
HIE_34@O	GLN_493@HE21	GLN_493@NE2	0.0001	2.9269	142.9827
TYR_41@HE2	GLN_498@HE22	GLN_498@NE2	0.0001	2.9521	141.643
TYR_41@HD2	GLN_498@HE21	GLN_498@NE2	0.0001	2.9686	143.9007
LEU_45@HD22	THR_500@HG1	THR_500@OG1	0.0001	2.8458	145.7076
LEU_79@HG	TYR_489@HH	TYR_489@OH	0.0001	2.9424	143.892
LEU_79@HG	GLY_485@HA2	GLY_485@CA	0.0001	2.9499	138.6384
MET_82@HB3	PHE_486@HB2	PHE_486@CB	0.0001	2.9484	150.005
MET_82@HG3	PHE_486@HD2	PHE_486@CD2	0.0001	2.9436	137.6149
TYR_83@HH	TYR_489@HE1	TYR_489@CE1	0.0001	2.9702	150.6937
TYR_83@HE2	TYR_489@HH	TYR_489@OH	0.0001	2.8111	139.1897
PRO_84@HD3	PHE_486@HE2	PHE_486@CE2	0.0001	2.9715	147.9218
THR_324@HG22	VAL_503@HG23	VAL_503@CG2	0.0001	2.9448	138.6061
GLN_325@NE2	GLN_506@HE21	GLN_506@NE2	0.0001	2.9757	156.1756
GLN_325@HE22	GLN_506@HE21	GLN_506@NE2	0.0001	2.8712	136.8776
LYS_353@HE3	ASN_501@HD21	ASN_501@ND2	0.0001	2.8386	138.0893
LYS_353@O	ASN_501@HD22	ASN_501@ND2	0.0001	2.9015	166.2686
SER_19@H3	GLY_476@HA3	GLY_476@CA	0.0001	2.8315	138.0492
SER_19@H3	ALA_475@HB1	ALA_475@CB	0.0001	2.9066	141.5036

#Acceptor	DonorH	Donor	Frac	AvgDist	AvgAng
SER_19@HA	ALA_475@HB3	ALA_475@CB	0.0001	2.9196	140.1529
SER_19@HB2	GLY_476@HA3	GLY_476@CA	0.0001	2.8697	156.4172
SER_19@HB3	GLY_476@HA3	GLY_476@CA	0.0001	2.997	138.2646
SER_19@HG	SER_477@H	SER_477@N	0.0001	2.7712	154.5457
ILE_21@HD11	PHE_486@HZ	PHE_486@CZ	0.0001	2.8706	145.542
ILE_21@HD13	PHE_486@HZ	PHE_486@CZ	0.0001	2.8969	141.3182
ILE_21@HD13	PHE_486@HE2	PHE_486@CE2	0.0001	2.8189	137.455
GLU_23@HG3	ALA_475@HB3	ALA_475@CB	0.0001	2.9055	135.6258
GLN_24@HB3	ASN_487@HB2	ASN_487@CB	0.0001	2.9434	138.6345
GLN_24@HB3	TYR_489@HH	TYR_489@OH	0.0001	2.695	136.5982
GLN_24@HG2	ASN_487@HD21	ASN_487@ND2	0.0001	2.6467	140.9132
THR_27@HG21	ALA_475@HB1	ALA_475@CB	0.0001	2.8628	136.6902
THR_27@HG22	PHE_456@HZ	PHE_456@CZ	0.0001	2.9529	135.4904
THR_27@HG23	TYR_489@HD2	TYR_489@CD2	0.0001	2.9827	139.7372
THR_27@HG23	ALA_475@HB1	ALA_475@CB	0.0001	2.9598	144.9695
THR_27@HG23	ALA_475@HB3	ALA_475@CB	0.0001	2.9627	139.728
THR_27@HG1	TYR_473@HE2	TYR_473@CE2	0.0001	2.8971	135.2963
ASP_30@CG	LYS_417@HZ1	LYS_417@NZ	0.0001	2.9838	147.2433
LYS_31@HB2	LEU_455@HD21	LEU_455@CD2	0.0001	2.9867	137.4458
LYS_31@HG2	GLN_493@HE22	GLN_493@NE2	0.0001	2.8454	144.2069
LYS_31@HG3	GLN_493@HE21	GLN_493@NE2	0.0001	2.923	135.3849
LYS_31@HG3	LEU_455@HD21	LEU_455@CD2	0.0001	2.9381	156.8567
LYS_31@HD2	TYR_489@HD1	TYR_489@CD1	0.0001	2.8886	136.8374
LYS_31@HD3	GLN_493@HE21	GLN_493@NE2	0.0001	2.9161	168.0313
LYS_31@HE2	TYR_489@HB3	TYR_489@CB	0.0001	2.7837	149.9962
LYS_31@HE3	PHE_456@HE2	PHE_456@CE2	0.0001	2.9235	172.5031
LYS_31@HZ2	LEU_455@HD23	LEU_455@CD2	0.0001	2.8884	135.0702
LYS_31@HZ3	GLN_493@HE21	GLN_493@NE2	0.0001	2.9677	136.8157
LYS_31@HZ3	GLN_493@HA	GLN_493@CA	0.0001	2.9518	143.5641
LYS_31@O	GLN_493@HE22	GLN_493@NE2	0.0001	2.9734	153.3401
HIE_34@HB2	GLN_493@HG2	GLN_493@CG	0.0001	2.972	139.4442
HIE_34@HE1	ARG_403@HH22	ARG_403@NH2	0.0001	2.9146	137.5505
HIE_34@HE1	ARG_403@HH21	ARG_403@NH2	0.0001	2.981	136.1026
HIE_34@HE2	LYS_417@HZ1	LYS_417@NZ	0.0001	2.8788	136.9498
HIE_34@HD2	GLN_493@HG3	GLN_493@CG	0.0001	2.9998	148.2169
HIE_34@HD2	GLN_493@HG2	GLN_493@CG	0.0001	2.9492	137.0648
HIE_34@HD2	LYS_417@HZ1	LYS_417@NZ	0.0001	2.9155	137.7797
HIE_34@C	GLN_493@HE22	GLN_493@NE2	0.0001	2.9813	141.5996
GLU_35@H	GLN_493@HE21	GLN_493@NE2	0.0001	2.9627	140.2188
GLU_35@OE2	GLN_493@HE22	GLN_493@NE2	0.0001	2.9415	142.4129
GLU_37@OE2	TYR_505@HH	TYR_505@OH	0.0001	2.8456	140.2538
ASP_38@HB3	TYR_449@HH	TYR_449@OH	0.0001	2.6816	149.4596
TYR_41@CZ	THR_500@HG1	THR_500@OG1	0.0001	2.9672	170.6568
TYR_41@OH	GLN_498@HE22	GLN_498@NE2	0.0001	2.9576	163.1294
GLN_42@HE22	GLN_498@HE21	GLN_498@NE2	0.0001	2.9583	160.5637
LEU_45@HD11	THR_500@HG1	THR_500@OG1	0.0001	2.8359	151.313
LEU_45@HD21	THR_500@HG1	THR_500@OG1	0.0001	2.9079	141.2521
LEU_45@HD22	GLN_498@HE21	GLN_498@NE2	0.0001	2.9019	139.0507
LEU_45@HD23	THR_500@HG1	THR_500@OG1	0.0001	2.9296	138.9503
LEU_79@HD11	PHE_486@HD1	PHE_486@CD1	0.0001	2.9748	154.4524
LEU_79@HD11	PHE_486@HD2	PHE_486@CD2	0.0001	2.9812	143.1567
LEU_79@HD11	TYR_489@HE1	TYR_489@CE1	0.0001	2.9724	136.3322
LEU_79@HD12	PHE_486@H	PHE_486@N	0.0001	2.7717	138.967
LEU_79@HD12	PHE_486@HD2	PHE_486@CD2	0.0001	2.937	147.2427
LEU_79@HD12	TYR_489@HE1	TYR_489@CE1	0.0001	2.9587	138.6848
LEU_79@HD13	PHE_486@HD1	PHE_486@CD1	0.0001	2.8919	142.0528
LEU_79@CD2	TYR_489@HH	TYR_489@OH	0.0001	2.9906	163.1326
LEU_79@HD23	PHE_486@HB2	PHE_486@CB	0.0001	2.9643	137.8831
MET_82@HG2	PHE_486@HD1	PHE_486@CD1	0.0001	2.9875	142.8271
MET_82@HG2	PHE_486@HD2	PHE_486@CD2	0.0001	2.9978	135.4084
MET_82@HE1	PHE_486@HD1	PHE_486@CD1	0.0001	2.9091	138.5407
MET_82@HE3	PHE_486@HB2	PHE_486@CB	0.0001	2.8903	139.4878
MET_82@HE3	PHE_486@H	PHE_486@N	0.0001	2.9903	143.1004
TYR_83@HH	PHE_486@HD2	PHE_486@CD2	0.0001	2.996	135.2301
TYR_83@HE2	PHE_486@HE2	PHE_486@CE2	0.0001	2.9855	137.4725
THR_324@HG21	VAL_503@HG22	VAL_503@CG2	0.0001	2.9958	141.284

#Acceptor	DonorH	Donor	Frac	AvgDist	AvgAng
THR_324@HG22	VAL_503@HG22	VAL_503@CG2	0.0001	2.9975	141.9244
THR_324@HG23	VAL_503@HG21	VAL_503@CG2	0.0001	2.893	140.7034
THR_324@HG23	VAL_503@HG12	VAL_503@CG1	0.0001	2.9942	136.7498
THR_324@HG23	VAL_503@HG23	VAL_503@CG2	0.0001	2.9879	149.2147
THR_324@HG1	VAL_503@HG13	VAL_503@CG1	0.0001	2.9828	138.5788
GLN_325@HB3	VAL_503@HG13	VAL_503@CG1	0.0001	2.9731	144.6424
GLN_325@HE21	VAL_503@HG21	VAL_503@CG2	0.0001	2.9947	147.279
GLN_325@HE21	VAL_503@HG22	VAL_503@CG2	0.0001	2.988	139.3946
GLN_325@HE21	VAL_503@HG23	VAL_503@CG2	0.0001	2.816	144.799
ASN_330@HD21	THR_500@HA	THR_500@CA	0.0001	2.901	143.2861
ASN_330@HD22	THR_500@HB	THR_500@CB	0.0001	2.8906	143.1138
LYS_353@HB3	TYR_505@HB3	TYR_505@CB	0.0001	2.9724	137.958
LYS_353@HD2	GLN_498@HE22	GLN_498@NE2	0.0001	2.8213	140.2612
LYS_353@HE2	GLN_498@HG2	GLN_498@CG	0.0001	2.8065	142.2572
LYS_353@HE2	GLY_496@H	GLY_496@N	0.0001	2.993	136.7793
LYS_353@HE2	ASN_501@HD21	ASN_501@ND2	0.0001	2.9222	135.8248
LYS_353@HZ1	GLN_498@HG2	GLN_498@CG	0.0001	2.7944	135.5879
LYS_353@HZ1	GLN_498@HE21	GLN_498@NE2	0.0001	2.9654	140.9285
LYS_353@HZ3	TYR_449@HH	TYR_449@OH	0.0001	2.9646	136.8547
LYS_353@HZ3	GLN_498@HB2	GLN_498@CB	0.0001	2.9512	145.906
ALA_386@HB2	TYR_505@HH	TYR_505@OH	0.0001	2.9136	140.5008

Table S3. Hydrogen bond analysis of S protein (DELTA PLUS)-ACE2 complex during the last 20 ns of MD simulation with S protein as acceptor and ACE2 as donor

#Acceptor	DonorH	Donor	Frac	AvgDist	AvgAng
GLN_498@OE1	GLN_42@HE21	GLN_42@NE2	0.7617	2.85	162.6269
PHE_486@O	TYR_83@HH	TYR_83@OH	0.7469	2.7524	155.9339
GLN_498@OE1	LYS_353@HZ2	LYS_353@NZ	0.5296	2.796	154.6215
GLY_496@O	LYS_353@HZ3	LYS_353@NZ	0.4418	2.8306	155.7951
GLN_498@OE1	LYS_353@HZ3	LYS_353@NZ	0.2943	2.7992	155.7832
GLY_496@O	LYS_353@HZ1	LYS_353@NZ	0.266	2.8247	156.8619
ALA_475@O	SER_19@HG	SER_19@OG	0.0892	2.7309	159.9891
GLN_493@OE1	LYS_31@HZ3	LYS_31@NZ	0.0727	2.7803	156.3293
ALA_475@O	GLN_24@HE22	GLN_24@NE2	0.0712	2.8541	158.5407
GLY_502@HA3	GLY_354@HA3	GLY_354@CA	0.0509	2.9316	142.7164
GLN_498@OE1	LYS_353@HZ1	LYS_353@NZ	0.0393	2.7963	153.3046
GLN_493@OE1	LYS_31@HZ1	LYS_31@NZ	0.0389	2.7776	155.531
ALA_475@O	SER_19@H3	SER_19@N	0.0362	2.8325	152.5473
GLY_496@O	LYS_353@HZ2	LYS_353@NZ	0.0337	2.8355	155.6598
TYR_489@HB3	LYS_31@HE3	LYS_31@CE	0.0311	2.9013	147.7997
TYR_505@HH	ARG_393@HH22	ARG_393@NH2	0.0292	2.9091	144.1933
ALA_475@O	SER_19@H1	SER_19@N	0.0285	2.8338	152.6704
ALA_475@O	SER_19@H2	SER_19@N	0.0279	2.8292	152.2275
TYR_489@HH	PHE_28@HB2	PHE_28@CB	0.0276	2.8704	148.7951
GLN_493@OE1	LYS_31@HZ2	LYS_31@NZ	0.0276	2.7634	156.2306
TYR_489@HB2	LYS_31@HE3	LYS_31@CE	0.0267	2.9055	148.0868
THR_500@HG1	ARG_357@HH21	ARG_357@NH2	0.0225	2.8592	139.5305
ASN_501@OD1	LYS_353@HZ3	LYS_353@NZ	0.0225	2.8465	146.2969
PHE_490@O	LYS_31@HZ1	LYS_31@NZ	0.0221	2.8647	155.6311
TYR_490@OH	HIE_34@HE2	HIE_34@NE2	0.0192	2.8435	152.6456
GLN_493@HE21	GLU_34@HB2	GLU_34@CB	0.0186	2.8777	145.2207
GLU_484@OE2	LYS_31@HZ1	LYS_31@NZ	0.0162	2.7928	156.5559
SER_477@OG	GLN_24@HE21	GLN_24@NE2	0.0146	2.8861	157.1783
PHE_490@O	LYS_31@HZ3	LYS_31@NZ	0.013	2.8611	157.4532
ASN_501@HD21	LYS_353@HD2	LYS_353@CD	0.0118	2.9233	146.88
THR_500@HG1	TYR_41@HH	TYR_41@OH	0.0103	2.8102	140.0509
GLU_484@OE2	LYS_31@HZ2	LYS_31@NZ	0.01	2.8132	154.5051
PHE_490@HB3	LYS_31@HE3	LYS_31@CE	0.01	2.9018	144.1297
GLN_493@HE22	LYS_31@HE2	LYS_31@CE	0.0095	2.9085	154.2185
TYR_489@HH	PHE_28@HD1	PHE_28@CD1	0.0083	2.874	148.4554
PHE_490@O	LYS_31@HZ2	LYS_31@NZ	0.008	2.8577	157.392
TYR_505@OH	ARG_393@HH22	ARG_393@NH2	0.0077	2.9061	151.2319
THR_500@O	ASN_330@HD21	ASN_330@ND2	0.0076	2.889	148.8327
TYR_489@HE1	PHE_28@HB2	PHE_28@CB	0.007	2.9387	140.7699
ASN_487@HD21	GLN_24@HG2	GLN_24@CG	0.007	2.8726	146.6654
ASN_501@OD1	LYS_353@HE3	LYS_353@CE	0.0069	2.9642	141.6958

#Acceptor	DonorH	Donor	Frac	AvgDist	AvgAng
TYR_489@HH	TYR_83@HH	TYR_83@OH	0.0056	2.9113	143.0294
SER_477@OG	SER_19@HG	SER_19@OG	0.0053	2.7736	159.3709
GLU_484@OE2	LYS_31@HZ3	LYS_31@NZ	0.0052	2.7987	153.1001
LEU_492@O	LYS_31@HZ1	LYS_31@NZ	0.0049	2.834	146.2359
GLN_493@HE22	LYS_31@HG3	LYS_31@CG	0.0046	2.9074	146.7257
SER_477@OG	SER_19@H2	SER_19@N	0.0043	2.8827	151.0749
ASN_501@HD21	LYS_353@HZ3	LYS_353@NZ	0.0043	2.9263	147.3254
PHE_456@HE2	LYS_31@HD2	LYS_31@CD	0.004	2.9596	144.6522
SER_477@OG	SER_19@H1	SER_19@N	0.004	2.88	149.4937
TYR_489@HD1	LYS_31@HE3	LYS_31@CE	0.004	2.9277	148.0687
GLN_493@HE21	LYS_31@HE2	LYS_31@CE	0.0034	2.9143	152.4459
GLN_493@HE21	GLU_34@HA	GLU_34@CA	0.0033	2.8865	140.4119
LEU_455@HD21	HIE_34@HD2	HIE_34@CD2	0.0031	2.9526	143.8924
GLY_446@O	GLN_42@HE21	GLN_42@NE2	0.0031	2.8462	152.1806
PHE_486@H	LEU_79@HD22	LEU_79@CD2	0.0031	2.8983	154.559
TYR_449@OH	GLN_42@HE22	GLN_42@NE2	0.003	2.8788	160.1911
THR_500@HB	ASN_330@HD21	ASN_330@ND2	0.003	2.7325	141.843
THR_500@O	TYR_41@HH	TYR_41@OH	0.0029	2.8197	140.3216
PHE_486@HB3	LEU_79@HB3	LEU_79@CB	0.0027	2.9563	140.1469
PHE_456@HZ	LYS_31@HB2	LYS_31@CB	0.0024	2.9667	143.6434
TYR_489@HE1	PHE_28@HD1	PHE_28@CD1	0.0024	2.9559	146.1379
LEU_455@HD23	HIE_34@HD2	HIE_34@CD2	0.0024	2.9506	142.2451
THR_500@HG22	ARG_357@HH22	ARG_357@NH2	0.0022	2.8814	141.8752
TYR_449@HH	GLN_42@HE22	GLN_42@NE2	0.0022	2.8657	139.9421
SER_477@OG	SER_19@H3	SER_19@N	0.0022	2.8766	148.1033
THR_500@HG23	ARG_357@HH22	ARG_357@NH2	0.0022	2.8607	142.2146
PHE_486@HB3	LEU_79@HD23	LEU_79@CD2	0.0021	2.9483	143.4274
GLN_493@HE21	GLU_34@HB3	GLU_34@CB	0.0021	2.8802	147.8154
PHE_486@HB3	LEU_79@HD22	LEU_79@CD2	0.0021	2.9457	143.3842
GLN_493@HE21	HIE_34@HB2	HIE_34@CB	0.0021	2.8436	144.8066
PHE_486@HA	LEU_79@HD12	LEU_79@CD1	0.0019	2.9363	143.1053
GLU_484@OE1	LYS_31@HZ1	LYS_31@NZ	0.0019	2.8643	151.2437
LEU_455@HD22	HIE_34@HD2	HIE_34@CD2	0.0018	2.9326	140.5806
GLU_484@OE1	LYS_31@HZ2	LYS_31@NZ	0.0018	2.8657	145.9138
GLY_476@O	SER_19@HG	SER_19@OG	0.0018	2.8324	154.5037
THR_500@HG21	ARG_357@HH22	ARG_357@NH2	0.0018	2.8671	141.6625
ASN_501@HD21	LYS_353@HZ1	LYS_353@NZ	0.0016	2.9324	147.6596
ASN_487@OD1	GLN_24@HE21	GLN_24@NE2	0.0016	2.8524	155.2198
PHE_486@HE2	TYR_83@HA	TYR_83@CA	0.0015	2.9536	143.8536
GLN_498@HB3	LYS_353@HZ3	LYS_353@NZ	0.0015	2.873	139.8889
PHE_486@H	LEU_79@HD21	LEU_79@CD2	0.0015	2.8641	150.3868
ASN_501@OD1	LYS_353@HZ1	LYS_353@NZ	0.0015	2.8809	143.5074
GLN_493@HE22	HIE_34@HB3	HIE_34@CB	0.0014	2.9163	141.2822
PHE_486@HA	LEU_79@HD11	LEU_79@CD1	0.0014	2.9423	144.776
PHE_486@HB3	MET_82@HG3	MET_82@CG	0.0014	2.954	142.6347
PHE_456@HE2	LYS_31@HD3	LYS_31@CD	0.0013	2.9441	141.0005
PHE_486@HB3	LEU_79@HD21	LEU_79@CD2	0.0013	2.9483	143.336
PHE_486@H	LEU_79@HD23	LEU_79@CD2	0.0013	2.9122	150.053
PHE_490@H	LYS_31@HE3	LYS_31@CE	0.0013	2.9053	155.4732
ALA_475@HB1	GLN_24@HG2	GLN_24@CG	0.0012	2.9598	143.9654
GLY_502@H	GLY_354@HA3	GLY_354@CA	0.0011	2.8853	140.0995
ALA_475@HB3	GLN_24@HG2	GLN_24@CG	0.0011	2.9553	139.6264
SER_477@HG	SER_19@H2	SER_19@N	0.001	2.8986	143.9432
PHE_486@HA	LEU_79@HD13	LEU_79@CD1	0.001	2.9344	143.136
GLN_493@HE21	HIE_34@HB3	HIE_34@CB	0.001	2.8123	142.6308
ALA_475@HB2	GLN_24@HG2	GLN_24@CG	0.0009	2.9648	142.7728
ASN_487@HD21	GLN_24@HB3	GLN_24@CB	0.0009	2.8947	141.8748
PHE_490@HD2	LYS_31@HZ2	LYS_31@NZ	0.0009	2.7934	140.4045
LEU_455@HD21	LYS_31@HA	LYS_31@CA	0.0009	2.9584	141.652
LEU_455@HD22	LYS_31@HA	LYS_31@CA	0.0009	2.9309	142.8706
TYR_489@HH	GLN_24@HB3	GLN_24@CB	0.0009	2.9455	139.5012
PHE_456@HE2	LYS_31@HB2	LYS_31@CB	0.0008	2.9581	142.2351
PHE_486@HB2	TYR_83@HE1	TYR_83@CE1	0.0008	2.9312	140.4354
PHE_486@HD2	MET_82@HG2	MET_82@CG	0.0008	2.9465	144.7541
ASN_487@OD1	GLN_24@HE22	GLN_24@NE2	0.0008	2.8722	157.5241
TYR_489@HB3	LYS_31@HE2	LYS_31@CE	0.0008	2.9027	153.4334

#Acceptor	DonorH	Donor	Frac	AvgDist	AvgAng
TYR_490@HH	HIE_34@HE2	HIE_34@NE2	0.0008	2.8556	147.3363
PHE_456@HE2	LYS_31@HE2	LYS_31@CE	0.0008	2.9256	145.4956
PHE_486@HD2	MET_82@HB2	MET_82@CB	0.0008	2.9687	139.4599
ASN_501@OD1	LYS_353@HZ2	LYS_353@NZ	0.0008	2.8499	147.0682
LEU_455@HD23	LYS_31@HA	LYS_31@CA	0.0007	2.9653	140.5412
ALA_475@HB1	SER_19@HB2	SER_19@CB	0.0007	2.9518	140.5485
GLY_476@HA2	GLN_24@HE22	GLN_24@NE2	0.0007	2.9171	144.5766
GLY_476@HA2	SER_19@H3	SER_19@N	0.0007	2.8805	146.0407
LEU_455@HD12	HIE_34@HD2	HIE_34@CD2	0.0006	2.9128	138.83
LEU_455@HD21	LYS_31@HD3	LYS_31@CD	0.0006	2.9507	139.4919
PHE_456@HE1	THR_203@HG21	THR_203@CG2	0.0006	2.9698	140.6532
ALA_475@HB1	GLN_24@HA	GLN_24@CA	0.0006	2.9496	144.1276
ALA_475@HB3	SER_19@HB2	SER_19@CB	0.0006	2.948	144.4791
SER_477@HG	GLN_24@HE21	GLN_24@NE2	0.0006	2.9456	150.1385
GLU_484@OE1	LYS_31@HZ3	LYS_31@NZ	0.0006	2.8536	151.2224
GLN_493@HE21	LYS_31@HZ2	LYS_31@NZ	0.0006	2.8527	142.2417
GLN_498@HB3	LYS_353@HZ1	LYS_353@NZ	0.0006	2.8738	139.298
PHE_456@HE1	THR_203@HG23	THR_203@CG2	0.0006	2.947	139.4134
PHE_456@HE1	THR_203@HG22	THR_203@CG2	0.0006	2.9601	140.1919
SER_477@HG	SER_19@H1	SER_19@N	0.0006	2.9072	146.6717
ASN_487@HD22	GLN_24@HB3	GLN_24@CB	0.0006	2.9176	146.5044
PHE_490@HD2	LYS_31@HZ1	LYS_31@NZ	0.0006	2.853	140.5816
GLN_493@HE21	GLU_34@HG2	GLU_34@CG	0.0006	2.7922	145.6271
LEU_455@HD11	HIE_34@HD2	HIE_34@CD2	0.0006	2.9252	140.9257
ALA_475@HB3	GLN_24@HA	GLN_24@CA	0.0006	2.9344	142.1119
SER_477@HG	SER_19@HG	SER_19@OG	0.0006	2.8845	147.2817
ASN_487@HD21	GLN_24@HE22	GLN_24@NE2	0.0006	2.8448	146.6136
LEU_492@O	LYS_31@HZ3	LYS_31@NZ	0.0006	2.8355	140.7594
GLN_498@HE21	GLN_42@HE21	GLN_42@NE2	0.0006	2.8878	138.5443
THR_500@HG22	ASN_330@HD21	ASN_330@ND2	0.0006	2.9016	139.0798
THR_500@HG23	ASN_330@HD21	ASN_330@ND2	0.0006	2.8709	146.6314
ASN_501@HD21	LYS_353@HZ2	LYS_353@NZ	0.0006	2.9322	150.0548
TYR_473@HE2	THR_203@HG22	THR_203@CG2	0.0005	2.9462	140.8059
TYR_489@HE2	THR_203@HG21	THR_203@CG2	0.0005	2.9517	140.3534
GLN_493@HG3	HIE_34@HB3	HIE_34@CB	0.0005	2.955	139.2365
TYR_490@HE2	HIE_34@HE2	HIE_34@NE2	0.0004	2.919	143.7824
ALA_475@HB2	THR_203@HG22	THR_203@CG2	0.0004	2.9623	141.25
GLY_476@HA2	GLN_24@HE21	GLN_24@NE2	0.0004	2.8142	144.3313
GLY_485@HA2	LEU_79@HG	LEU_79@CG	0.0004	2.9625	139.003
PHE_486@HD1	MET_82@HG3	MET_82@CG	0.0004	2.9477	143.8501
LEU_492@O	LYS_31@HZ2	LYS_31@NZ	0.0004	2.8559	145.7755
GLN_493@HE21	LYS_31@HZ3	LYS_31@NZ	0.0004	2.9243	146.2707
GLN_498@HB2	LYS_353@HZ3	LYS_353@NZ	0.0004	2.9084	137.9377
GLN_498@HB3	LYS_353@HZ2	LYS_353@NZ	0.0004	2.8818	139.9277
THR_500@HG21	ASN_330@HD21	ASN_330@ND2	0.0004	2.7836	138.5448
LEU_455@HD13	HIE_34@HD2	HIE_34@CD2	0.0004	2.9537	139.5158
PHE_456@HZ	LYS_31@HD2	LYS_31@CD	0.0004	2.9659	146.3586
PHE_456@HE2	LYS_31@HG3	LYS_31@CG	0.0004	2.9586	142.2457
ALA_475@HB2	GLN_24@HA	GLN_24@CA	0.0004	2.9283	143.1111
GLY_476@HA2	SER_19@H2	SER_19@N	0.0004	2.8636	148.8319
SER_477@HB2	GLN_24@HE21	GLN_24@NE2	0.0004	2.8781	148.8998
GLY_485@HA2	LEU_79@HD12	LEU_79@CD1	0.0004	2.9306	144.3084
GLY_485@HA2	LEU_79@HD13	LEU_79@CD1	0.0004	2.9083	137.7341
TYR_489@HE1	PHE_28@HA	PHE_28@CA	0.0004	2.9485	139.5588
PHE_490@HB3	LYS_31@HE2	LYS_31@CE	0.0004	2.9209	141.0345
GLN_493@HE21	LYS_31@HZ1	LYS_31@NZ	0.0004	2.8691	145.8653
VAL_445@O	GLN_42@HE21	GLN_42@NE2	0.0003	2.9244	162.1188
TYR_490@HH	HIE_34@HB3	HIE_34@CB	0.0003	2.9423	149.9062
LEU_455@HD11	HIE_34@HE2	HIE_34@NE2	0.0003	2.8153	141.5463
LEU_455@HD13	HIE_34@HE2	HIE_34@NE2	0.0003	2.8752	141.1249
PHE_456@HZ	THR_203@HG23	THR_203@CG2	0.0003	2.9465	140.8937
SER_477@HG	SER_19@H3	SER_19@N	0.0003	2.8361	145.8822
PHE_486@HD2	MET_82@HB3	MET_82@CB	0.0003	2.9402	141.1693
ASN_487@HA	GLN_24@HG2	GLN_24@CG	0.0003	2.9292	142.3041
ASN_487@HD21	GLN_24@HE21	GLN_24@NE2	0.0003	2.92	142.4646
GLN_493@HE21	GLU_34@HG3	GLU_34@CG	0.0003	2.7572	144.7837

#Acceptor	DonorH	Donor	Frac	AvgDist	AvgAng
GLY_496@HA3	LYS_353@HD2	LYS_353@CD	0.0003	2.961	138.0924
GLN_498@HB2	LYS_353@HZ2	LYS_353@NZ	0.0003	2.8844	140.1964
GLN_498@HE21	TYR_41@HE2	TYR_41@CE2	0.0003	2.9098	145.1988
LEU_455@HD22	LYS_31@HE2	LYS_31@CE	0.0003	2.9085	151.553
LEU_455@HD23	LYS_31@HD3	LYS_31@CD	0.0003	2.9699	141.7042
ALA_475@O	GLN_24@HE21	GLN_24@NE2	0.0003	2.8733	145.5608
GLY_476@HA2	SER_19@HB3	SER_19@CB	0.0003	2.9412	149.2868
GLY_485@HA2	LEU_79@HD11	LEU_79@CD1	0.0003	2.9434	140.7895
PHE_486@HA	LEU_79@HD23	LEU_79@CD2	0.0003	2.9374	140.7439
TYR_489@HE2	THR_203@HG23	THR_203@CG2	0.0003	2.9497	139.8746
PHE_490@H	LYS_31@HE2	LYS_31@CE	0.0003	2.7908	153.8618
PHE_490@HD2	LYS_31@HZ3	LYS_31@NZ	0.0003	2.8855	143.2908
GLN_498@HB2	LYS_353@HZ1	LYS_353@NZ	0.0003	2.9013	138.277
GLN_498@NE2	GLN_42@HE21	GLN_42@NE2	0.0003	2.952	143.5371
GLN_498@HE21	LEU_221@HD23	LEU_221@CD2	0.0003	2.9331	139.4522
THR_500@OG1	TYR_41@HH	TYR_41@OH	0.0003	2.7828	148.826
ASN_501@HA	ASP_531@HB2	ASP_531@CB	0.0003	2.9791	148.7893
TYR_505@HD1	GLY_354@HA3	GLY_354@CA	0.0003	2.9442	138.6542
PHE_456@HZ	THR_203@HG21	THR_203@CG2	0.0003	2.9108	137.2239
PHE_456@HZ	LYS_31@HG3	LYS_31@CG	0.0003	2.9532	141.501
TYR_473@HE2	THR_203@HG21	THR_203@CG2	0.0003	2.9401	143.9598
TYR_473@HE2	THR_203@HG23	THR_203@CG2	0.0003	2.9705	151.6093
ALA_475@HB2	SER_19@HB2	SER_19@CB	0.0003	2.9708	139.017
ALA_475@HB2	THR_203@HG23	THR_203@CG2	0.0003	2.9555	144.7954
ALA_475@HB3	GLN_24@HE22	GLN_24@NE2	0.0003	2.9106	151.049
GLY_476@HA2	SER_19@H1	SER_19@N	0.0003	2.9095	142.3304
PHE_486@HA	LEU_79@HB3	LEU_79@CB	0.0003	2.9633	147.4196
PHE_486@HB2	TYR_83@HH	TYR_83@OH	0.0003	2.8181	143.352
PHE_486@HD1	LEU_79@HD22	LEU_79@CD2	0.0003	2.9659	139.1905
TYR_489@HD1	LYS_31@HG2	LYS_31@CG	0.0003	2.9765	145.9413
TYR_489@HE2	THR_203@HG22	THR_203@CG2	0.0003	2.9161	140.4646
PHE_490@HB3	LYS_31@HZ2	LYS_31@NZ	0.0003	2.7488	136.9723
PHE_490@O	LYS_31@HE3	LYS_31@CE	0.0003	2.9735	138.1705
ASN_501@HD21	LYS_353@HE3	LYS_353@CE	0.0003	2.8972	136.5399
ALA_475@HB1	SER_19@HG	SER_19@OG	0.0002	2.754	142.8996
ALA_475@HB1	THR_203@HG22	THR_203@CG2	0.0002	2.9628	142.2673
GLY_485@HA2	LEU_79@HD21	LEU_79@CD2	0.0002	2.9245	139.1427
GLY_485@HA3	LEU_79@HD21	LEU_79@CD2	0.0002	2.9285	145.5813
PHE_486@HA	LEU_79@HD22	LEU_79@CD2	0.0002	2.9675	153.5374
PHE_486@HA	PHE_28@HE1	PHE_28@CE1	0.0002	2.9524	145.2852
PHE_486@HB2	LEU_79@HD11	LEU_79@CD1	0.0002	2.9451	139.2443
PHE_486@HD1	LEU_79@HD23	LEU_79@CD2	0.0002	2.9685	138.3434
PHE_486@HD1	LEU_79@HD21	LEU_79@CD2	0.0002	2.9181	137.9441
PHE_486@HZ	ILE_21@HG22	ILE_21@CG2	0.0002	2.9677	137.4221
PHE_486@HZ	ILE_21@HB	ILE_21@CB	0.0002	2.9702	137.1145
TYR_489@HB3	LYS_31@HD2	LYS_31@CD	0.0002	2.9165	136.198
TYR_489@HE2	THR_203@HB	THR_203@CB	0.0002	2.9467	136.6897
GLN_493@HE22	LYS_31@HG2	LYS_31@CG	0.0002	2.9412	148.9568
GLN_498@HE21	LEU_221@HD21	LEU_221@CD2	0.0002	2.9079	140.4364
GLN_498@HE21	LEU_221@HD22	LEU_221@CD2	0.0002	2.9577	141.4534
PHE_456@HZ	THR_203@HG22	THR_203@CG2	0.0001	2.9589	138.3042
ALA_475@HB1	THR_203@HG23	THR_203@CG2	0.0001	2.9403	138.9847
ALA_475@HB2	GLN_24@HE22	GLN_24@NE2	0.0001	2.8833	138.0241
ALA_475@HB3	THR_203@HG22	THR_203@CG2	0.0001	2.9713	142.4842
GLY_476@O	SER_19@H1	SER_19@N	0.0001	2.8129	148.3096
SER_477@HB3	SER_19@H1	SER_19@N	0.0001	2.8896	147.6574
SER_477@HB3	SER_19@H2	SER_19@N	0.0001	2.8479	153.2609
GLY_485@HA2	LEU_79@HD22	LEU_79@CD2	0.0001	2.9075	143.1487
GLY_485@HA3	LEU_79@HD23	LEU_79@CD2	0.0001	2.9406	144.0634
GLY_485@HA3	LEU_79@HD22	LEU_79@CD2	0.0001	2.9431	137.4216
PHE_486@HB2	MET_82@HG3	MET_82@CG	0.0001	2.9707	146.8448
PHE_486@HB3	MET_82@HB3	MET_82@CB	0.0001	2.9547	136.5482
PHE_486@HB3	MET_82@HE3	MET_82@CE	0.0001	2.9323	141.0912
PHE_486@HE1	ILE_21@HG22	ILE_21@CG2	0.0001	2.9071	138.2061
PHE_486@HZ	ILE_21@HG23	ILE_21@CG2	0.0001	2.9538	140.3563
TYR_489@HB2	LYS_31@HE2	LYS_31@CE	0.0001	2.9135	142.6864

#Acceptor	DonorH	Donor	Frac	AvgDist	AvgAng
TYR_489@HD1	LYS_31@HE2	LYS_31@CE	0.0001	2.9685	137.083
TYR_489@OH	GLN_24@HE22	GLN_24@NE2	0.0001	2.9248	150.6566
PHE_490@HB3	LYS_31@HZ1	LYS_31@NZ	0.0001	2.9364	142.472
GLN_493@HE22	LYS_31@HD3	LYS_31@CD	0.0001	2.9473	141.7078
GLN_493@HE22	GLU_34@HB3	GLU_34@CB	0.0001	2.9574	146.7574
GLY_496@HA3	LYS_353@HD3	LYS_353@CD	0.0001	2.9627	136.1118
GLY_496@HA3	LYS_353@HZ2	LYS_353@NZ	0.0001	2.8882	147.8981
GLN_498@OE1	GLN_42@HE22	GLN_42@NE2	0.0001	2.9287	153.4892
THR_500@OG1	ARG_357@HH22	ARG_357@NH2	0.0001	2.8851	137.7324
TYR_505@HH	ARG_393@HH12	ARG_393@NH1	0.0001	2.8669	143.2007
TYR_505@HE2	GLU_213@HG2	GLU_213@CG	0.0001	2.9374	138.0287
ARG_403@HH12	HIE_34@HE1	HIE_34@CE1	0.0001	2.9203	137.4055
TYR_449@HH	LYS_353@HZ3	LYS_353@NZ	0.0001	2.9782	140.7679
LEU_455@HD23	LYS_31@HB2	LYS_31@CB	0.0001	2.9344	138.3504
LEU_455@HD23	LYS_31@HG2	LYS_31@CG	0.0001	2.9762	141.5878
ALA_475@HB1	THR_203@HG21	THR_203@CG2	0.0001	2.9645	147.3316
ALA_475@HB2	SER_19@HG	SER_19@OG	0.0001	2.8738	168.3474
ALA_475@HB3	THR_203@HG23	THR_203@CG2	0.0001	2.9367	140.1343
ALA_475@HB3	GLU_199@HG2	GLU_199@CG	0.0001	2.8954	137.1358
ALA_475@HB3	SER_19@HB3	SER_19@CB	0.0001	2.9647	141.2835
GLY_476@HA2	GLN_24@HG2	GLN_24@CG	0.0001	2.99	137.4262
GLY_476@HA2	SER_19@HG	SER_19@OG	0.0001	2.9854	149.9233
GLY_476@HA3	SER_19@HB3	SER_19@CB	0.0001	2.9539	144.5986
GLY_476@O	SER_19@H3	SER_19@N	0.0001	2.8288	160.4226
SER_477@H	GLN_24@HE21	GLN_24@NE2	0.0001	2.9763	139.6423
LYS_478@HE2	MET_82@HE3	MET_82@CE	0.0001	2.8942	138.9289
GLU_484@OE2	LYS_31@HE2	LYS_31@CE	0.0001	2.9591	150.0526
GLY_485@HA2	MET_82@HE3	MET_82@CE	0.0001	2.9429	140.2759
GLY_485@HA3	LEU_79@HD11	LEU_79@CD1	0.0001	2.9704	148.8234
PHE_486@HA	LEU_79@HD21	LEU_79@CD2	0.0001	2.8917	142.8044
PHE_486@HB2	MET_82@HE1	MET_82@CE	0.0001	2.9743	144.2113
PHE_486@HB2	LEU_79@HD13	LEU_79@CD1	0.0001	2.9751	146.213
PHE_486@HB2	LEU_79@HB3	LEU_79@CB	0.0001	2.9309	136.5832
PHE_486@HB3	MET_82@HE2	MET_82@CE	0.0001	2.941	138.5892
PHE_486@HD1	MET_82@HE2	MET_82@CE	0.0001	2.9993	143.0728
PHE_486@HE1	ILE_21@HG21	ILE_21@CG2	0.0001	2.9625	135.6652
PHE_486@HZ	ILE_21@HG21	ILE_21@CG2	0.0001	2.8512	139.7958
PHE_486@HD2	MET_82@HG3	MET_82@CG	0.0001	2.9017	138.9832
PHE_486@O	GLN_24@HE22	GLN_24@NE2	0.0001	2.8225	149.2634
ASN_487@ND2	GLN_24@HE21	GLN_24@NE2	0.0001	2.852	153.7898
ASN_487@ND2	GLN_24@HE22	GLN_24@NE2	0.0001	2.9504	166.4325
TYR_489@HD1	LYS_31@HD2	LYS_31@CD	0.0001	2.9492	136.7002
GLN_493@HG3	HIE_34@HE2	HIE_34@NE2	0.0001	2.6572	138.0086
GLN_493@OE1	LYS_31@HE2	LYS_31@CE	0.0001	2.988	146.1966
GLN_493@HE21	LYS_31@HD2	LYS_31@CD	0.0001	2.9916	145.8675
GLN_493@HE21	LYS_31@HG3	LYS_31@CG	0.0001	2.8905	146.2895
GLN_498@HE22	GLN_42@HE21	GLN_42@NE2	0.0001	2.9323	143.0358
THR_500@HG1	ARG_357@HH22	ARG_357@NH2	0.0001	2.8423	137.5348
ASN_501@HA	TYR_41@HH	TYR_41@OH	0.0001	2.9735	141.336
ASN_501@OD1	TYR_41@HH	TYR_41@OH	0.0001	2.8299	144.1006
TYR_505@HD1	LYS_353@HA	LYS_353@CA	0.0001	2.9736	146.0777
TYR_505@HD2	LYS_353@HG2	LYS_353@CG	0.0001	2.981	137.4576
GLY_447@HA2	GLN_42@HE21	GLN_42@NE2	0.0001	2.9888	136.6312
GLY_447@HA3	GLN_42@HE21	GLN_42@NE2	0.0001	2.9478	145.6086
TYR_449@HE2	LEU_215@HD21	LEU_215@CD2	0.0001	2.9837	137.8593
LEU_455@HD12	HIE_34@HE2	HIE_34@NE2	0.0001	2.7513	141.0951
LEU_455@HD21	LYS_31@HB2	LYS_31@CB	0.0001	2.9618	153.388
LEU_455@HD22	LYS_31@HG2	LYS_31@CG	0.0001	2.9747	143.6599
LEU_455@HD22	LYS_31@HD3	LYS_31@CD	0.0001	2.9559	146.9374
LEU_455@HD22	LYS_31@HD2	LYS_31@CD	0.0001	2.9542	140.5601
LEU_455@HD23	LYS_31@HG3	LYS_31@CG	0.0001	2.9884	137.792
LEU_455@HD23	LYS_31@HD2	LYS_31@CD	0.0001	2.9833	154.9432
PHE_456@HE2	LYS_31@HG2	LYS_31@CG	0.0001	2.936	140.3013
ALA_475@HB1	THR_203@HG1	THR_203@OG1	0.0001	2.9983	151.7762
ALA_475@HB1	GLN_24@HG3	GLN_24@CG	0.0001	2.9874	142.9422
ALA_475@HB1	THR_203@HB	THR_203@CB	0.0001	2.8559	138.5303

#Acceptor	DonorH	Donor	Frac	AvgDist	AvgAng
ALA_475@HB2	THR_203@HG21	THR_203@CG2	0.0001	2.9285	140.8499
ALA_475@HB2	SER_19@H2	SER_19@N	0.0001	2.9386	137.826
ALA_475@HB2	GLN_24@HB3	GLN_24@CB	0.0001	2.9404	137.6659
ALA_475@HB2	GLU_199@HG2	GLU_199@CG	0.0001	2.9658	135.6623
ALA_475@HB3	THR_203@HG21	THR_203@CG2	0.0001	2.9731	139.458
ALA_475@HB3	GLN_24@HG3	GLN_24@CG	0.0001	2.9921	141.128
ALA_475@HB3	SER_19@H3	SER_19@N	0.0001	2.9919	143.0893
GLY_476@H	GLN_24@HG2	GLN_24@CG	0.0001	2.6831	138.9757
GLY_476@HA2	SER_19@HB2	SER_19@CB	0.0001	2.948	147.4706
GLY_476@HA3	GLN_24@HE22	GLN_24@NE2	0.0001	2.7748	136.6382
GLY_476@O	SER_19@H2	SER_19@N	0.0001	2.7655	147.4564
SER_477@H	SER_19@HB3	SER_19@CB	0.0001	2.8721	141.0348
SER_477@HB3	SER_19@HG	SER_19@OG	0.0001	2.802	143.3746
SER_477@HB3	GLN_24@HE21	GLN_24@NE2	0.0001	2.9862	138.0429
SER_477@HG	SER_19@HB2	SER_19@CB	0.0001	2.9172	140.4556
LYS_478@HE2	MET_82@HE1	MET_82@CE	0.0001	2.9867	135.7628
GLY_485@HA2	MET_82@HE1	MET_82@CE	0.0001	2.8719	137.1384
GLY_485@HA2	LEU_79@HD23	LEU_79@CD2	0.0001	2.9569	136.0214
GLY_485@HA3	LEU_79@HD13	LEU_79@CD1	0.0001	2.9391	146.6317
PHE_486@H	LEU_79@HD13	LEU_79@CD1	0.0001	2.9681	155.4683
PHE_486@HA	PHE_28@HD1	PHE_28@CD1	0.0001	2.9699	135.8478
PHE_486@HA	TYR_83@HH	TYR_83@OH	0.0001	2.6123	140.637
PHE_486@HA	PHE_28@HB2	PHE_28@CB	0.0001	2.9816	145.4058
PHE_486@HB3	LEU_79@HD13	LEU_79@CD1	0.0001	2.9378	139.0487
PHE_486@HD1	MET_82@HE3	MET_82@CE	0.0001	2.9762	146.9878
PHE_486@HD1	LEU_79@HD12	LEU_79@CD1	0.0001	2.9677	136.3812
PHE_486@HD1	LEU_79@HD11	LEU_79@CD1	0.0001	2.9609	146.7274
PHE_486@HE1	MET_82@HE1	MET_82@CE	0.0001	2.9663	152.6114
PHE_486@HE1	LEU_79@HD22	LEU_79@CD2	0.0001	2.9927	149.827
PHE_486@HE1	MET_82@HE2	MET_82@CE	0.0001	2.9824	153.7346
PHE_486@HE1	ILE_21@HG23	ILE_21@CG2	0.0001	2.9432	143.9999
PHE_486@HE2	MET_82@HB3	MET_82@CB	0.0001	2.9272	151.5617
PHE_486@HE2	PRO_84@HD3	PRO_84@CD	0.0001	2.9452	138.0964
PHE_486@HE2	MET_82@HG3	MET_82@CG	0.0001	2.947	136.9381
PHE_486@HE2	MET_82@HB2	MET_82@CB	0.0001	2.9808	143.2266
PHE_486@HD2	LEU_79@HD11	LEU_79@CD1	0.0001	2.9892	135.1371
ASN_487@HD22	GLN_24@HE21	GLN_24@NE2	0.0001	2.8084	140.5718
ASN_487@HD22	GLN_24@HG2	GLN_24@CG	0.0001	2.9992	137.1202
ASN_487@O	GLN_24@HE22	GLN_24@NE2	0.0001	2.9742	142.7022
TYR_489@HB3	LYS_31@HG2	LYS_31@CG	0.0001	2.9722	142.4048
TYR_489@HB3	LYS_31@HZ1	LYS_31@NZ	0.0001	2.8708	136.6345
TYR_489@HB3	LYS_31@HG3	LYS_31@CG	0.0001	2.9838	139.5712
TYR_489@HD1	PHE_28@HB2	PHE_28@CB	0.0001	2.8658	140.8775
TYR_489@OH	TYR_83@HH	TYR_83@OH	0.0001	2.8593	137.7247
TYR_489@HD2	LYS_31@HE3	LYS_31@CE	0.0001	2.9305	151.2229
PHE_490@HB3	LYS_31@HZ3	LYS_31@NZ	0.0001	2.9503	137.5527
PHE_490@HD2	LYS_31@HE2	LYS_31@CE	0.0001	2.8106	137.1622
GLN_493@HG2	LYS_31@HZ1	LYS_31@NZ	0.0001	2.9966	144.9149
GLN_493@HG2	LYS_31@HZ3	LYS_31@NZ	0.0001	2.986	139.4922
GLN_493@HG3	HIE_34@HD2	HIE_34@CD2	0.0001	2.9082	138.9442
GLN_493@HG3	HIE_34@HB2	HIE_34@CB	0.0001	2.9991	136.242
GLN_493@NE2	LYS_31@HZ1	LYS_31@NZ	0.0001	2.8597	136.6004
GLN_493@HE21	LYS_31@HE3	LYS_31@CE	0.0001	2.9223	140.5127
GLN_493@HE22	LYS_31@HE3	LYS_31@CE	0.0001	2.9953	143.8377
GLN_493@HE22	GLU_34@HB2	GLU_34@CB	0.0001	2.8887	162.5548
GLY_496@HA3	LYS_353@HZ3	LYS_353@NZ	0.0001	2.926	141.5763
GLY_496@HA3	ASP_214@HB2	ASP_214@CB	0.0001	2.9973	136.3663
GLY_496@HA3	LYS_353@HZ1	LYS_353@NZ	0.0001	2.9747	136.7692
GLN_498@HG2	TYR_41@HE2	TYR_41@CE2	0.0001	2.9922	143.8445
GLN_498@HE21	TYR_41@HD2	TYR_41@CD2	0.0001	2.9752	138.9267
THR_500@HA	ASN_330@HD21	ASN_330@ND2	0.0001	2.9962	146.2513
THR_500@HB	ARG_357@HH21	ARG_357@NH2	0.0001	2.9375	136.8901
THR_500@HG1	TYR_41@HE2	TYR_41@CE2	0.0001	2.8893	138.9589
THR_500@HG1	LEU_221@HD23	LEU_221@CD2	0.0001	2.8372	151.011
VAL_503@HG11	GLN_325@HE22	GLN_325@NE2	0.0001	2.7305	144.5766
VAL_503@HG13	GLN_325@HE22	GLN_325@NE2	0.0001	2.8216	136.53

#Acceptor	DonorH	Donor	Frac	AvgDist	AvgAng
VAL_503@HG22	GLN_325@HE22	GLN_325@NE2	0.0001	2.7744	135.0187
TYR_505@HE1	GLY_354@HA3	GLY_354@CA	0.0001	2.9922	136.4845
TYR_505@HE2	LYS_353@HE3	LYS_353@CE	0.0001	2.917	150.2936

Table S4. Hydrogen bond analysis of S protein (DELTA PLUS)-ACE2 complex during the last 20 ns of MD simulation with S protein as donor and ACE2 as acceptor.

#Acceptor	DonorH	Donor	Frac	AvgDist	AvgAng
LYS_353@O	GLY_502@H	GLY_502@N	0.7457	2.8646	161.8695
GLN_42@OE1	GLN_498@HE21	GLN_498@NE2	0.5394	2.8778	162.0907
ASP_355@OD1	THR_500@HG1	THR_500@OG1	0.5362	2.7176	161.986
GLU_37@OE1	TYR_505@HH	TYR_505@OH	0.3708	2.7545	158.3531
GLU_35@OE1	GLN_493@HE21	GLN_493@NE2	0.324	2.8351	161.1112
GLU_35@OE2	GLN_493@HE21	GLN_493@NE2	0.3167	2.8327	160.5401
TYR_41@OH	THR_500@HG1	THR_500@OG1	0.3115	2.7967	159.4389
ASP_38@OD2	TYR_449@HH	TYR_449@OH	0.2225	2.6572	165.2554
GLN_24@OE1	ASN_487@HD21	ASN_487@ND2	0.2041	2.8419	154.2866
GLN_24@OE1	ASN_487@HD22	ASN_487@ND2	0.1991	2.8281	159.9813
TYR_41@HH	THR_500@HG1	THR_500@OG1	0.0753	2.8559	145.6898
GLY_354@HA3	GLY_502@HA3	GLY_502@CA	0.0466	2.929	142.0585
GLU_37@OE2	TYR_505@HH	TYR_505@OH	0.0416	2.7415	158.9966
TYR_83@OH	ASN_487@HD22	ASN_487@ND2	0.0343	2.9069	158.8668
GLN_24@O	TYR_489@HH	TYR_489@OH	0.0285	2.8375	146.1125
PHE_28@HB2	TYR_489@HH	TYR_489@OH	0.0236	2.7997	146.9589
ARG_357@HH21	THR_500@HG1	THR_500@OG1	0.019	2.8474	140.4169
LYS_31@HE3	TYR_489@HB3	TYR_489@CB	0.0172	2.8971	146.0249
ASN_330@HD21	THR_500@HB	THR_500@CB	0.0154	2.8729	148.8812
TYR_83@OH	TYR_489@HH	TYR_489@OH	0.0138	2.8786	145.4164
GLU_35@HB2	GLN_493@HE21	GLN_493@NE2	0.0129	2.8044	144.4727
LYS_31@HE3	PHE_490@HB3	PHE_490@CB	0.012	2.9147	147.2295
GLN_24@HG2	ASN_487@HD21	ASN_487@ND2	0.0115	2.8459	147.0977
ASP_38@OD1	TYR_449@HH	TYR_449@OH	0.0111	2.7789	159.8995
TYR_83@HH	TYR_489@HH	TYR_489@OH	0.0106	2.8668	143.9956
HIE_34@O	GLN_493@HE21	GLN_493@NE2	0.0096	2.8603	158.2311
HIE_34@HB2	GLN_493@HE21	GLN_493@NE2	0.0083	2.8558	153.1276
GLU_35@OE1	GLN_493@HE22	GLN_493@NE2	0.008	2.8266	158.906
LYS_31@HE3	TYR_489@HB2	TYR_489@CB	0.0075	2.8893	144.6467
LYS_353@HD2	ASN_501@HD21	ASN_501@ND2	0.0072	2.8639	140.2198
HIE_34@HB3	GLN_493@HE21	GLN_493@NE2	0.0071	2.8389	147.1803
PHE_28@HD1	TYR_489@HH	TYR_489@OH	0.0067	2.8022	144.713
PHE_28@HB2	TYR_489@HE1	TYR_489@CE1	0.0059	2.9491	143.6993
LYS_31@HD2	PHE_456@HE2	PHE_456@CE2	0.0056	2.9468	142.6428
GLN_24@HE21	SER_477@H	SER_477@N	0.0053	2.853	148.8498
GLU_35@HG2	GLN_493@HE21	GLN_493@NE2	0.005	2.8284	144.9133
LYS_353@HZ3	ASN_501@HD21	ASN_501@ND2	0.0049	2.9196	143.2186
GLU_35@OE2	GLN_493@HE22	GLN_493@NE2	0.0045	2.8167	160.2129
GLN_24@OE1	SER_477@H	SER_477@N	0.0036	2.8966	156.5255
GLU_35@HA	GLN_493@HE21	GLN_493@NE2	0.0034	2.8697	143.8172
LEU_79@HD22	PHE_486@HB3	PHE_486@CB	0.0031	2.9414	141.5071
LEU_79@HD23	PHE_486@HB3	PHE_486@CB	0.0029	2.9472	139.7617
GLN_24@HE22	GLY_476@HA2	GLY_476@CA	0.0029	2.904	144.5995
LYS_31@HB2	PHE_456@HZ	PHE_456@CZ	0.0028	2.9503	143.7167
GLU_35@HG3	GLN_493@HE21	GLN_493@NE2	0.0025	2.8292	145.8733
HIE_34@O	GLN_493@HE22	GLN_493@NE2	0.0024	2.8673	151.2401
LYS_353@HZ1	ASN_501@HD21	ASN_501@ND2	0.0024	2.9481	144.8508
PHE_28@HD1	TYR_489@HE1	TYR_489@CE1	0.0024	2.9477	141.5601
ALA_562@O	TYR_505@HH	TYR_505@OH	0.0023	2.799	154.2864
ASP_355@HB2	ASN_501@HA	ASN_501@CA	0.0022	2.9531	140.9498
ASP_355@OD2	THR_500@HG1	THR_500@OG1	0.0022	2.7343	163.0719
LYS_31@HZ2	PHE_490@HD2	PHE_490@CD2	0.0022	2.913	155.3666
LEU_79@HD21	PHE_486@HB3	PHE_486@CB	0.0021	2.9517	140.274
GLU_37@CD	TYR_505@HH	TYR_505@OH	0.0021	2.9674	141.8368
TYR_83@HA	PHE_486@HE2	PHE_486@CE2	0.0019	2.9373	143.565
LEU_79@HB3	PHE_486@HB3	PHE_486@CB	0.0018	2.9523	139.6199
LYS_353@HZ3	GLN_498@HB2	GLN_498@CB	0.0018	2.9334	146.0938
LYS_353@HZ3	GLN_498@HB3	GLN_498@CB	0.0018	2.9046	143.9938
LEU_79@HD12	PHE_486@HA	PHE_486@CA	0.0016	2.9341	142.6928

#Acceptor	DonorH	Donor	Frac	AvgDist	AvgAng
HIE_34@HD2	LEU_455@HD22	LEU_455@CD2	0.0015	2.9401	141.6774
ARG_357@HH22	THR_500@HG23	THR_500@CG2	0.0015	2.9094	142.5465
LEU_79@HD11	PHE_486@HA	PHE_486@CA	0.0015	2.9258	140.8005
GLN_24@HE21	GLY_476@HA2	GLY_476@CA	0.0014	2.9278	148.7741
LYS_31@HD3	PHE_456@HE2	PHE_456@CE2	0.0014	2.9548	142.3731
HIE_34@HD2	LEU_455@HD21	LEU_455@CD2	0.0014	2.9324	141.1251
GLN_24@NE2	ASN_487@HD21	ASN_487@ND2	0.0014	2.9323	154.3663
TYR_41@HE2	THR_500@HG1	THR_500@OG1	0.0013	2.8683	141.9563
LEU_79@HD13	PHE_486@HA	PHE_486@CA	0.0013	2.9433	142.6886
ARG_357@HH22	THR_500@HG21	THR_500@CG2	0.0013	2.9059	141.2752
LYS_31@HB2	PHE_456@HE2	PHE_456@CE2	0.0013	2.9523	141.5388
LYS_31@HE3	PHE_490@H	PHE_490@N	0.0013	2.85	144.1528
GLU_35@HB3	GLN_493@HE21	GLN_493@NE2	0.0013	2.7804	144.5164
GLN_42@HE22	TYR_449@HH	TYR_449@OH	0.0013	2.9013	138.1338
PHE_28@HA	TYR_489@HE1	TYR_489@CE1	0.0012	2.9397	142.5587
HIE_34@HD2	LEU_455@HD23	LEU_455@CD2	0.0012	2.945	142.2385
GLN_24@HG2	ALA_475@HB3	ALA_475@CB	0.0011	2.9577	140.3279
LYS_31@HG3	GLN_493@HE22	GLN_493@NE2	0.001	2.8362	140.1682
ARG_357@HH22	THR_500@HG22	THR_500@CG2	0.001	2.9083	141.0212
GLN_24@HE21	ASN_487@HD21	ASN_487@ND2	0.001	2.9003	146.7817
GLN_24@HE22	ASN_487@HD21	ASN_487@ND2	0.001	2.9518	147.2901
LYS_31@HZ1	PHE_490@HD2	PHE_490@CD2	0.001	2.9136	149.9808
LYS_353@HD2	GLY_496@HA3	GLY_496@CA	0.001	2.9476	140.7766
THR_27@HG21	PHE_456@HE1	PHE_456@CE1	0.0009	2.9523	141.3087
GLN_24@HG2	ALA_475@HB2	ALA_475@CB	0.0008	2.97	141.1918
LYS_31@HZ3	PHE_490@HD2	PHE_490@CD2	0.0008	2.9225	149.8294
HIE_34@HD2	LEU_455@HD12	LEU_455@CD1	0.0008	2.9276	140.4254
THR_27@HG22	PHE_456@HE1	PHE_456@CE1	0.0008	2.9608	140.9979
THR_27@HG23	PHE_456@HE1	PHE_456@CE1	0.0008	2.9346	140.6422
LYS_31@HE2	PHE_490@HB3	PHE_490@CB	0.0008	2.9314	145.959
LEU_79@HD22	PHE_486@H	PHE_486@N	0.0008	2.763	140.8188
ARG_393@HH22	TYR_505@HH	TYR_505@OH	0.0008	2.8443	139.2554
SER_19@H3	GLY_476@HA2	GLY_476@CA	0.0007	2.9315	144.7675
GLN_24@HG2	ALA_475@HB1	ALA_475@CB	0.0007	2.9415	139.0451
THR_27@HG22	TYR_489@HE2	TYR_489@CE2	0.0007	2.9554	143.7762
THR_27@HG23	TYR_489@HE2	TYR_489@CE2	0.0007	2.9685	141.6838
LYS_31@O	GLN_493@HE21	GLN_493@NE2	0.0007	2.9086	151.0236
TYR_83@HE1	PHE_486@HB2	PHE_486@CB	0.0007	2.9494	145.8423
LYS_353@HZ2	GLN_498@HB2	GLN_498@CB	0.0007	2.9279	143.0811
SER_19@HG	GLY_476@HA2	GLY_476@CA	0.0006	2.9158	143.0573
SER_19@O	SER_477@HG	SER_477@OG	0.0006	2.7817	151.501
GLN_24@HB3	ASN_487@HD21	ASN_487@ND2	0.0006	2.8582	140.7524
GLN_42@HE21	TYR_449@HH	TYR_449@OH	0.0006	2.8405	152.8571
LEU_79@HD21	PHE_486@H	PHE_486@N	0.0006	2.7786	140.184
ARG_357@HH21	THR_500@HB	THR_500@CB	0.0006	2.9146	140.3985
HIE_34@HE2	LEU_455@HD13	LEU_455@CD1	0.0006	2.9132	141.4809
MET_82@HG2	PHE_486@HD2	PHE_486@CD2	0.0006	2.9393	148.5074
MET_82@HG3	PHE_486@HB3	PHE_486@CB	0.0006	2.9566	142.2645
TYR_83@HH	ASN_487@HA	ASN_487@CA	0.0006	2.9251	137.9052
SER_19@HB2	ALA_475@HB3	ALA_475@CB	0.0006	2.9398	146.617
GLN_24@HG2	ASN_487@HD22	ASN_487@ND2	0.0006	2.8473	140.0199
GLN_24@CD	ASN_487@HD22	ASN_487@ND2	0.0006	2.9632	141.0629
GLN_24@NE2	SER_477@H	SER_477@N	0.0006	2.9561	146.8479
THR_27@HG21	TYR_489@HE2	TYR_489@CE2	0.0006	2.9424	140.9048
THR_27@HG23	PHE_456@HZ	PHE_456@CZ	0.0006	2.9449	142.6209
LYS_31@HE2	TYR_489@HB3	TYR_489@CB	0.0006	2.8318	143.5287
LEU_79@HB3	PHE_486@HA	PHE_486@CA	0.0006	2.957	139.9004
LYS_353@HZ2	ASN_501@HD21	ASN_501@ND2	0.0006	2.9472	139.4837
SER_19@HB2	ALA_475@HB1	ALA_475@CB	0.0005	2.9359	143.5322
GLN_24@HA	ALA_475@HB2	ALA_475@CB	0.0005	2.9359	142.2693
GLN_24@HE21	GLY_476@HA3	GLY_476@CA	0.0005	2.9636	142.5421
THR_27@HG22	TYR_473@HE2	TYR_473@CE2	0.0005	2.9482	145.2395
LYS_31@HE2	PHE_456@HE2	PHE_456@CE2	0.0005	2.9202	143.5743
HIE_34@HD2	LEU_455@HD13	LEU_455@CD1	0.0005	2.9319	141.7644
TYR_41@HH	THR_500@HB	THR_500@CB	0.0005	2.9457	138.7949
LEU_79@HD11	GLY_485@HA2	GLY_485@CA	0.0005	2.9282	141.6001

#Acceptor	DonorH	Donor	Frac	AvgDist	AvgAng
LEU_79@HD13	GLY_485@HA2	GLY_485@CA	0.0005	2.9591	141.8722
MET_82@HB3	PHE_486@HD2	PHE_486@CD2	0.0005	2.9419	144.1209
SER_19@HB3	GLY_476@HA2	GLY_476@CA	0.0004	2.9138	142.0516
GLN_24@HA	ALA_475@HB3	ALA_475@CB	0.0004	2.9439	140.8209
GLN_24@HA	ALA_475@HB1	ALA_475@CB	0.0004	2.9329	140.5454
THR_27@HG22	ALA_475@HB2	ALA_475@CB	0.0004	2.9553	140.6346
PHE_28@HD1	PHE_486@HA	PHE_486@CA	0.0004	2.9614	143.1493
LYS_31@HG3	PHE_456@HE2	PHE_456@CE2	0.0004	2.9705	142.7041
LYS_31@HZ2	PHE_490@HB3	PHE_490@CB	0.0004	2.9034	164.1125
HIE_34@HE2	LEU_455@HD11	LEU_455@CD1	0.0004	2.8999	140.1724
LEU_79@HD12	GLY_485@HA2	GLY_485@CA	0.0004	2.8998	139.9699
LEU_79@HD23	PHE_486@HD1	PHE_486@CD1	0.0004	2.9506	143.262
ARG_357@HH22	THR_500@HG1	THR_500@OG1	0.0004	2.8344	153.6208
SER_19@H1	GLY_476@HA2	GLY_476@CA	0.0004	2.9308	140.6889
SER_19@H2	GLY_476@HA2	GLY_476@CA	0.0004	2.8821	143.4103
SER_19@HG	ALA_475@HB3	ALA_475@CB	0.0004	2.929	156.5068
THR_27@HG21	TYR_473@HE2	TYR_473@CE2	0.0004	2.9655	142.6016
PHE_28@HE1	PHE_486@HA	PHE_486@CA	0.0004	2.975	148.9641
LYS_31@HA	LEU_455@HD22	LEU_455@CD2	0.0004	2.9012	138.2636
LYS_31@HG2	TYR_489@HD1	TYR_489@CD1	0.0004	2.9655	143.7304
LYS_31@HG3	PHE_456@HZ	PHE_456@CZ	0.0004	2.9338	139.3692
LYS_31@HZ1	PHE_490@HB3	PHE_490@CB	0.0004	2.9576	158.6229
HIE_34@HB3	GLN_493@HG3	GLN_493@CG	0.0004	2.9774	142.0232
HIE_34@HB3	GLN_493@HE22	GLN_493@NE2	0.0004	2.9023	142.138
GLU_35@CD	GLN_493@HE21	GLN_493@NE2	0.0004	2.9487	145.0771
LEU_79@HD21	PHE_486@HD1	PHE_486@CD1	0.0004	2.9406	145.9087
THR_27@HG21	PHE_456@HZ	PHE_456@CZ	0.0003	2.9368	137.4422
THR_27@HG22	PHE_456@HZ	PHE_456@CZ	0.0003	2.9605	141.7286
LYS_31@HD3	LEU_455@HD22	LEU_455@CD2	0.0003	2.9573	141.3431
LYS_31@HE2	LEU_455@HD22	LEU_455@CD2	0.0003	2.9074	145.71
LYS_31@HE2	GLN_493@HE22	GLN_493@NE2	0.0003	2.8604	139.7394
LYS_31@O	GLN_493@HE22	GLN_493@NE2	0.0003	2.8779	145.8615
HIE_34@HE2	LEU_455@HD12	LEU_455@CD1	0.0003	2.9097	147.2645
GLN_42@NE2	TYR_449@HH	TYR_449@OH	0.0003	2.8702	160.3342
LEU_79@HD23	PHE_486@H	PHE_486@N	0.0003	2.7612	143.3177
ASN_330@HD21	THR_500@HG23	THR_500@CG2	0.0003	2.8861	142.1
GLY_354@HA3	GLY_502@H	GLY_502@N	0.0003	2.8381	141.7612
SER_19@HB2	GLY_476@HA2	GLY_476@CA	0.0003	2.8882	140.0593
SER_19@HG	ALA_475@HB1	ALA_475@CB	0.0003	2.9015	148.8556
ILE_21@HG22	PHE_486@HE1	PHE_486@CE1	0.0003	2.9276	139.4943
GLN_24@HB3	ASN_487@HD22	ASN_487@ND2	0.0003	2.8456	140.6882
GLN_24@HG3	ASN_487@HD21	ASN_487@ND2	0.0003	2.8342	148.4843
THR_27@HG23	TYR_473@HE2	TYR_473@CE2	0.0003	2.8987	143.262
LYS_31@HA	LEU_455@HD21	LEU_455@CD2	0.0003	2.9288	137.14
LYS_31@HE3	TYR_489@HD1	TYR_489@CD1	0.0003	2.9362	139.1708
HIE_34@HD2	LEU_455@HD11	LEU_455@CD1	0.0003	2.9483	139.298
TYR_83@HH	PHE_486@HB2	PHE_486@CB	0.0003	2.8953	147.7178
LYS_353@HZ1	GLN_498@HB2	GLN_498@CB	0.0003	2.9216	139.1715
LYS_353@HZ2	GLN_498@HB3	GLN_498@CB	0.0003	2.8792	144.6262
SER_19@O	SER_477@H	SER_477@N	0.0003	2.9502	145.3239
ILE_21@HG23	PHE_486@HZ	PHE_486@CZ	0.0003	2.9369	140.5528
GLN_24@NE2	ASN_487@HD22	ASN_487@ND2	0.0003	2.9168	141.2719
THR_27@HG23	ALA_475@HB1	ALA_475@CB	0.0003	2.9608	140.5863
LYS_31@HD3	LEU_455@HD21	LEU_455@CD2	0.0003	2.9648	138.0408
LYS_31@HZ3	GLN_493@HE21	GLN_493@NE2	0.0003	2.8894	138.0343
LEU_79@HD22	PHE_486@HA	PHE_486@CA	0.0003	2.9402	142.2471
MET_82@HB3	PHE_486@HB3	PHE_486@CB	0.0003	2.9295	139.798
TYR_83@HH	PHE_486@HA	PHE_486@CA	0.0003	2.8632	139.8404
ASN_330@HD21	THR_500@HG21	THR_500@CG2	0.0003	2.8915	143.2212
SER_19@HG	SER_477@HG	SER_477@OG	0.0002	2.8469	137.456
ILE_21@HB	PHE_486@HZ	PHE_486@CZ	0.0002	2.9648	139.3811
ILE_21@HG22	PHE_486@HZ	PHE_486@CZ	0.0002	2.9789	138.625
GLN_24@OE1	LYS_478@HZ3	LYS_478@NZ	0.0002	2.8845	140.5679
GLN_24@HE22	GLY_476@HA3	GLY_476@CA	0.0002	2.8978	144.1689
THR_27@HG21	ALA_475@HB1	ALA_475@CB	0.0002	2.9702	140.2013
THR_27@HG22	ALA_475@HB3	ALA_475@CB	0.0002	2.973	137.7062

#Acceptor	DonorH	Donor	Frac	AvgDist	AvgAng
LYS_31@HG2	GLN_493@HE22	GLN_493@NE2	0.0002	2.9102	140.6752
LYS_31@HZ3	PHE_490@HB3	PHE_490@CB	0.0002	2.9242	149.2656
ASP_38@CG	TYR_449@HH	TYR_449@OH	0.0002	2.9826	149.2794
GLN_42@HE21	GLY_447@HA3	GLY_447@CA	0.0002	2.9582	144.3228
LEU_45@HD21	GLN_498@HE21	GLN_498@NE2	0.0002	2.9001	142.6398
LEU_45@HD23	GLN_498@HE21	GLN_498@NE2	0.0002	2.9416	141.3903
LEU_79@HD21	GLY_485@HA2	GLY_485@CA	0.0002	2.9478	143.1619
LEU_79@HD22	PHE_486@HD1	PHE_486@CD1	0.0002	2.9848	143.6293
SER_19@OG	SER_477@HG	SER_477@OG	0.0001	2.7932	156.6464
SER_19@HG	ALA_475@HB2	ALA_475@CB	0.0001	2.9178	146.3168
GLN_24@HB3	TYR_489@HH	TYR_489@OH	0.0001	2.9277	135.4175
GLN_24@HE21	PHE_486@HE1	PHE_486@CE1	0.0001	2.9235	143.4159
GLN_24@HE22	SER_477@H	SER_477@N	0.0001	2.8913	149.8073
LYS_31@HD2	PHE_456@HZ	PHE_456@CZ	0.0001	2.9509	141.3766
LYS_31@HD2	TYR_489@HB3	TYR_489@CB	0.0001	2.9462	141.8983
LYS_31@HD3	LEU_455@HD23	LEU_455@CD2	0.0001	2.9228	137.2354
GLU_35@H	GLN_493@HE21	GLN_493@NE2	0.0001	2.9521	162.5284
GLN_42@OE1	TYR_449@HH	TYR_449@OH	0.0001	2.909	143.6085
LEU_79@HD13	GLY_485@HA3	GLY_485@CA	0.0001	2.9649	142.3092
LEU_79@HD21	GLY_485@HA3	GLY_485@CA	0.0001	2.9231	137.9805
MET_82@HB2	PHE_486@HB3	PHE_486@CB	0.0001	2.9598	138.7062
MET_82@HB2	PHE_486@HD2	PHE_486@CD2	0.0001	2.9639	137.4125
TYR_83@HH	PHE_486@HD2	PHE_486@CD2	0.0001	2.966	144.6757
GLY_354@HA3	TYR_505@HD1	TYR_505@CD1	0.0001	2.926	137.9715
ILE_21@HG21	LYS_478@HE3	LYS_478@CE	0.0001	2.8568	147.3588
ILE_21@HG21	PHE_486@HZ	PHE_486@CZ	0.0001	2.9014	147.0823
ILE_21@HG21	PHE_486@HE1	PHE_486@CE1	0.0001	2.9461	138.4748
GLN_24@HG2	ASN_487@HA	ASN_487@CA	0.0001	2.9631	158.2187
GLN_24@OE1	LYS_478@HZ1	LYS_478@NZ	0.0001	2.7788	146.2934
GLN_24@OE1	LYS_478@HZ2	LYS_478@NZ	0.0001	2.852	159.8205
GLN_24@HE21	ASN_487@HD22	ASN_487@ND2	0.0001	2.8674	136.8845
GLN_24@HE22	ALA_475@HB3	ALA_475@CB	0.0001	2.9207	142.1349
GLN_24@HE22	ASN_487@HA	ASN_487@CA	0.0001	2.9775	150.2591
THR_27@HB	ALA_475@HB2	ALA_475@CB	0.0001	2.962	135.6361
THR_27@HG23	ALA_475@HB3	ALA_475@CB	0.0001	2.9558	143.2219
THR_27@HG23	ALA_475@HB2	ALA_475@CB	0.0001	2.9064	139.9062
ASP_30@HB3	PHE_456@HZ	PHE_456@CZ	0.0001	2.992	141.549
LYS_31@HA	LEU_455@HD23	LEU_455@CD2	0.0001	2.9062	138.8643
LYS_31@HG2	LEU_455@HD23	LEU_455@CD2	0.0001	2.9624	137.5776
LYS_31@HG3	LEU_455@HD22	LEU_455@CD2	0.0001	2.9852	136.5063
LYS_31@HG3	TYR_489@HB3	TYR_489@CB	0.0001	2.9153	137.6398
LYS_31@HE2	PHE_490@H	PHE_490@N	0.0001	2.7458	139.0401
LYS_31@HE2	TYR_489@HD1	TYR_489@CD1	0.0001	2.9816	140.6477
LYS_31@HZ2	GLN_493@HE21	GLN_493@NE2	0.0001	2.7996	145.5352
HIE_34@HE2	GLN_493@HG3	GLN_493@CG	0.0001	2.8885	166.1311
HIE_34@HD2	GLN_493@HG3	GLN_493@CG	0.0001	2.9484	140.0183
ASP_38@HB2	TYR_505@HH	TYR_505@OH	0.0001	2.8801	140.6832
TYR_41@HE2	GLN_498@HE21	GLN_498@NE2	0.0001	2.8432	141.8108
GLN_42@HG2	GLN_498@HE21	GLN_498@NE2	0.0001	2.9106	148.1852
LEU_45@HD22	GLN_498@HE21	GLN_498@NE2	0.0001	2.6193	135.7806
LEU_79@HG	GLY_485@HA2	GLY_485@CA	0.0001	2.969	137.5303
LEU_79@HD11	PHE_486@HB2	PHE_486@CB	0.0001	2.9645	137.4337
LEU_79@HD12	PHE_486@HB2	PHE_486@CB	0.0001	2.9855	140.4561
LEU_79@HD22	GLY_485@HA3	GLY_485@CA	0.0001	2.9319	148.6603
LEU_79@HD23	PHE_486@HA	PHE_486@CA	0.0001	2.8629	139.6098
LEU_79@HD23	GLY_485@HA2	GLY_485@CA	0.0001	2.9941	139.8508
MET_82@HG3	PHE_486@HD2	PHE_486@CD2	0.0001	2.9247	143.5971
MET_82@HE1	GLY_485@HA2	GLY_485@CA	0.0001	2.9404	145.7253
MET_82@HE2	PHE_486@HD1	PHE_486@CD1	0.0001	2.9672	140.0558
TYR_83@HE2	ASN_487@HD22	ASN_487@ND2	0.0001	2.8795	143.7345
ASN_330@HD21	THR_500@HG22	THR_500@CG2	0.0001	2.8195	154.5195
LYS_353@HD3	GLY_496@HA3	GLY_496@CA	0.0001	2.9702	148.887
LYS_353@HZ1	GLN_498@HB3	GLN_498@CB	0.0001	2.9736	142.1171
ARG_357@HH22	THR_500@HB	THR_500@CB	0.0001	2.9116	137.6746
SER_19@H1	SER_477@HB3	SER_477@CB	0.0001	2.8753	148.0122
SER_19@H2	SER_477@HB3	SER_477@CB	0.0001	2.7104	147.12

#Acceptor	DonorH	Donor	Frac	AvgDist	AvgAng
SER_19@H3	ALA_475@HB1	ALA_475@CB	0.0001	2.9849	144.9198
SER_19@HB2	SER_477@HA	SER_477@CA	0.0001	2.9836	140.9217
SER_19@HB2	ALA_475@HB2	ALA_475@CB	0.0001	2.9409	143.4888
SER_19@HB3	GLY_476@HA3	GLY_476@CA	0.0001	2.9838	138.5254
SER_19@HB3	ALA_475@HB1	ALA_475@CB	0.0001	2.8942	136.1844
SER_19@OG	ASN_487@HD21	ASN_487@ND2	0.0001	2.9	140.9847
SER_19@OG	SER_477@H	SER_477@N	0.0001	2.9963	135.4734
ILE_21@HG22	LYS_478@HZ3	LYS_478@NZ	0.0001	2.9852	147.296
ILE_21@HG23	PHE_486@HE1	PHE_486@CE1	0.0001	2.8881	137.8229
ILE_21@HG12	PHE_486@HZ	PHE_486@CZ	0.0001	2.9214	150.0773
GLU_199@HG2	ALA_475@HB2	ALA_475@CB	0.0001	2.9214	135.726
GLU_199@HG2	ALA_475@HB3	ALA_475@CB	0.0001	2.9892	158.4207
GLN_24@HB3	ALA_475@HB2	ALA_475@CB	0.0001	2.9622	140.306
GLN_24@HG2	GLY_476@H	GLY_476@N	0.0001	2.6378	142.5597
GLN_24@HG3	ALA_475@HB1	ALA_475@CB	0.0001	2.9722	139.0334
GLN_24@HE21	LYS_478@HZ3	LYS_478@NZ	0.0001	2.9774	146.5251
GLN_24@HE22	ALA_475@HB2	ALA_475@CB	0.0001	2.9064	140.0795
THR_27@HA	PHE_456@HZ	PHE_456@CZ	0.0001	2.9407	135.7287
THR_27@HB	ALA_475@HB1	ALA_475@CB	0.0001	2.9827	137.3533
THR_27@HG21	ALA_475@HB2	ALA_475@CB	0.0001	2.9703	166.5768
THR_27@HG22	ALA_475@HB1	ALA_475@CB	0.0001	2.96	140.7449
PHE_28@HA	TYR_489@HH	TYR_489@OH	0.0001	2.9853	152.1561
PHE_28@HB2	TYR_489@HD1	TYR_489@CD1	0.0001	2.908	147.7125
PHE_28@HB2	PHE_486@HA	PHE_486@CA	0.0001	2.968	143.7004
LYS_31@HB2	LEU_455@HD21	LEU_455@CD2	0.0001	2.8759	140.8908
LYS_31@HB2	LEU_455@HD23	LEU_455@CD2	0.0001	2.9982	140.6849
LYS_31@HG2	LEU_455@HD22	LEU_455@CD2	0.0001	2.9669	146.4018
LYS_31@HG2	PHE_456@HZ	PHE_456@CZ	0.0001	2.9539	140.1566
LYS_31@HG2	PHE_456@HE2	PHE_456@CE2	0.0001	2.9946	138.8892
LYS_31@HG3	LEU_455@HD23	LEU_455@CD2	0.0001	2.9796	135.3757
LYS_31@HG3	LEU_455@HD21	LEU_455@CD2	0.0001	2.8983	135.8335
LYS_31@HD2	LEU_455@HD23	LEU_455@CD2	0.0001	2.9943	147.6328
LYS_31@HD3	GLN_493@HE22	GLN_493@NE2	0.0001	2.8574	137.1457
LYS_31@HD3	TYR_489@HB3	TYR_489@CB	0.0001	2.9831	140.3697
LYS_31@HE2	PHE_490@HD2	PHE_490@CD2	0.0001	2.9288	155.7327
LYS_31@HE2	LEU_455@HD23	LEU_455@CD2	0.0001	2.8461	138.6133
LYS_31@HE2	GLN_493@HE21	GLN_493@NE2	0.0001	2.8706	139.3472
HIE_34@HE1	ARG_403@HH12	ARG_403@NH1	0.0001	2.8957	137.6996
HIE_34@HE2	TYR_453@HE2	TYR_453@CE2	0.0001	2.9522	136.664
HIE_34@HD2	TYR_453@HE2	TYR_453@CE2	0.0001	2.998	143.6574
GLU_35@N	GLN_493@HE21	GLN_493@NE2	0.0001	2.9831	146.3237
GLU_37@HG2	TYR_505@HE2	TYR_505@CE2	0.0001	2.9757	140.2224
ASP_38@HB3	TYR_449@HH	TYR_449@OH	0.0001	2.8977	143.7069
TYR_41@HD2	GLN_498@HE21	GLN_498@NE2	0.0001	2.9922	135.4949
GLN_42@NE2	GLN_498@HE21	GLN_498@NE2	0.0001	2.9367	139.0831
GLN_42@HE21	GLN_498@HE22	GLN_498@NE2	0.0001	2.9363	137.4352
LEU_45@HD21	THR_500@HG23	THR_500@CG2	0.0001	2.9293	139.8341
LEU_45@HD21	THR_500@HG1	THR_500@OG1	0.0001	2.8423	150.5823
LEU_45@HD21	THR_500@HG22	THR_500@CG2	0.0001	2.9811	141.6654
LEU_45@HD22	THR_500@HG1	THR_500@OG1	0.0001	2.8377	146.7542
LEU_79@HA	PHE_486@HB3	PHE_486@CB	0.0001	2.975	136.7518
LEU_79@HG	PHE_486@HD1	PHE_486@CD1	0.0001	2.985	145.7967
LEU_79@HD11	PHE_486@HD1	PHE_486@CD1	0.0001	2.9127	136.5247
LEU_79@HD12	GLY_485@HA3	GLY_485@CA	0.0001	2.9047	142.841
LEU_79@HD12	PHE_486@HD1	PHE_486@CD1	0.0001	2.9327	166.0909
LEU_79@HD12	PHE_486@HD2	PHE_486@CD2	0.0001	2.9999	159.8704
LEU_79@HD13	PHE_486@HD1	PHE_486@CD1	0.0001	2.9715	138.1426
LEU_79@HD13	PHE_486@HB2	PHE_486@CB	0.0001	2.8782	139.4572
LEU_79@HD21	PHE_486@HA	PHE_486@CA	0.0001	2.9701	135.0502
LEU_79@HD22	GLY_485@HA2	GLY_485@CA	0.0001	2.996	142.2138
LEU_79@HD23	GLY_485@HA3	GLY_485@CA	0.0001	2.9519	139.5702
MET_82@HB2	PHE_486@HE2	PHE_486@CE2	0.0001	2.9274	137.6187
MET_82@HG3	PHE_486@HB2	PHE_486@CB	0.0001	2.9643	136.7597
MET_82@HE1	PHE_486@HE1	PHE_486@CE1	0.0001	2.8779	135.2679
TYR_83@HH	ASN_487@HD22	ASN_487@ND2	0.0001	2.676	144.02
TYR_83@HE2	ASN_487@HD21	ASN_487@ND2	0.0001	2.8944	149.0634

#Acceptor	DonorH	Donor	Frac	AvgDist	AvgAng
PRO_260@HD3	PHE_486@HE2	PHE_486@CE2	0.0001	2.8853	136.0338
GLN_501@HE22	VAL_503@HG11	VAL_503@CG1	0.0001	2.9994	135.9487
ASN_330@HD21	THR_500@HA	THR_500@CA	0.0001	2.9907	136.6161
LYS_353@HE3	ASN_501@HD21	ASN_501@ND2	0.0001	2.9225	137.869
ARG_357@HH21	THR_500@HG21	THR_500@CG2	0.0001	2.9508	139.1807

Table S5A. List of atom-atom interactions (Hydrogen bonds) across protein-ligand interface in ACE2 (Chain A)-Spike Protein (Chain B) (Delta variant) complex from PDBsum server.

	ACE2					SARS-CoV-2 S protein (Delta)				
Sl. No	Atom no.	Atom name	Res name	Res no.	Hydrogen bonds	Atom no.	Atom name	Res name	Res no.	Distance
1	1	N	SER	19	<-->	6025	O	ALA	475	3.04
2	45	OE1	GLN	24	<-->	6106	ND2	ASN	487	2.79
3	94	OD2	ASP	30	<-->	5538	NZ	LYS	417	2.68
4	103	NZ	LYS	31	<-->	6083	OE2	GLU	484	2.8
5	103	NZ	LYS	31	<-->	6158	OE1	GLN	493	2.85
6	141	OE2	GLU	35	<-->	6159	NE2	GLN	493	2.74
7	163	OD2	ASP	38	<-->	5787	OH	TYR	449	2.53
8	192	OH	TYR	41	<-->	6215	OG1	THR	500	2.74
9	192	OH	TYR	41	<-->	6215	OG1	THR	500	2.74
10	203	NE2	GLN	42	<-->	5767	O	GLY	446	2.83
11	203	NE2	GLN	42	<-->	5787	OH	TYR	449	2.85
12	530	OH	TYR	83	<-->	6105	OD1	ASN	487	3.3
13	2725	O	LYS	353	<-->	6226	N	GLY	502	2.82
14	2723	NZ	LYS	353	<-->	6183	O	GLY	496	2.84
15	2723	NZ	LYS	353	<-->	6200	OE1	GLN	498	2.78

Table S5B. List of atom-atom interactions (Non-bonded contacts) across the protein-ligand interface in ACE2 (Chain A)-Spike Protein (Chain B) (Delta variant) complex from PDBsum server

	ACE2					SARS-CoV-2 S protein (Delta)				
Sl.no.	Atom no.	Atom name	Res name	Res no.	Non-bonded contacts	Atom no.	Atom name	Res name	Res no.	Distance
1	1	N	SER	19	<-->	6025	O	ALA	475	3.04
2	43	CG	GLN	24	<-->	6025	O	ALA	475	3.44
3	43	CG	GLN	24	<-->	6106	ND2	ASN	487	3.89
4	44	CD	GLN	24	<-->	6104	CG	ASN	487	3.86
5	44	CD	GLN	24	<-->	6106	ND2	ASN	487	3.09
6	45	OE1	GLN	24	<-->	6027	CA	GLY	476	3.34
7	45	OE1	GLN	24	<-->	6104	CG	ASN	487	3.77
8	45	OE1	GLN	24	<-->	6106	ND2	ASN	487	2.79
9	46	NE2	GLN	24	<-->	6106	ND2	ASN	487	3.38
10	68	C	THR	27	<-->	6123	CE2	TYR	489	3.74
11	69	O	THR	27	<-->	5860	CZ	PHE	456	3.55
12	69	O	THR	27	<-->	6123	CE2	TYR	489	3.6
13	67	OG1	THR	27	<-->	5858	CD1	PHE	456	3.6
14	67	OG1	THR	27	<-->	5859	CE1	PHE	456	3.07
15	67	OG1	THR	27	<-->	5860	CZ	PHE	456	3.38
16	67	OG1	THR	27	<-->	6008	CE2	TYR	473	3.85
17	67	OG1	THR	27	<-->	6124	CD2	TYR	489	3.79
18	67	OG1	THR	27	<-->	6123	CE2	TYR	489	3.49
19	66	CG2	THR	27	<-->	6023	CB	ALA	475	3.31
20	70	N	PHE	28	<-->	6122	OH	TYR	489	3.69
21	71	CA	PHE	28	<-->	6122	OH	TYR	489	3.46
22	72	CB	PHE	28	<-->	6122	OH	TYR	489	3.43
23	95	C	ASP	30	<-->	5851	CD2	LEU	455	3.85
24	96	O	ASP	30	<-->	5851	CD2	LEU	455	3.74
25	92	CG	ASP	30	<-->	5538	NZ	LYS	417	3.8
26	93	OD1	ASP	30	<-->	5850	CD1	LEU	455	3.79
27	94	OD2	ASP	30	<-->	5537	CE	LYS	417	3.19
28	94	OD2	ASP	30	<-->	5538	NZ	LYS	417	2.68

ACE2					Non-bonded contacts	SARS-CoV-2 S protein (Delta)				
Sl.no.	Atom no.	Atom name	Res name	Res no.		Atom no.	Atom name	Res name	Res no.	Distance
29	94	OD2	ASP	30	<-->	5849	CG	LEU	455	3.86
30	94	OD2	ASP	30	<-->	5850	CD1	LEU	455	3.89
31	94	OD2	ASP	30	<-->	5859	CE1	PHE	456	3.44
32	101	CD	LYS	31	<-->	6158	OE1	GLN	493	3.43
33	102	CE	LYS	31	<-->	6083	OE2	GLU	484	3.16
34	102	CE	LYS	31	<-->	6158	OE1	GLN	493	3.7
35	103	NZ	LYS	31	<-->	6081	CD	GLU	484	3.63
36	103	NZ	LYS	31	<-->	6082	OE1	GLU	484	3.66
37	103	NZ	LYS	31	<-->	6083	OE2	GLU	484	2.8
38	103	NZ	LYS	31	<-->	6157	CD	GLN	493	3.86
39	103	NZ	LYS	31	<-->	6158	OE1	GLN	493	2.85
40	127	CB	HIS	34	<-->	5830	OH	TYR	453	3.67
41	128	CG	HIS	34	<-->	5830	OH	TYR	453	3.81
42	129	ND1	HIS	34	<-->	5850	CD1	LEU	455	3.78
43	129	ND1	HIS	34	<-->	5851	CD2	LEU	455	3.57
44	132	CD2	HIS	34	<-->	5830	OH	TYR	453	3.35
45	130	CE1	HIS	34	<-->	5850	CD1	LEU	455	3.49
46	131	NE2	HIS	34	<-->	5850	CD1	LEU	455	3.69
47	139	CD	GLU	35	<-->	6159	NE2	GLN	493	3.69
48	141	OE2	GLU	35	<-->	6157	CD	GLN	493	3.49
49	141	OE2	GLU	35	<-->	6158	OE1	GLN	493	3.33
50	141	OE2	GLU	35	<-->	6159	NE2	GLN	493	2.74
51	154	OE1	GLU	37	<-->	6249	CE2	TYR	505	3.87
52	155	OE2	GLU	37	<-->	6250	CD2	TYR	505	3.76
53	155	OE2	GLU	37	<-->	6249	CE2	TYR	505	3.34
54	161	CG	ASP	38	<-->	5785	CE1	TYR	449	3.71
55	161	CG	ASP	38	<-->	5787	OH	TYR	449	3.37
56	162	OD1	ASP	38	<-->	5785	CE1	TYR	449	3.64
57	162	OD1	ASP	38	<-->	5786	CZ	TYR	449	3.88
58	162	OD1	ASP	38	<-->	5787	OH	TYR	449	3.49
59	162	OD1	ASP	38	<-->	6181	CA	GLY	496	3.53
60	163	OD2	ASP	38	<-->	5785	CE1	TYR	449	3.26
61	163	OD2	ASP	38	<-->	5786	CZ	TYR	449	3.31
62	163	OD2	ASP	38	<-->	5787	OH	TYR	449	2.53
63	189	CD1	TYR	41	<-->	6199	CD	GLN	498	3.77
64	189	CD1	TYR	41	<-->	6200	OE1	GLN	498	3.49
65	190	CE1	TYR	41	<-->	6198	CG	GLN	498	3.88
66	190	CE1	TYR	41	<-->	6199	CD	GLN	498	3.76
67	190	CE1	TYR	41	<-->	6200	OE1	GLN	498	3.53
68	190	CE1	TYR	41	<-->	6222	OD1	ASN	501	3.61
69	193	CE2	TYR	41	<-->	6222	OD1	ASN	501	3.67
70	191	CZ	TYR	41	<-->	6215	OG1	THR	500	3.81
71	191	CZ	TYR	41	<-->	6222	OD1	ASN	501	3.24
72	192	OH	TYR	41	<-->	6216	C	THR	500	3.52
73	192	OH	TYR	41	<-->	6217	O	THR	500	3.6
74	192	OH	TYR	41	<-->	6213	CB	THR	500	3.43
75	192	OH	TYR	41	<-->	6215	OG1	THR	500	2.74
76	192	OH	TYR	41	<-->	6218	N	ASN	501	3.71
77	192	OH	TYR	41	<-->	6222	OD1	ASN	501	3.33
78	201	CD	GLN	42	<-->	5767	O	GLY	446	3.83
79	201	CD	GLN	42	<-->	5787	OH	TYR	449	3.85
80	201	CD	GLN	42	<-->	6201	NE2	GLN	498	3.47
81	202	OE1	GLN	42	<-->	6201	NE2	GLN	498	3.58
82	203	NE2	GLN	42	<-->	5766	C	GLY	446	3.66
83	203	NE2	GLN	42	<-->	5767	O	GLY	446	2.83
84	203	NE2	GLN	42	<-->	5786	CZ	TYR	449	3.73
85	203	NE2	GLN	42	<-->	5787	OH	TYR	449	2.85
86	203	NE2	GLN	42	<-->	6201	NE2	GLN	498	3.05

ACE2					Non-bonded contacts	SARS-CoV-2 S protein (Delta)				
Sl.no.	Atom no.	Atom name	Res name	Res no.		Atom no.	Atom name	Res name	Res no.	Distance
87	517	CB	MET	82	<-->	6095	CE1	PHE	486	3.52
88	517	CB	MET	82	<-->	6096	CZ	PHE	486	3.67
89	519	SD	MET	82	<-->	6093	CG	PHE	486	3.77
90	519	SD	MET	82	<-->	6094	CD1	PHE	486	3.62
91	519	SD	MET	82	<-->	6095	CE1	PHE	486	3.85
92	528	CE1	TYR	83	<-->	6095	CE1	PHE	486	3.81
93	528	CE1	TYR	83	<-->	6105	OD1	ASN	487	3.6
94	529	CZ	TYR	83	<-->	6095	CE1	PHE	486	3.87
95	529	CZ	TYR	83	<-->	6105	OD1	ASN	487	3.89
96	530	OH	TYR	83	<-->	6094	CD1	PHE	486	3.79
97	530	OH	TYR	83	<-->	6095	CE1	PHE	486	3.7
98	530	OH	TYR	83	<-->	6105	OD1	ASN	487	3.3
99	530	OH	TYR	83	<-->	6122	OH	TYR	489	3.76
100	2551	OD1	ASN	330	<-->	6212	CA	THR	500	3.49
101	2551	OD1	ASN	330	<-->	6217	O	THR	500	3.73
102	2551	OD1	ASN	330	<-->	6213	CB	THR	500	3.23
103	2551	OD1	ASN	330	<-->	6214	CG2	THR	500	3.29
104	2718	CA	LYS	353	<-->	6244	CG	TYR	505	3.52
105	2718	CA	LYS	353	<-->	6245	CD1	TYR	505	3.79
106	2718	CA	LYS	353	<-->	6250	CD2	TYR	505	3.58
107	2724	C	LYS	353	<-->	6243	CB	TYR	505	3.85
108	2724	C	LYS	353	<-->	6244	CG	TYR	505	3.5
109	2724	C	LYS	353	<-->	6245	CD1	TYR	505	3.32
110	2724	C	LYS	353	<-->	6246	CE1	TYR	505	3.79
111	2725	O	LYS	353	<-->	6219	CA	ASN	501	3.64
112	2725	O	LYS	353	<-->	6224	C	ASN	501	3.59
113	2725	O	LYS	353	<-->	6220	CB	ASN	501	3.84
114	2725	O	LYS	353	<-->	6226	N	GLY	502	2.82
115	2725	O	LYS	353	<-->	6227	CA	GLY	502	3.61
116	2725	O	LYS	353	<-->	6229	O	GLY	502	3.63
117	2725	O	LYS	353	<-->	6243	CB	TYR	505	3.36
118	2725	O	LYS	353	<-->	6244	CG	TYR	505	3.47
119	2725	O	LYS	353	<-->	6245	CD1	TYR	505	3.37
120	2719	CB	LYS	353	<-->	6221	CG	ASN	501	3.87
121	2719	CB	LYS	353	<-->	6222	OD1	ASN	501	3.84
122	2719	CB	LYS	353	<-->	6243	CB	TYR	505	3.89
123	2721	CD	LYS	353	<-->	6183	O	GLY	496	3.88
124	2721	CD	LYS	353	<-->	6200	OE1	GLN	498	3.7
125	2721	CD	LYS	353	<-->	6221	CG	ASN	501	3.73
126	2721	CD	LYS	353	<-->	6222	OD1	ASN	501	3.54
127	2721	CD	LYS	353	<-->	6223	ND2	ASN	501	3.52
128	2722	CE	LYS	353	<-->	6183	O	GLY	496	3.8
129	2722	CE	LYS	353	<-->	6200	OE1	GLN	498	3.78
130	2723	NZ	LYS	353	<-->	6181	CA	GLY	496	3.82
131	2723	NZ	LYS	353	<-->	6182	C	GLY	496	3.71
132	2723	NZ	LYS	353	<-->	6183	O	GLY	496	2.84
133	2723	NZ	LYS	353	<-->	6199	CD	GLN	498	3.64
134	2723	NZ	LYS	353	<-->	6200	OE1	GLN	498	2.78
135	2723	NZ	LYS	353	<-->	6201	NE2	GLN	498	3.64
136	2726	N	GLY	354	<-->	6245	CD1	TYR	505	3.65
137	2726	N	GLY	354	<-->	6246	CE1	TYR	505	3.72
138	2728	C	GLY	354	<-->	6226	N	GLY	502	3.64
139	2728	C	GLY	354	<-->	6227	CA	GLY	502	3.7
140	2729	O	GLY	354	<-->	6226	N	GLY	502	3.8
141	2729	O	GLY	354	<-->	6227	CA	GLY	502	3.46
142	2730	N	ASP	355	<-->	6226	N	GLY	502	3.7
143	2732	CB	ASP	355	<-->	6217	O	THR	500	3.38
144	2733	CG	ASP	355	<-->	6217	O	THR	500	3.32

ACE2					Non-bonded contacts	SARS-CoV-2 S protein (Delta)				
Sl.no.	Atom no.	Atom name	Res name	Res no.		Atom no.	Atom name	Res name	Res no.	Distance
145	2735	OD2	ASP	355	<-->	6217	O	THR	500	3.4
146	2735	OD2	ASP	355	<-->	6213	CB	THR	500	3.85
147	2757	NH2	ARG	357	<-->	6213	CB	THR	500	3.42
148	2757	NH2	ARG	357	<-->	6215	OG1	THR	500	3.65
149	2757	NH2	ARG	357	<-->	6214	CG2	THR	500	3.7

Table S5C. List of atom-atom interactions (Salt bridge) across the protein-ligand interface in ACE2 (Chain A)-Spike Protein (Chain B) (Delta variant) complex from PDBsum server.

ACE2					Salt bridge	SARS-CoV-2 S protein (Delta)				
Sl.no.	Atom no.	Atom name	Res name	Res no.		Atom no.	Atom name	Res name	Res no.	Distance
1	94	OD2	ASP	30	<-->	5538	NZ	LYS	417	2.68
2	103	NZ	LYS	31	<-->	6082	OE1	GLU	484	2.8

Table S6A. List of atom-atom interactions (Hydrogen bonds) across the protein-ligand interface in ACE2 (Chain A)-Spike Protein (Chain B) (Delta-Plus variant) complex from PDBsum server.

ACE2					Hydrogen bonds	SARS-CoV-2 S protein (Delta-Plus)				
Sl.no.	Atom no.	Res name	Res name	Atom no.		Atom no.	Atom name	Res name	Res no.	Distance
1	1	N	SER	19	<-->	11761	O	ALA	475	2.79
2	88	OE1	GLN	24	<-->	11915	ND2	ASN	487	2.52
3	207	NZ	LYS	31	<-->	11876	OE2	GLU	484	2.53
4	207	NZ	LYS	31	<-->	12016	OE1	GLN	493	2.91
5	276	OE2	GLU	35	<-->	12017	NE2	GLN	493	2.79
6	313	OD2	ASP	38	<-->	11288	OH	TYR	449	2.51
7	368	OH	TYR	41	<-->	12122	OG1	THR	500	2.59
8	368	OH	TYR	41	<-->	12122	OG1	THR	500	2.59
9	388	NE2	GLN	42	<-->	11288	OH	TYR	449	2.53
10	4966	ND2	ASN	330	<-->	12125	O	THR	500	3
11	5309	O	LYS	353	<-->	12140	N	GLY	502	3.14
12	5304	NZ	LYS	353	<-->	12060	O	GLY	496	2.49
13	5304	NZ	LYS	353	<-->	12092	OE1	GLN	498	2.87

Table S6B. List of atom-atom interactions (Non-bonded contacts) across the protein-ligand interface in ACE2 (Chain A)-Spike Protein (Chain B) (Delta-Plus variant) complex from PDBsum server.

ACE2					Non-bonded contacts	SARS-CoV-2 S protein (Delta-Plus)				
Sl.no.	Atom no.	Atom name	Res name	Res no.		Atom no.	Atom name	Res name	Res no.	Distance
1	1	N	SER	19	<-->	11761	O	ALA	475	2.79
2	81	CB	GLN	24	<-->	11761	O	ALA	475	3.52
3	81	CB	GLN	24	<-->	11914	OD1	ASN	487	3.71
4	84	CG	GLN	24	<-->	11914	OD1	ASN	487	3.71
5	87	CD	GLN	24	<-->	11914	OD1	ASN	487	3.86
6	87	CD	GLN	24	<-->	11915	ND2	ASN	487	3.38
7	88	OE1	GLN	24	<-->	11913	CG	ASN	487	3.31
8	88	OE1	GLN	24	<-->	11914	OD1	ASN	487	3.35
9	88	OE1	GLN	24	<-->	11915	ND2	ASN	487	2.52
10	139	O	THR	27	<-->	11429	CE1	PHE	456	3.78
11	139	O	THR	27	<-->	11431	CZ	PHE	456	3.22
12	130	CB	THR	27	<-->	11756	CB	ALA	475	3.7
13	132	CG2	THR	27	<-->	11429	CE1	PHE	456	3.77
14	132	CG2	THR	27	<-->	11431	CZ	PHE	456	3.76
15	132	CG2	THR	27	<-->	11731	CD2	TYR	473	3.79

	ACE2				Non-bonded contacts	SARS-CoV-2 S protein (Delta-Plus)				
Sl.no.	Atom no.	Atom name	Res name	Res no.		Atom no.	Atom name	Res name	Res no.	Distance
16	132	CG2	THR	27	<-->	11729	CE2	TYR	473	3.48
17	132	CG2	THR	27	<-->	11756	CB	ALA	475	3.51
18	132	CG2	THR	27	<-->	11948	CD2	TYR	489	3.8
19	132	CG2	THR	27	<-->	11946	CE2	TYR	489	3.74
20	140	N	PHE	28	<-->	11946	CE2	TYR	489	3.8
21	142	CA	PHE	28	<-->	11946	CE2	TYR	489	3.79
22	142	CA	PHE	28	<-->	11943	CZ	TYR	489	3.86
23	142	CA	PHE	28	<-->	11944	OH	TYR	489	3.5
24	144	CB	PHE	28	<-->	11944	OH	TYR	489	3.14
25	147	CG	PHE	28	<-->	11944	OH	TYR	489	3.61
26	148	CD1	PHE	28	<-->	11944	OH	TYR	489	3.18
27	189	C	ASP	30	<-->	11413	CD2	LEU	455	3.81
28	190	O	ASP	30	<-->	11413	CD2	LEU	455	3.69
29	183	CB	ASP	30	<-->	11429	CE1	PHE	456	3.52
30	183	CB	ASP	30	<-->	11431	CZ	PHE	456	3.74
31	188	OD2	ASP	30	<-->	11407	CG	LEU	455	3.44
32	188	OD2	ASP	30	<-->	11409	CD1	LEU	455	3.12
33	188	OD2	ASP	30	<-->	11413	CD2	LEU	455	3.79
34	188	OD2	ASP	30	<-->	11429	CE1	PHE	456	3.31
35	191	N	LYS	31	<-->	11431	CZ	PHE	456	3.55
36	195	CB	LYS	31	<-->	11938	CG	TYR	489	3.85
37	195	CB	LYS	31	<-->	11948	CD2	TYR	489	3.8
38	198	CG	LYS	31	<-->	11938	CG	TYR	489	3.57
39	198	CG	LYS	31	<-->	11939	CD1	TYR	489	3.55
40	201	CD	LYS	31	<-->	12016	OE1	GLN	493	3.31
41	204	CE	LYS	31	<-->	11874	CD	GLU	484	3.67
42	204	CE	LYS	31	<-->	11875	OE1	GLU	484	3.85
43	204	CE	LYS	31	<-->	11876	OE2	GLU	484	2.77
44	204	CE	LYS	31	<-->	12016	OE1	GLN	493	3.67
45	207	NZ	LYS	31	<-->	11874	CD	GLU	484	3.47
46	207	NZ	LYS	31	<-->	11875	OE1	GLU	484	3.64
47	207	NZ	LYS	31	<-->	11876	OE2	GLU	484	2.53
48	207	NZ	LYS	31	<-->	12016	OE1	GLN	493	2.91
49	251	CB	HIS	34	<-->	11368	OH	TYR	453	3.84
50	254	CG	HIS	34	<-->	11409	CD1	LEU	455	3.78
51	254	CG	HIS	34	<-->	11413	CD2	LEU	455	3.67
52	255	ND1	HIS	34	<-->	11409	CD1	LEU	455	3.62
53	255	ND1	HIS	34	<-->	11413	CD2	LEU	455	3.56
54	260	CD2	HIS	34	<-->	11370	CE2	TYR	453	3.43
55	260	CD2	HIS	34	<-->	11367	CZ	TYR	453	3.81
56	260	CD2	HIS	34	<-->	11368	OH	TYR	453	3.42
57	260	CD2	HIS	34	<-->	11409	CD1	LEU	455	3.43
58	256	CE1	HIS	34	<-->	11409	CD1	LEU	455	3.08
59	256	CE1	HIS	34	<-->	11413	CD2	LEU	455	3.9
60	258	NE2	HIS	34	<-->	11409	CD1	LEU	455	2.95
61	271	CG	GLU	35	<-->	12017	NE2	GLN	493	3.74
62	274	CD	GLU	35	<-->	12017	NE2	GLN	493	3.3
63	276	OE2	GLU	35	<-->	12015	CD	GLN	493	3.49
64	276	OE2	GLU	35	<-->	12016	OE1	GLN	493	3.3
65	276	OE2	GLU	35	<-->	12017	NE2	GLN	493	2.79
66	301	OE2	GLU	37	<-->	12185	CE2	TYR	505	3.67
67	311	CG	ASP	38	<-->	11285	CE1	TYR	449	3.47

ACE2					Non-bonded contacts	SARS-CoV-2 S protein (Delta-Plus)				
Sl.no.	Atom no.	Atom name	Res name	Res no.		Atom no.	Atom name	Res name	Res no.	Distance
68	311	CG	ASP	38	<-->	11287	CZ	TYR	449	3.87
69	311	CG	ASP	38	<-->	11288	OH	TYR	449	3.35
70	312	OD1	ASP	38	<-->	11285	CE1	TYR	449	3.58
71	312	OD1	ASP	38	<-->	11288	OH	TYR	449	3.48
72	312	OD1	ASP	38	<-->	12056	CA	GLY	496	3.27
73	313	OD2	ASP	38	<-->	11285	CE1	TYR	449	2.84
74	313	OD2	ASP	38	<-->	11287	CZ	TYR	449	3.06
75	313	OD2	ASP	38	<-->	11288	OH	TYR	449	2.51
76	372	CD2	TYR	41	<-->	12091	CD	GLN	498	3.55
77	372	CD2	TYR	41	<-->	12092	OE1	GLN	498	3.27
78	365	CE1	TYR	41	<-->	12134	OD1	ASN	501	3.63
79	370	CE2	TYR	41	<-->	12085	CB	GLN	498	3.87
80	370	CE2	TYR	41	<-->	12088	CG	GLN	498	3.67
81	370	CE2	TYR	41	<-->	12091	CD	GLN	498	3.55
82	370	CE2	TYR	41	<-->	12092	OE1	GLN	498	3.33
83	370	CE2	TYR	41	<-->	12134	OD1	ASN	501	3.89
84	367	CZ	TYR	41	<-->	12122	OG1	THR	500	3.69
85	367	CZ	TYR	41	<-->	12134	OD1	ASN	501	3.36
86	368	OH	TYR	41	<-->	12124	C	THR	500	3.46
87	368	OH	TYR	41	<-->	12125	O	THR	500	3.68
88	368	OH	TYR	41	<-->	12116	CB	THR	500	3.27
89	368	OH	TYR	41	<-->	12122	OG1	THR	500	2.59
90	368	OH	TYR	41	<-->	12126	N	ASN	501	3.63
91	368	OH	TYR	41	<-->	12134	OD1	ASN	501	3.41
92	383	CG	GLN	42	<-->	11288	OH	TYR	449	3.48
93	386	CD	GLN	42	<-->	11288	OH	TYR	449	3.4
94	386	CD	GLN	42	<-->	12093	NE2	GLN	498	3.54
95	388	NE2	GLN	42	<-->	11252	C	GLY	446	3.56
96	388	NE2	GLN	42	<-->	11253	O	GLY	446	3.45
97	388	NE2	GLN	42	<-->	11254	N	GLY	447	3.87
98	388	NE2	GLN	42	<-->	11290	CE2	TYR	449	3.68
99	388	NE2	GLN	42	<-->	11287	CZ	TYR	449	3.52
100	388	NE2	GLN	42	<-->	11288	OH	TYR	449	2.53
101	388	NE2	GLN	42	<-->	12093	NE2	GLN	498	3.39
102	428	CD2	LEU	45	<-->	11246	O	VAL	445	3.57
103	1001	O	MET	82	<-->	11898	CZ	PHE	486	3.42
104	989	CB	MET	82	<-->	11894	CD1	PHE	486	3.88
105	989	CB	MET	82	<-->	11896	CE1	PHE	486	3.2
106	989	CB	MET	82	<-->	11898	CZ	PHE	486	3.52
107	995	SD	MET	82	<-->	11894	CD1	PHE	486	3.76
108	1019	CD2	TYR	83	<-->	11898	CZ	PHE	486	3.7
109	1017	CE2	TYR	83	<-->	11896	CE1	PHE	486	3.14
110	1017	CE2	TYR	83	<-->	11898	CZ	PHE	486	3.16
111	1017	CE2	TYR	83	<-->	11914	OD1	ASN	487	3.6
112	1014	CZ	TYR	83	<-->	11896	CE1	PHE	486	3.12
113	1014	CZ	TYR	83	<-->	11898	CZ	PHE	486	3.71
114	1015	OH	TYR	83	<-->	11905	O	PHE	486	3.28
115	1015	OH	TYR	83	<-->	11894	CD1	PHE	486	3.45
116	1015	OH	TYR	83	<-->	11896	CE1	PHE	486	3.09
117	1015	OH	TYR	83	<-->	11914	OD1	ASN	487	3.57
118	1015	OH	TYR	83	<-->	11944	OH	TYR	489	3.27
119	4964	CG	ASN	330	<-->	12118	CG2	THR	500	3.77

ACE2					Non-bonded contacts	SARS-CoV-2 S protein (Delta-Plus)				
Sl.no.	Atom no.	Atom name	Res name	Res no.		Atom no.	Atom name	Res name	Res no.	Distance
120	4965	OD1	ASN	330	<-->	12116	CB	THR	500	3.82
121	4965	OD1	ASN	330	<-->	12118	CG2	THR	500	3.25
122	4966	ND2	ASN	330	<-->	12114	CA	THR	500	3.48
123	4966	ND2	ASN	330	<-->	12124	C	THR	500	3.68
124	4966	ND2	ASN	330	<-->	12125	O	THR	500	3
125	4966	ND2	ASN	330	<-->	12116	CB	THR	500	3.45
126	4966	ND2	ASN	330	<-->	12118	CG2	THR	500	3.8
127	5290	CA	LYS	353	<-->	12174	CB	TYR	505	3.8
128	5290	CA	LYS	353	<-->	12177	CG	TYR	505	3.31
129	5290	CA	LYS	353	<-->	12178	CD1	TYR	505	3.72
130	5290	CA	LYS	353	<-->	12187	CD2	TYR	505	3.32
131	5290	CA	LYS	353	<-->	12185	CE2	TYR	505	3.74
132	5308	C	LYS	353	<-->	12174	CB	TYR	505	3.43
133	5308	C	LYS	353	<-->	12177	CG	TYR	505	3.18
134	5308	C	LYS	353	<-->	12178	CD1	TYR	505	3.22
135	5308	C	LYS	353	<-->	12187	CD2	TYR	505	3.8
136	5309	O	LYS	353	<-->	12128	CA	ASN	501	3.6
137	5309	O	LYS	353	<-->	12138	C	ASN	501	3.82
138	5309	O	LYS	353	<-->	12130	CB	ASN	501	3.43
139	5309	O	LYS	353	<-->	12133	CG	ASN	501	3.87
140	5309	O	LYS	353	<-->	12140	N	GLY	502	3.14
141	5309	O	LYS	353	<-->	12146	O	GLY	502	3.86
142	5309	O	LYS	353	<-->	12174	CB	TYR	505	2.81
143	5309	O	LYS	353	<-->	12177	CG	TYR	505	3.11
144	5309	O	LYS	353	<-->	12178	CD1	TYR	505	3.33
145	5292	CB	LYS	353	<-->	12177	CG	TYR	505	3.88
146	5292	CB	LYS	353	<-->	12187	CD2	TYR	505	3.72
147	5295	CG	LYS	353	<-->	12187	CD2	TYR	505	3.89
148	5301	CE	LYS	353	<-->	12060	O	GLY	496	2.99
149	5301	CE	LYS	353	<-->	12092	OE1	GLN	498	3.69
150	5301	CE	LYS	353	<-->	12135	ND2	ASN	501	3.68
151	5304	NZ	LYS	353	<-->	12056	CA	GLY	496	3.52
152	5304	NZ	LYS	353	<-->	12059	C	GLY	496	3.36
153	5304	NZ	LYS	353	<-->	12060	O	GLY	496	2.49
154	5304	NZ	LYS	353	<-->	12091	CD	GLN	498	3.8
155	5304	NZ	LYS	353	<-->	12092	OE1	GLN	498	2.87
156	5304	NZ	LYS	353	<-->	12093	NE2	GLN	498	3.89
157	5310	N	GLY	354	<-->	12178	CD1	TYR	505	3.45
158	5310	N	GLY	354	<-->	12180	CE1	TYR	505	3.82
159	5312	CA	GLY	354	<-->	12140	N	GLY	502	3.69
160	5312	CA	GLY	354	<-->	12142	CA	GLY	502	3.76
161	5312	CA	GLY	354	<-->	12178	CD1	TYR	505	3.76
162	5315	C	GLY	354	<-->	12140	N	GLY	502	3.14
163	5315	C	GLY	354	<-->	12142	CA	GLY	502	3.3
164	5316	O	GLY	354	<-->	12140	N	GLY	502	3.26
165	5316	O	GLY	354	<-->	12142	CA	GLY	502	2.95
166	5317	N	ASP	355	<-->	12140	N	GLY	502	3.33
167	5319	CA	ASP	355	<-->	12125	O	THR	500	3.9
168	5319	CA	ASP	355	<-->	12140	N	GLY	502	3.86
169	5321	CB	ASP	355	<-->	12125	O	THR	500	3.04
170	5324	CG	ASP	355	<-->	12124	C	THR	500	3.74
171	5324	CG	ASP	355	<-->	12125	O	THR	500	2.79

ACE2					Non-bonded contacts	SARS-CoV-2 S protein (Delta-Plus)				
Sl.no.	Atom no.	Atom name	Res name	Res no.		Atom no.	Atom name	Res name	Res no.	Distance
172	5325	OD1	ASP	355	<-->	12125	O	THR	500	3.2
173	5326	OD2	ASP	355	<-->	12124	C	THR	500	3.66
174	5326	OD2	ASP	355	<-->	12125	O	THR	500	3.06
175	5326	OD2	ASP	355	<-->	12116	CB	THR	500	3.38
176	5326	OD2	ASP	355	<-->	12122	OG1	THR	500	3.75
177	5368	NH2	ARG	357	<-->	12116	CB	THR	500	3.15
178	5368	NH2	ARG	357	<-->	12122	OG1	THR	500	3.61
179	5368	NH2	ARG	357	<-->	12118	CG2	THR	500	3.23

Table S6C. List of atom-atom interactions (Salt bridges) across the protein-ligand interface in ACE2 (Chain A)-Spike Protein (Chain B) (Delta-Plus variant) complex from PDBsum server

ACE2					Salt bridges	SARS-CoV-2 S protein (Delta-Plus)				
Sl.no.	Atom no.	Atom name	Res name	Res no.		Atom no.	Atom name	Res name	Res no.	Distance
1	207	NZ	LYS	31	<-->	11876	OE2	GLU	484	2.53